Identification of Components Controlling Meristem Homeostasis

by

Lindsey Ann Gish

A dissertation submitted in the partial fulfillment
of the requirements for the degree of
Doctor of Philosophy
(Molecular, Cellular and Developmental Biology)
in the University of Michigan
2013

Doctoral Committee:

Professor Steven E. Clark, Chair
Assistant Professor Patrick J. Hu
Professor Jianming Li
Professor John W. Schiefelbein

Dedicated to Timothy Q. Mouse

Acknowledgments

I would like to take the time to acknowledge and extend my gratitude to the people who have helped me along during my graduate career and made all of this possible. Whether it has been in advice, support, or in the role of the sounding board, each individual mentioned here has played their part in helping me shape my thesis and myself.

To Steven Clark, my advisor and guide through the jungle of autorads and negative results, thank you for your level head. Your ability to cut through the chaos of data spewed forth from my notebooks these years has been instrumental in shaping my thesis into its final form. Thank you for your advice and guidance.

The members of my committee, Patrick Hu, Jianming Li, and John Schiefelbein have provided me with invaluable suggestion and ideas throughout the development of all of my projects. Thank you for your time and attention and for helping me stay on track.

I had the benefit of working under several knowledgeable and helpful post-docs during my time in the lab. Thanks goes to Jennifer Gagne for initiating me

into the world of graduate school research and for those first few years of mentorship. I would also like to thank Linqu Han for introducing me to the facets of the protein realm. And to Yongfeng Guo, a very special thank you for cloning advice and general encouragement.

I have had many friends within the department who have shared these years with me. I will miss my lab mate Chunghee Lee and wish luck to him and his family. There are also many people who have moved on to bigger things that I miss seeing around the building. Graduate school life would not have been nearly as interesting without the companionship of my plant ladies, Yana Wieckowski, Amy Klocko, and Nicola Harrison-Lowe, Sherilyn Grill and non-plant lady Lisa Sramkoski. You have truly helped me maintain my sanity throughout the years.

There are countless others in the department who helped me with all things needed for life and working, too many to name here but I want to mention Laura Olsen, Mary Carr, Jackie Glebe and Ed Grant.

My family and friends outside of Ann Arbor, your support and understanding throughout my education has seen me through and I could not have done it without you.

To my husband and almost four and a half years of long distance, I think we have earned this together. I cannot wait to finally live with you.

Table of Contents

List of Figures

List of Tables

Abstract

Plants maintain a pool of stem cells throughout their lives from which they draw to produce the organs of the adult plant body. This strictly regulated pool of stem cells is contained within structures known as meristems. There are several signal transduction pathways known that are involved in meristem homeostasis. While a number of factors reflecting different regulatory pathways controlling meristem function are known, our understanding of most of these pathways have significant gaps. This thesis research has been to attempt to identify novel components involved in meristem maintenance. Using a variety of approaches, several were identified and characterized.

The first novel component, CCI1, was identified in a protein-protein interaction screen with CLAVATA pathway kinases CLV1 and BAM1. CCI1 is a previously uncharacterized protein with no known or identifiable domains or motifs. I have shown that CCI1 directly binds to the receptor proteins and has phosphoinositide-binding activity *in vitro*. I have also shown that CCI1 partitions into detergent-resistant membrane (DRM) microdomains with other CLV pathway components. This partitioning is essential for CCI1 interaction with some CLV components, but not others, when tested in transient expression.

The second component characterized was a spontaneous, novel missense allele of *BLR*. BLR is a homeodomain protein of the BELL family of

TALE homeodomain proteins, which has been previously shown to be essential for internode elongation and floral evocation. The mutation I characterized is a unique allele with dominant negative characteristics that disrupt meristem homeostasis. Genetic interaction analyses as well as protein localization and DNA binding studies suggest that this mutant of BLR disrupts function of the SHOOTMERISTEMLESS transcription factor, known to be essential for meristem maintenance.

Finally, I characterized two mutants generated in an EMS enhancer screen in the *poltergeist* (*pol*) mutant background. While *pol pll1* double mutants lack stem cells, the *pol* single mutant provides a genetically sensitized background. I mapped two different mutants to *AGO10* and *TONSOKU* (*TSK*). Both genes have been shown to play important roles in meristem maintenance. The specific *tsk* mutation identified is previously uncharacterized; however the impact of *tsk* mutants on meristem homeostasis may be an indirect consequence of defects in polarized cell divisions.

Chapter One

Introduction to Signal transduction and the plant meristem

The basics of plant development and meristem architecture

The formation of the plant body occurs in two developmental stages [1]. The juvenile/seedling body plan is established during embryogenesis. The embryonic structure of higher plants such as *Arabidopsis thaliana* includes cotyledons, hypocotyl and root (Figure 1.1A). The embryo also contains two populations of undifferentiated cells termed meristems necessary for post-embryonic growth. The root apical meristem (RAM) is located at the basal end of the embryo and is the source of all subsequent root tissue (Figure 1.1A). The shoot apical meristem (SAM) is located at the apical end of the embryo, between the two cotyledons in the case of the dicotyledonous model plant *Arabidopsis thaliana* (Figure 1.1A). All post-embryonic aerial plant tissues and organs are ultimately derived from the SAM.

The cell divisions precipitating the emergence of a histologically recognizable SAM occur relatively late in embryogenesis, after much of the rest of the embryo is formed. However, the expression of determinants necessary for

meristem initiation and maintenance can be detected much earlier in development. Subsequent asymmetric cell divisions result in restriction of these meristem promoting factors to the shoot meristem [2]. Because plant cells cannot move relative to one another, asymmetric cell division is vital in establishing positional information as well as specifying cell fate.

The adult shoot meristems (SMs) contains a population of undifferentiated pluripotent stem cells in what is known as the central zone surrounded by the differentiating and proliferating daughter cells in the peripheral zone (Figure 1.1B). The cells of the central zone divide very slowly [3]. As these cells divide, they gradually are displaced from the meristem center in a 360° slow-motion cascade. As their positional cues change they begin to proliferate, differentiate, and become incorporated into incipient organ primordia.

The SM is organized into three cell layers termed L1, L2 and L3. The L1 and L2 cells undergo anticlinal divisions and so are able to remain clonally distinct. The cells of the L3 layer divide both anticlinally and periclinally (Figure 1.1B). In the vegetative and inflorescence shoot meristems, the L1 stem cells are the progenitors for the epidermis, L2 stem cells are progenitors for the mesophyll and L3 stem cells form the mesophyll and vasculature [4]. In the floral meristem, the L1 and L2 layers give rise to the epidermis and mesophyll of the sepals and petals while the stamens and carpels contain L1 epidermal, L2 subepidermal and L3 derived core tissue [5].

Initially, the SM is a vegetative meristem, producing the leaves of the rosette (Figure 1.2). After receiving the appropriate environmental cues, the vegetative SM makes the transition to an inflorescence SM, which will produce floral primordia with internode elongation between subsequent primordia. Flowers respecify stem cells to form a flower meristem. Unlike the vegetative and inflorescence meristems, floral meristems are determinate in that they produce a finite number of floral organs and then terminate. The organs of the flower are arranged in four concentric circles, or whorls, and develop from outermost to innermost (Figure 1.1C). The wild-type flower meristem produces, from outermost to innermost whorl, four sepals, four petals, six stamens and two carpels before terminating.

Meristem maintenance through CLAVATA signal transduction

The cells of multicellular organisms do not exist in isolation and are constantly receiving signals that drive physiological and developmental processes. The mechanisms involved between signal and cellular response is known as signal transduction. Signal transduction pathways often utilize protein receptors at the plasma membrane which receive extracellular ligand signals. These receptors then begin the transduction of the signal into the cell, leading to a cellular response often in the form of changes in gene regulation.

As the cells of the meristem divide and differentiate, they must also maintain a population of undifferentiated stem cells. The balance between

differentiation and proliferation must be maintained throughout the life of the plant so that reiterative organ formation can be sustained. Too many meristematic cells lead to fasciation and flower defects; too few and the meristem will terminate, reducing organogenic capacity and plant architecture. A major signal transduction pathway responsible for stem cell homeostasis is the CLAVATA pathway (Figure 1.3). Derived from the Latin word for club (clava), CLAVATA describes the club-like appearance of the silique fruit of plants with mutations in the pathways, resulting from an overgrowth of floral meristematic cells. The larger flower meristem forms supernumerary floral organs. Because the number of organs formed correlates to stem cell number on the early flower meristem, floral organ number is a convenient readout for meristem size.

The founding member of the pathway, *CLV1*, encodes a leucine rich repeat (LRR) transmembrane receptor kinase (Figure 1.4) [6]. *clv1* null alleles, including T-DNA insertional alleles, display only minor accumulation stem cells within the shoot and flower meristems. The most severe changes in stem cell number in *clv1* mutants are observed in dominant-negative alleles. These *clv1* alleles have missense mutations in the LRR and/or kinase domains [7,8]. As identified by in situ hybridization, *CLV1* expression is found highly specific within the central region of shoot and floral meristems [6].

CLV2 encodes a transmembrane receptor protein with 21 LRRs and a short cytoplasmic tail (Figure 1.4). Mutations in *CLV2* also lead to increased meristem size and floral organ number but the effects are consistently less severe than that of dominant-negative *clv1* alleles. *CLV2* expression is found

throughout the plant [9]. The expression pattern correlates with the pleiotropic phenotypes of *clv2* mutants which include multiple floral organ defects and a significant reduction in time to flowering when grown under short day conditions. In addition, *clv2* meristem phenotypes are suppressed under short day conditions [10]

CLV3 encodes a peptide ligand for the receptors of the pathway (Figure 1.4). It is a member of the CLE-containing family of proteins. CLE proteins are found in all land plants, including 32 different CLE-encoding genes in Arabidopsis [11]. CLV3 is secreted and proteolytically processed to release its CLE domain, which can then bind the extracellular receptors of CLV1, CLV2 and BAM1 [12] [13]. The *clv3-2* null allele has the most severe accumulation of stem cells found among *clv* mutants, consistent with its role as an upstream activator of all the CLV receptor components. *CLV3* is expressed in the center of the meristem in the L1, L2 and L3 layers [14] overlapping with CLV1 expression and marking the stem cell population.

BAM1/2/3 are CLV1-related LRR receptor kinases also involved in CLAVATA signaling. In contrast to *clv1* mutants, single loss-of-function *bam* alleles have no phenotype. Multiple *bam* mutations lead to smaller and terminated meristems [15]. In accordance with the role of BAM receptors in promoting stem cell maintenance, *bam1 bam2* suppress the stem cell accumulation phenotype of *clv3*. However, when combined with a *clv1* mutation, *bam1* and *bam2* enhance the *clv1* mutant phenotype [16]. A model resolving these data proposes two roles for BAM receptors in the meristem. *BAM1* and

BAM2 transcripts within the meristem identified by RNA in situ hybridization are most readily detected on the meristem periphery, with very low levels in the meristem center. In the meristem center BAM is redundant with CLV1 but weakly functional because of the low expression levels. At the periphery of the meristem, the high level of BAM receptors are able to insulate the meristem center from superfluous CLE ligands.

bam1 bam2 also exhibit many pleiotropic phenotypes play indicating that *BAM1/2* play important roles in vascular patterning as well as anther and ovule development [15]. Interestingly, when over-expressed within the meristem, *BAM1* and *BAM2* can partially rescue the *clv1* mutant phenotype and *CLV1* expression driven by the *ERECTA* promoter can fully rescue the *bam1 bam2* mutant phenotype, suggesting a strong conservation of biochemical function. Thus, the different developmental roles played by CLV1 and BAM are likely controlled primarily by expression patterns and signaling partners. [16].

CORYNE (CRN) was identified as a CLAVATA signaling pathway component in a screen for suppressors of *CLV3* over-expression, which leads to meristem termination [17] [18]. The two identified *crn* alleles both contain missense mutations within the transmembrane domain, resulting in enlarged meristems as well as defects in stamen development. In addition, the *crn* mutation suppresses the short pedicel phenotype of the *erecta* mutation. CRN is a transmembrane pseudokinase, meaning it has lost its enzymatic activity as tested by its inability to autophosporylate *in vitro* (Figure 1.4). In addition, CRN does not require kinase activity for wild type function [19]. This suggests CRN

may function structurally as a scaffolding protein for signal transduction complexes.

There is a great deal of biochemical and genetic evidence that several protein receptor complex combinations are receiving and relaying CLV signaling. In various experiments utilizing co-immunoprecipitation, FRET, and firefly luciferase complementation the most predominant interactions are those of CLV1 homodimers, and CLV1/BAM and CLV2/CRN heterodimers [20-22] Genetically, *crn* and *clv2* mutants are epistatic to one another, suggesting they work together in the pathway [17]. The pleiotropic phenotypes of *clv2* and *crn* mutations, and the additive effect of mutations of each with *clv1* mutations, imply they operate in separate signaling complexes within CLV signaling. Supporting evidence for separate signaling complexes, over-expression of *BAM1* or *BAM2* completely rescues the *clv2* mutant phenotype, presumably bypassing the need for the CLV2/CRN signaling complex [13].

WUSCHEL (*WUS*) encodes a homedomain-containing transcription factor that is required for embryonic meristem initiation and adult meristem maintenance. Mutations in *WUS* lead to seedlings with no SAM. Postembryonic growth in *wus* mutants consists of repeated adventitious shoot formation lacking functional meristems. *wus* mutants are fully epistatic to *clv* mutations, suggesting that *WUS* is the key target of the CLV pathway [2]. *WUS* expression can be detected as early as the 16-cell-stage embryo [2]. As embryogenesis progresses, *WUS* expression becomes restricted to a small patch of cells in the center of the meristem beneath the L3 in what is known as the Organizing Center

(OC)[2]. *WUS* expression in the OC is necessary for maintenance of the SM. WUS protein moves from the cells of the OC to the *CLV3* expressing central zone cells, and directly activates *CLV3* transcription [23]. WUS presumably activates additional targets to maintain stem cell identity (Figure 1.3). Mutations in the CLV pathway components discussed thus far lead to increased expression of *WUS* within the meristem, demonstrating negative regulation of *WUS* by the CLAVATA pathway (Figure 1.3) [18,24]. The enlarged meristems of *clv* mutants is the result of the reduction of negative regulation which shifts *WUS* expression up one cell layer relative to wild type and also expands expression laterally.

The only signaling intermediates identified so far in the CLAVATA pathway are the related and redundant type 2C phosphatases POL and PLL1 [25-27]. Identified in a *clv* mutant suppressor screen, mutations in *POL* and *PLL1* do not have any gross identifiable phenotypes as single mutants. The *pol pll1* double mutant develops severe embryonic basal patterning defects and are seedling lethal as they lack root structure [28]. When the apical portion of a *pol pll1* seedling was grafted onto the basal portion of a wild-type seedling, the resulting plant phenocopies the *wus* mutant [29]. *pol pll1* grafted plants are unable to maintain *WUS* expression. The vegetative meristems reiteratively terminate and the inflorescence produces flowers which also terminate prematurely, resulting in flowers with a reduced number of organs. The CLV/CRN components act through POL and PLL1 to restrict *WUS* expression as demonstrated by *pol pll1* double mutant epistasis to *clv* mutations and the ability of *WUS* over-expression to rescue the double mutant phenotype [29] (Figure 1.3).

Relatively few kinase-interacting proteins have been identified in plants. The only CLV1 kinase interacting protein identified to date is KAPP [30,31]. KAPP is a protein phosphatase that interacts with many phosphorylated RLKs and is thought to act in a number of signal transduction pathways [32,33]. While constitutive expression of *KAPP* in Arabidopsis leads to a slight increase in carpel number and reduction of KAPP mRNA can rescue the *clv1* mutant phenotype, genetic interactions with other CLAVATA pathway components have not been reported [30,31].

Other meristem players

SHOOTMERISTEMLESS (STM) is a KNOX family transcription factor that functions to maintain meristem identity and is required for embryonic SAM formation. Much like *wus* mutants, *stm* mutants do not develop a SAM embryonically [34]. *STM* expression can be detected in the 32-64 cell stage embryo and becomes restricted to the center of the adult shoot and floral meristems [35]. Genetic evidence suggests WUS and STM operate in independent pathways. While *wus* is epistatic to *clv* mutations, *stm* and *clv* mutations are additive and display dominant cross-suppression interaction [36,37]. Additionally, mutations in *POL* recessively enhance *stm* mutant phenotypes [25]. Moreover, embryonic expression of the differentiation-promoting ligand CLV3 requires *WUS* and not *STM* [38]. Taken together, these data support separate pathways for WUS and STM function.

In the current model, WUS specifies the cells central in the meristem as stem cells, while STM specifically suppresses differentiation of the proliferating meristematic daughter cells. As cells on the meristem periphery organize into distinct organ primordia, *STM* expression is rapidly repressed, allowing the activation of differentiation factors, such as ASYMMETRIC LEAVES1 (AS1) [39]. AS1 is a MYB-domain transcription factor repressed by STM in stem cells. In organ founder cells, *STM* is repressed, allowing *AS1* expression, leading to the down-regulation of other three class I KNOX genes, *BP*, *KNAT2* and *KNAT6*, and differentiation. Thus, STM prevents differentiation by negatively regulating *AS1*.

This separation of stem cell specification and maintenance by WUS and differentiation antagonism during proliferation by STM is supported by the data that *WUS* expression in *stm* mutants allows for self-perpetuating meristematic activity while the converse, *STM* expression in the *wus* mutant, does not.

The search for signal transduction intermediates

Little is known about how the CLV signal is transduced from the plasma membrane to trigger the response of the *WUS* gene. Forward and reverse genetic methods have been all but exhausted in the search for CLV pathway signaling intermediates. Overlapping biochemical function, genetic redundancy, pleiotropic phenotypes and early developmental lethality are all possible explanations as to why pathways intermediates have been especially difficult to

identify using these screening methods. POL and CRN are both pathway components identified using enhancer/suppressor screens.

Phenotypic screens have identified many genes in developmental pathways, including most of the components of the CLAVATA pathway. Other members, such as the BAM receptors, have been identified by homology. Techniques such yeast two-hybrid and microarray expression analysis as well as the use of reporter genes are also popular methods of identifying gene function and interaction. Recent work on proteomics and gene-regulatory network mapping through FACS in Arabidopsis roots has led to a great deal of data and understanding of cell fate specification in root [40].

I have utilized multiple strategies in my attempt to identify meristem signaling pathway intermediates. In Chapter Two, I characterize CCI1, a CLV1 and BAM1 interacting protein identified in a yeast-based protein-protein interaction screen. Chapter Three discusses a spontaneous and unique mutation in *BELLRINGER*, which encodes a homedomain partner protein for STM. In chapter Four I map and analyze meristem mutant phenotypes to two previously characterized meristem maintenance factors AGO10 and TSK.

A

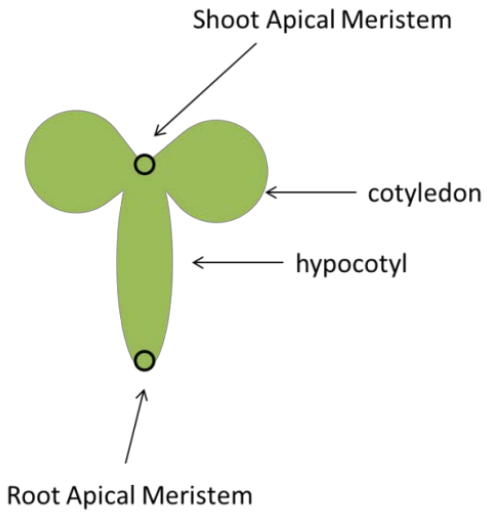

B

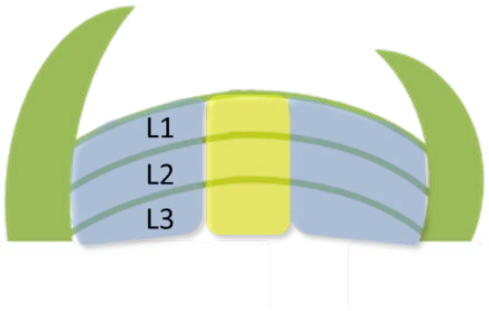

C

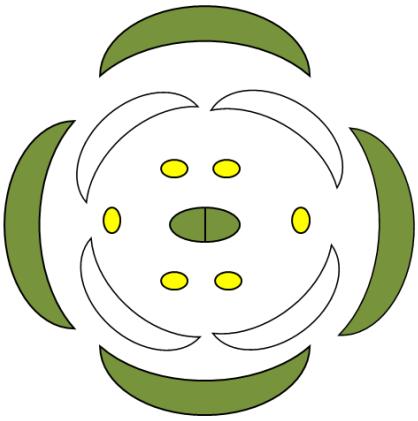

Figure 1.1 Arabidopsis embryo, meristem and flower structure.

A. The Arabidopsis embryo has a basic structure which includes the root and shoot meristems.
B. The SM has three clonally distinct cell layers. The central zone of stem cells is colored yellow while the more rapidly dividing peripheral zone is colored blue.
C. The Arabidopsis flower produces four concentric whorls of floral organs. From outermost to innermost: 4 sepals (green), 4 petals (white), 6 stamens (yellow), and 2 carpels (green).

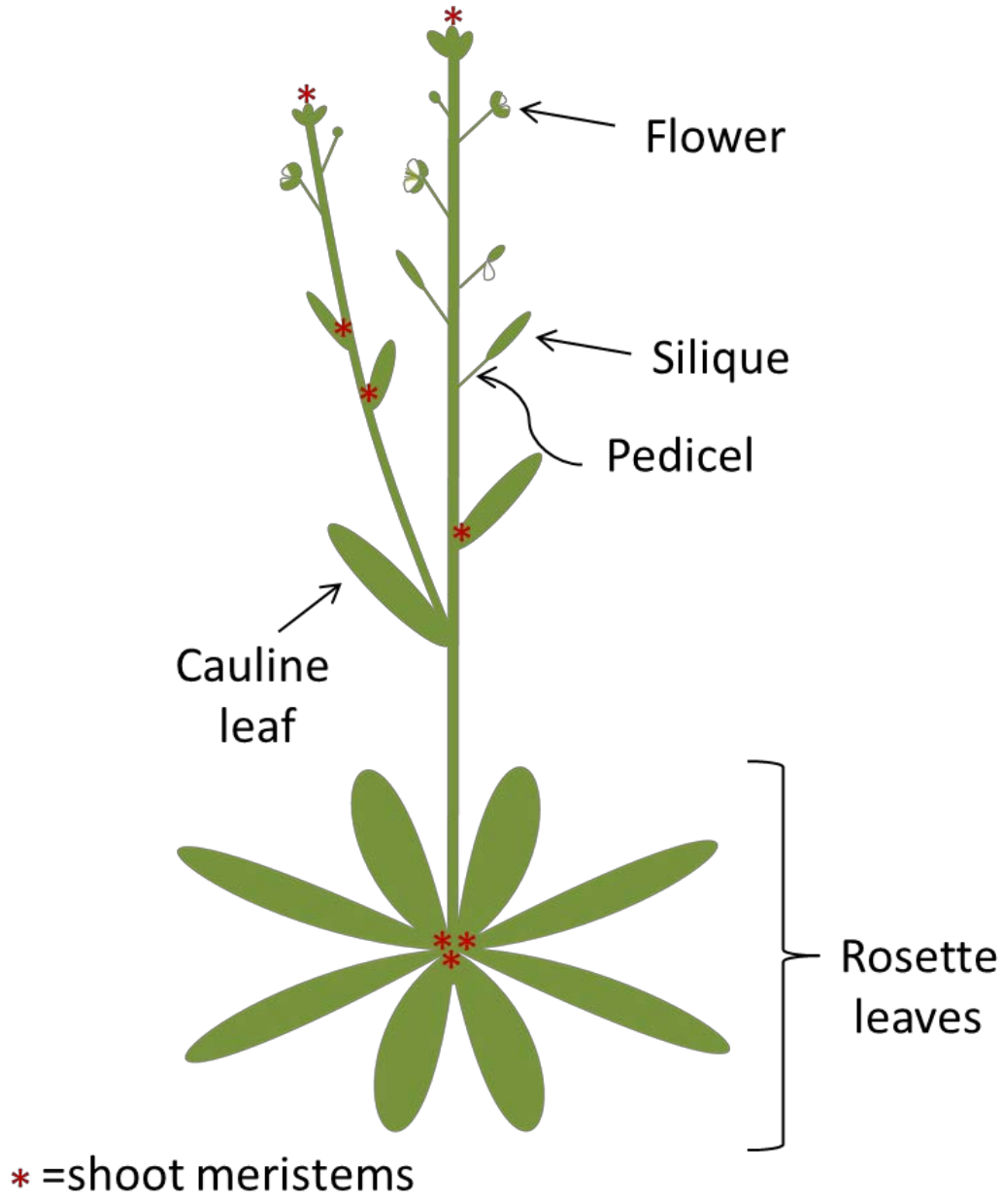

Figure 1.2 Structure of the adult Arabidopsis plant

The adult Arabidopsis plant with the location of shoot meristems indicated by asterisks.

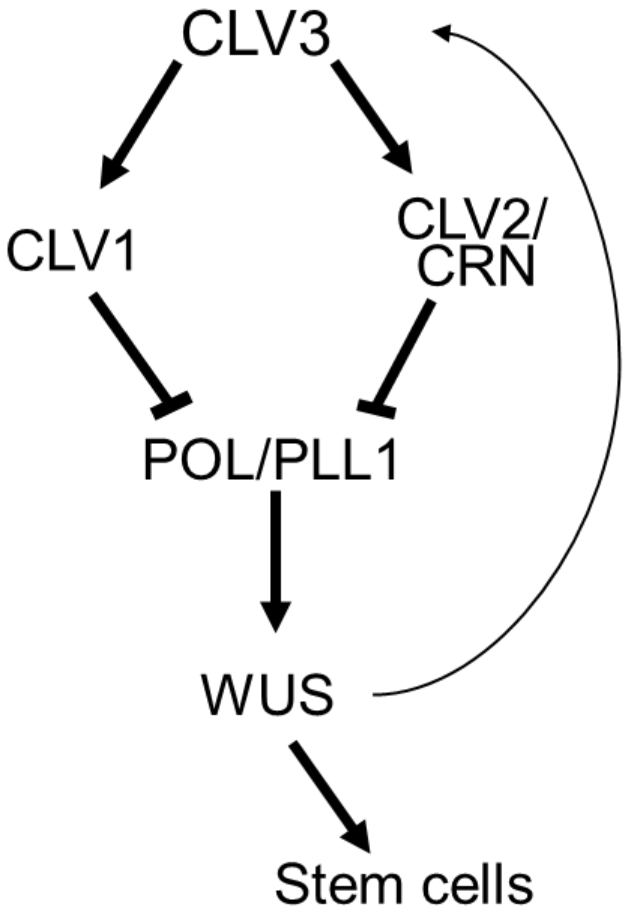

Figure 1.3 Model of genetic interactions of CLV pathway components

The feedback loop between CLV and WUS maintains a stable population of stem cells within the Arabidopsis meristem.

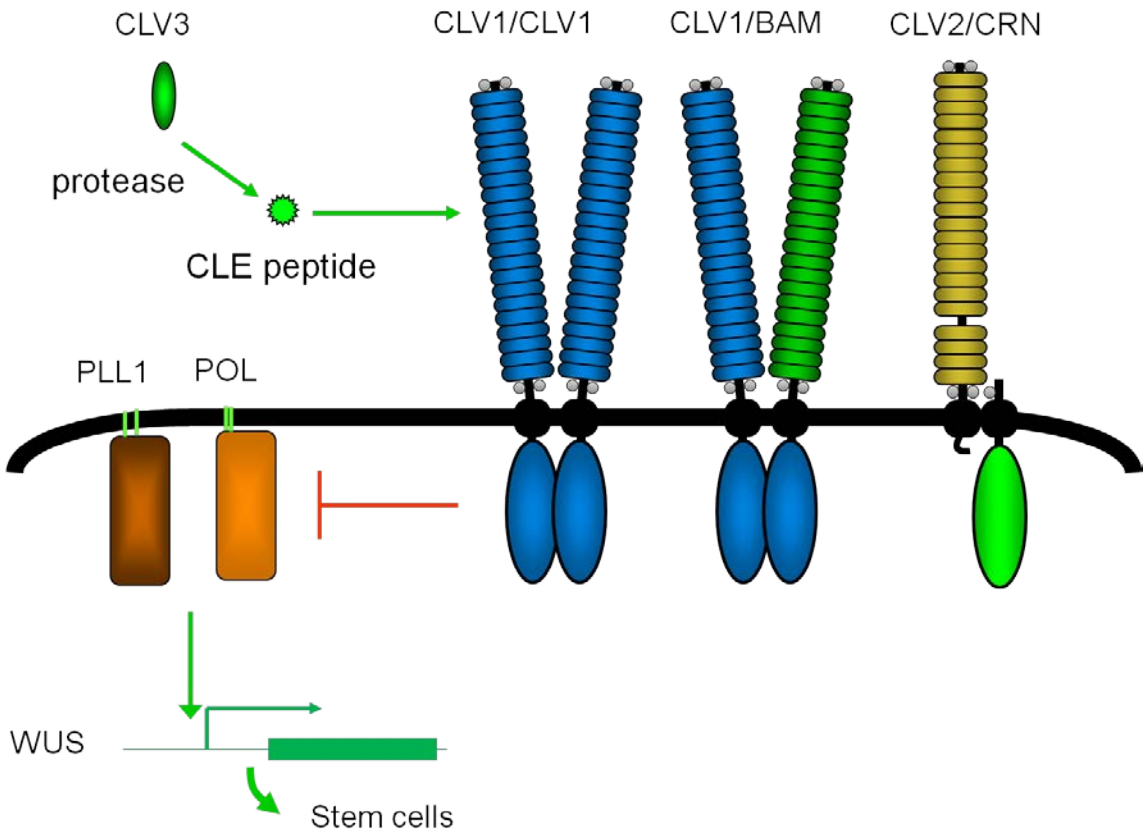

Figure 1.4 CLV pathway components biochemical model

The components of the CLV pathway identified to date are located at the plasma membrane and include several transmembrane receptor protein and kinases which negatively regulate membrane-associated phosphatases POL and PLL1 activity. POL and PLL1 work to maintain *WUS* expression, which ultimately specifies the stem cell fate.

References

1. Jürgens G (2001) Apical-basal pattern formation in Arabidopsis embryogenesis. Embo J 20: 3609-3616.

2. Mayer KF, Schoof H, Haecker A, Lenhard M, Jurgens G, et al. (1998) Role of *WUSCHEL* in regulating stem cell fate in the *Arabidopsis* shoot meristem. Cell 95: 805-815.

3. Laufs P, Grandjean O, Jonak C, Kieu K, Traas J (1998) Cellular parameters of the shoot apical meristem in Arabidopsis. Plant Cell 10: 1375-1390.

4. Steeves TA, Sussex IM (1989) Patterns in Plant Development. New York: Cambridge University Press.

5. Jenik PD, Irish VF (2000) Regulation of cell proliferation patterns by homeotic genes during Arabidopsis floral development. Development 127: 1267-1276.

6. Clark SE, Williams RW, Meyerowitz EM (1997) The *CLAVATA1* gene encodes a putative receptor kinase that controls shoot and floral meristem size in Arabidopsis. Cell 89: 575-585.

7. Clark SE, Running MP, Meyerowitz EM (1993) *CLAVATA1*, a regulator of meristem and flower development in Arabidopsis. Development 119: 397-418.

8. Diévart A, Dalal M, Tax FE, Lacey AD, Huttly A, et al. (2003) *CLAVATA1* dominant-negative alleles reveal functional overlap between multiple receptor kinases that regulate meristem and organ development. Plant Cell 15: 1198-1211.

9. Jeong S, Trotochaud AE, Clark SE (1999) The Arabidopsis *CLAVATA2* gene encodes a receptor-like protein required for the stability of the CLAVATA1 receptor-like kinase. Plant Cell 11: 1925-1934.

10. Kayes JM, Clark SE (1998) *CLAVATA2*, a regulator of meristem and organ development in *Arabidopsis*. Development 125: 3843-3851.

11. Cock JM, McCormick S (2001) A large family of genes that share homology with CLAVATA3. Plant Physiol 126: 939-942.

12. Ogawa M, Shinohara H, Sakagami Y, Matsubayashi Y (2008) Arabidopsis CLV3 peptide directly binds CLV1 ectodomain. Science 319: 294.

13. Guo Y, Han L, Hymes M, Denver R, Clark SE (2010) CLAVATA2 forms a distinct CLE-binding receptor complex regulating Arabidopsis stem cell specification. Plant J 63: 889-900.

14. Fletcher JC, Brand U, Running MP, Simon R, Meyerowitz EM (1999) Signaling of cell fate decisions by *CLAVATA3* in *Arabidopsis* shoot meristems. Science 283: 1911-1914.

15. DeYoung BJ, Bickle KL, Schrage KJ, Muskett P, Patel K, et al. (2006) The CLAVATA1-related BAM1, BAM2 and BAM3 receptor kinase-like proteins are required for meristem function in Arabidopsis. Plant J 45: 1-16.

16. DeYoung BJ, Clark SE (2008) BAM receptors regulate stem cell specification and organ development through complex interactions with CLAVATA signaling. Genetics 180: 895-904.

17. Muller R, Bleckmann A, Simon R (2008) The receptor kinase CORYNE of Arabidopsis transmits the stem cell-limiting signal CLAVATA3 independently of CLAVATA1. Plant Cell 20: 934-946.

18. Brand U, Fletcher JC, Hobe M, Meyerowitz EM, Simon R (2000) Dependence of stem cell fate in *Arabidopsis* on a feedback loop regulated by *CLV3* activity. Science 289: 617-619.

19. Nimchuk ZL, Tarr PT, Meyerowitz EM (2011) An evolutionarily conserved pseudokinase mediates stem cell production in plants. Plant Cell 23: 851-854.

20. Zhu Y, Wang Y, Li R, Song X, Wang Q, et al. (2010) Analysis of interactions among the CLAVATA3 receptors reveals a direct interaction between CLAVATA2 and CORYNE in Arabidopsis. Plant J 61: 223-233.

21. Bleckmann A, Weidtkamp-Peters S, Seidel CA, Simon R (2010) Stem cell signaling in Arabidopsis requires CRN to localize CLV2 to the plasma membrane. Plant Physiol 152: 166-176.

22. Guo Y, Clark SE (2010) Membrane distributions of two ligand-binding receptor complexes in the CLAVATA pathway. Plant Signal Behav 5: 1442-1445.

23. Yadav RK, Perales M, Gruel J, Girke T, Jonsson H, et al. (2011) WUSCHEL protein movement mediates stem cell homeostasis in the Arabidopsis shoot apex. Genes & Development 25: 2025-2030.

24. Schoof H, Lenhard M, Haecker A, Mayer KF, Jurgens G, et al. (2000) The stem cell population of *Arabidopsis* shoot meristems in maintained by a regulatory loop between the *CLAVATA* and *WUSCHEL* genes. Cell 100: 635-644.

25. Yu LP, Simon EJ, Trotochaud AE, Clark SE (2000) *POLTERGEIST* functions to regulate meristem development downstream of the *CLAVATA* loci. Development 127: 1661-1670.

26. Yu LP, Miller AK, Clark SE (2003) *POLTERGEIST* Encodes a Protein Phosphatase 2C that Regulates CLAVATA Pathways Controlling Stem Cell Identity at *Arabidopsis* Shoot and Flower Meristems. Curr Biol 13: 179-188.

27. Gagne JM, Clark SE (2010) The Arabidopsis stem sell factor POLTERGEIST is membrane localized and phospholipid stimulated. Plant Cell 22: 729-743.

28. Song SK, Clark SE (2005) POL and related phosphatases are dosage-sensitive regulators of meristem and organ development in Arabidopsis. Dev Biol 285: 272-284.

29. Song SK, Lee MM, Clark SE (2006) POL and PLL1 phosphatases are CLAVATA1 signaling intermediates required for Arabidopsis shoot and floral stem cells. Development 133: 4691-4698.

30. Williams RW, Wilson JM, Meyerowitz EM (1997) A possible role for kinase-associated protein phosphatase in the arabidopsis CLAVATA1 signaling pathway. Proc Natl Acad Sci USA 94: 10467-10472.

31. Stone JM, Trotochaud AE, Walker JC, Clark SE (1998) Control of meristem development by CLAVATA1 receptor kinase and kinase-associated protein phosphatase interactions. Plant Physiol 117: 1217-1225.

32. Gomez-Gomez L, Bauer Z, Boller T (2001) Both the extracellular leucine-rich repeat domain and the kinase activity of FSL2 are required for flagellin binding and signaling in Arabidopsis. Plant Cell 13: 1155-1163.

33. Becraft PW (2002) Receptor kinase signaling in plant development. Annu Rev Cell Dev Biol 18: 163-192.

34. Barton MK, Poethig RS (1993) Formation of the shoot apical meristem in *Arabidopsis thaliana*: An analysis of development in the wild type and *shoot meristemless* mutant. Development 119: 823-831.

35. Long JA, Moan EI, Medford JI, Barton MK (1996) A member of the KNOTTED class of homeodomain proteins encoded by the STM gene of *Arabidopsis*. Nature 379: 66-69.

36. Laux T, Mayer KF, Berger J, Jurgens G (1996) The WUSCHEL gene is required for shoot and floral meristem integrity in Arabidopsis. Development 122: 87-96.

37. Clark SE, Jacobsen SE, Levin JZ, Meyerowitz EM (1996) The *CLAVATA* and *SHOOT MERISTEMLESS* loci competitively regulate meristem activity in Arabidopsis. Development 122: 1567-1575.

38. Brand U, Grunewald M, Hobe M, Simon R (2002) Regulation of CLV3 Expression by Two Homeobox Genes in Arabidopsis. Plant Physiol 129: 565-575.

39. Byrne ME, Barley R, Curtis M, Arroyo JM, Dunham M, et al. (2000) *Asymmetric leaves1* mediates leaf patterning and stem cell function in *Arabidopsis*. Nature 408: 967-971.

40. Iyer-Pascuzzi AS, Benfey PN (2010) Fluorescence-activated cell sorting in plant developmental biology. Methods Mol Biol 655: 313-319.

Chapter Two

Characterization of a novel CLAVATA interacting factor

ABSTRACT

The CLAVATA (CLV) signaling pathway is essential for shoot meristem homeostasis in Arabidopsis. CLV acts to limit the expression domain of the stem cell-promoting factor WUSCHEL. The closely related receptor-kinases CLV1 and BAM1 are key components in this pathway; however, the downstream factors that link the receptors to WUSCHEL regulation are poorly understood. We have identified a novel receptor partner we term CCI1 through interaction screens with the CLV1 and BAM1 kinase domains. CCI1 directly interacted with the kinase domains of CLV1 and BAM1 receptors *in vitro*. CCI1 localized to the plasma membrane in transient expression assays. We present evidence that CCI1 membrane localization is the result of its phosphatidylinositide-binding activity. Furthermore, CLV signaling components and CCI1 both partition to detergent-resistant membrane microdomains characterized as lipid rafts.

INTRODUCTION

The aerial organs of the adult plant body are reiteratively initiated from a tightly maintained population of stem cells found at the shoot and flower meristems. Each meristem maintains a small number of stem cells in the center, surrounded by the more rapidly dividing and differentiating daughter cells [1]. The shoot meristems maintain a strict balance between proliferation and differentiation of stem cells throughout the life of the plant.

The shoot apical meristem (SAM) in Arabidopsis is composed of three stem cell layers (L1, L2, and L3). Directly beneath L3 stem cells is the Organizing Center (OC) defined by the expression of the transcription factor WUSCHEL (WUS) [2] Current evidence indicates that WUS protein moves from the OC to the overlying stem cell layers to maintain stem cell identity [3,4].

The components of the CLAVATA signaling transduction pathway act to spatially restrict *WUS* expression. The CLV pathway components include the CLV3 ligand, the leucine-rich repeat (LRR) receptor-kinase CLV1, the LRR receptor protein CLV2, and CRN, a transmembrane kinase-related protein. Mutations in the CLV components result in expanded *WUS* expression and an enlarged meristem [5].

In addition, the CLV1-related BAM1, BAM2 and BAM3 proteins fulfill both redundant and unique roles. In the meristem center, the weakly expressed BAM proteins act redundantly with CLV1 to limit meristem size. However, BAM1 and BAM2 are predominantly expressed on the meristem periphery [6]. Loss of BAM

receptors results in a reduction in stem cell accumulation [7]. In addition to their complex roles in meristem development, BAM receptors are expressed throughout the plant, and *bam1 bam2* double mutants exhibit pleiotropic developmental defects ranging from seedling lethality to reduced vascular branching to male sterility [6,8]. Critically, CLV1 and BAM receptors can cross-complement each other, indicating that the biochemical function of the individual receptors is largely interchangeable.

Several receptor complexes have been identified by various studies using both transient expression and *in vivo* analysis. The most commonly detected complexes are CLV1 and CLV1/BAM multimers and a complex of CLV2 and CRN [9-11]. Higher ordered interactions between CLV1 and CLV2 complexes have only been detected in in tobaccotransient expression.

The ligand, CLV3, is proteolytically processed to release the CLE peptide, which can then bind the extracellular domain of all of the detected receptor complexes [11,12]. CLV1, BAM1, BAM2 and CLV2 all have nearly identical binding affinities to the processed CLV3 ligand *in vitro* [11].

There is a conspicuous lack of understanding of signaling components between the CLV components and WUS. The only known verified signaling intermediates are the phosphatases POL and PLL1. Identified in a suppressor screen of the *clv* mutant phenotype, individual mutations in these phosphatases partially suppress the stem cell accumulation phenotype of *clv* mutants [13,14]. POL and PLL1 act downstream of CLV1 to maintain *WUS* expression [15]. As a

result, *pol pll1* double mutants fail to maintain *WUS* expression and phenocopy the meristem termination of *wus* mutants. The *pol pll1* meristem termination can be bypassed by ectopic *WUS* expression, placing POL/PLL1 downstream of CLV1 and upstream of WUS [15]. POL/PLL1 are plasma membrane localized in a fashion dependent on N-terminal myristoylation and palmitoylation [16]. This localization is required for protein function, as the *pol pll1* mutant phenotype can only be complemented by expression constructs with both of these acylation sites intact. In addition, POL and PLL1 are phospholipid binding proteins whose phosphatase activity is stimulated by PI(4)P.

In this study, we describe a novel protein CCI1 identified through interaction screens with both CLV1 and BAM1. We present evidence of CCI1 receptor interactions, plasma membrane localization, phospholipid binding, and membrane microdomain partitioning.

RESULTS

Identification of a novel CLV1-interacting protein

We performed a protein interaction screen using the yeast Cytotrap system that involves interactions at the yeast plasma membrane (Figure 2.1) [17]. Yeast at the restrictive temperature require that hSos (a Ras GEF) localize to the plasma membrane to replace the temperature sensitive cdc25 isoform. hSos was fused to the CLV1 and BAM1 kinase domain and placed into yeast along with cDNA library from Arabidopsis meristem tissue placed behind a N-

terminal myristoylation tag to drive plasma membrane localization. Only those yeast with a cDNA-encoded protein that bound to CLV1 or BAM1 would localize the hSos tag to the plasma membrane and survive at the restrictive temperature.We used as bait the kinase domains of both CLV1 (residues 697-980) and BAM1 (residues 699-1003) in separate screens. Because CLV1 and BAM1 can replace each other's function in Arabidopsis [6], we hypothesized that proteins interacting with both kinase domains were more likely to represent physiologically relevant partners. We sequenced 32 putative positive clones from yeast with the CLV1 bait protein and 52 clones from yeast with the BAM1 bait (Tables 2.1 and 2.2). Among these positives, two were identified from both CLV1 and BAM1 screens and only one, At5G65480, was identified multiple times in both screens. All positives for At5g65480 were full-length cDNAs, suggesting that interaction with CLV1 and BAM1 required the full-length protein.

At5g65480, which we have named *CCI1* (inspired from *C*lavata *c*omplex *i*nteractor) encodes a small protein of 153 amino acids. While having no known motifs, the genomes of all land plants we analyzed contained homologues of *CCI1* (Figure 2.2). Arabidopsis contains a second related protein encoded by At4g38060 that we named *CCI2* (Figure 2.2).

We first tested whether CCI1 directly interacts with the CLV1 kinase domain by expressing the corresponding proteins in *E. coli* as epitope-tagged fusion proteins. In pull-down experiments, GST-CCI1 showed direct interaction with the CLV1 kinase domain, but not in control reactions (Figure 2.3A). CCI2 also showed direct interaction with CLV1 (Figure 2.3A).

We next sought to determine whether the CLV1-CCI1 and BAM-CCI1 interactions could be replicated in a plant system. Because efforts to detect epitope-tagged CCI1 expressed in transgenic Arabidopsis were unsuccessful, we used transient expression in *N. benthamiana* to express the proteins [18]. We have successfully used this system to characterize CLV1 interactions both with CLV3 and with other signaling components [11,19]. To test the interactions between CCI1 and BAM1/CLV1, the full-length proteins were expressed as epitope tagged fusions under the cauliflower mosaic virus *35S* promoter. Two days after infiltration, leaf proteins were extracted and co-immunoprecipitation experiments were performed. When CCI1-FLAG and BAM1-GFP or CCI1-FLAG and CLV1-GFP were co-expressed in the same leaves we detected robust co-immunoprecipitation, suggesting a protein-protein interaction between CCI1-FLAG and the GFP-tagged full-length receptors (Figure 2.3B).

In addition to GFP-tagged BAM1 and CLV1, GFP-tagged full-length CRN, CLV2 and BRI1 were also tested for interaction with CCI1-FLAG. Unexpectedly, we observed co-immunoprecipitation between CCI1-FLAG and all of the tested proteins (Figure 2.3C). Co-immunoprecipitations were also detected when the epitope tags were switched (i.e., CCI1-GFP with BAM1-FLAG and CLV1-FLAG) (Figure 2.4). Additional control reactions demonstrated that proteins interactions were not a result of non-specific antibody interactions (Figure 2.3C). Hypothesizing that these associations might be formed spuriously after membrane isolation, we next tested whether the associations of CCI1 with CLV signaling components required co-expression, or could occur by mixing

membrane extracts expressing the corresponding proteins. These experiments revealed that co-expression is necessary for any interaction to occur, indicating that the CCI1-receptor interactions were not formed through spurious post-isolation interactions, but instead required that the proteins were expressed simultaneously in the same cells (Figure 2.3C).

CCI1 is plasma-membrane localized and binds phosphatidylinositols *in vitro*

Because CCI1 interacts with CLV1, which acts at the plasma membrane [20], we next tested whether CCI1 co-localized to the same subcellular compartment. CCI1 has no identifiable localization motif, nor any predicted transmembrane domain. Both CCI1-GFP and CCI1-FLAG were transiently expressed and localization was determined both by confocal microscopy and subcellular fractionation. The localization of CCI1-GFP was consistent with that of plasma membrane localization, with signal exclusively at the cell periphery (Figure 2.5A). However, the cytoplasm of these cells is largely appressed to the cell periphery, so that we could not exclude partitioning between the membrane and the cytoplasm. To resolve this issue, we fractionated extracts, separating membrane and soluble fractions. For CCI1-FLAG, we detected localization exclusively in the membrane fraction (Figure 2.5B). In addition, when these *N. benthamiana* leaf protein extracts were subjected to ultracentrifugation and fractionation by two-phase partitioning, CCI1-FLAG was detected in the plasma

membrane-enriched PEG phase, and was absent from the plasma membrane-depleted dextran phase [21], (Figure 2.5B). This localization of CCI1 is consistent with the plasma membrane-localized H+-ATPase PMA2, used as a control. These data collectively indicate that CCI1 is plasma membrane bound.

These results raised the question of what motif(s) within CCI1 were driving exclusive plasma-membrane localization. As mentioned, neither CCI1 nor any analyzed homologue contains a known membrane-localization motif. Furthermore, CCI1 membrane localization was independent of CLV1 co-expression. One possibility emerged from attempts to use CCI1 as a bait protein in the Cytotrap yeast system. Here we observed that CCI1 alone localized to the yeast plasma membrane (as evidenced by auto-activation, data not shown). As shown previously for the animal protein Tubby, Cytotrap auto-activation can result from lipid binding activity of the bait protein [22]. Furthermore, the CLV1 downstream signaling phosphatases POL and PLL1 autoactivate in the Cytotrap system, localize to the plasma membrane, and bind to phospholipids [16]. To test whether CCI1 has lipid-binding activity, *E.coli* expressed GST-CCI1 was incubated with lipid strips blotted with phosphatidylinositides and other lipids. The human FAPP protein, which has been shown to specifically bind phosphatidylinositol-4 phosphate (PI(4)P), was used as a positive control [23]. Full-length CCI1 bound PI-monophospates and cardolipin, with weak association observed to some PI-di- and tri-phosphates (Figure 2.6).

Examination of the protein sequence revealed that the N-terminal half of CCI1contains several polybasic stretches of amino acids, conserved across most

plant species, while the C-terminal domain has more extensive conservation across land plants (Figure 2.2). Several phosphatidylinositol-binding domains utilize polybasic patches to interact with negatively charged phosphates on the inositol head group of PI-mono and di-phosphates [24]. When the N- and C-terminal regions were expressed separately as fusion proteins, the N-terminal 83 amino acids of CCI1 were sufficient to bind a similar profile of lipids, while the C-terminal 70 amino acids showed no detectable binding (Figure 2.6). Deletion constructs targeting individual polybasic regions in the N-terminal portion appeared to attenuate but not abolish lipid binding activity (Figure 2.7).

Plasma membranes are not homogeneous with respect to protein and lipid-type distribution [25,26]. Isolation and visualization of membrane raft microdomains have suggested that specific protein and lipid enrichments in microdomains in the plasma membrane act as hubs to recruit signal transduction pathway components. Some microdomains are sufficiently enriched in sterols, phosphatidylinositols and saturated lipids that they become insoluble to specific detergent treatments [27,28]. Relative to the total plasma membrane, detergent-resistant membranes (DRMs) are enriched in phosphatidylinositides, such as PI(4)P and PI(4,5)P_2, over structural phospholipids such as phosphatidylcholine and phosphatidylethanolamine [29]. Furthermore, we have previously observed that CLV3 binding to the CLV1, BAM and CLV2 receptors could only be detected for receptors in DRM fractions, potentially reflecting lipid raft localization [11]. Taken together, we hypothesized CCI1 lipid binding might be associated with membrane microdomain partitioning as part of signaling complexes.

CCI1 was found in both the soluble membrane and detergent-insoluble membrane fractions from *N. benthamiana* transient expression. CLV2 partitions in a similar pattern in Arabidopsis, while BAM1 and BAM2 are found predominantly in the soluble membrane fraction with detectable partitioning to the DRM fraction (Figure 2.8A). To test if these receptors were truly localized to lipid rafts, we assayed their sedimentation in sucrose gradients. While the control clathrin was found exclusively in denser soluble membrane fractions, a fraction of CLV2 and all detectable CRN from Arabidopsis meristems were found in lighter fractions consistent with lipid raft partitioning (Figure 2.8B).

The potato sucrose transporter StSUT1 partitions to a DRM fraction of the membrane. Immunoprecipitation of StSUT1 from potato tissue co-immunoprecipitated over 40 associated proteins [30]. This broad array of interactions is thought to result from co-localization to the DRM fraction. In other words, immunoprecipitating a raft-localized protein can pull down the membrane microdomain and all of their associated proteins. Similarly, the co-immunoprecipitation of CCI1 with CLV signaling components could result from their co-localization to DRMs and not necessarily from direct protein-protein interactions. To test this hypothesis, co-IP experiments were performed on both total membrane and DRM-depleted soluble membrane fractions from *N. benthamiana* co-expressing CCI1-FLAG and CRN-GFP, as well as CCI1-FLAG and BAM2-GFP. When the DRM fraction was removed from the membrane fraction, the CCI1/BAM2 interaction was still detectable while the CCI1/CRN interaction was not (Figure 2.8C). This suggests the interaction between CCI1

and CRN depends on co-localization to the DRM and does not necessarily reflect a direct protein-protein interaction.

Genetic analysis of CCI1 function

We have characterized all three available alleles for At5g65480 (Figure 2.9). *cci1-1* is a JIC SM line (GT_5_40258), which contains an enhancer/suppressor-mutator mobile element inserted into At5g65480 [31]. The insertion in *cci1-1* is located 33bp after the start ATG; however, RT-PCR analysis readily detected transcripts from the downstream portion of the gene (Figure 2.10). Sequencing the insertion junction revealed that the insertion created an in-frame methionine, leading to a potentially functional gene product (Figure 2.11). Thus, we conclude that *cci1-1* is not a null allele and may not be hypomorphic. *cci1-1* plants lack any identifiable mutant phenotype. *cci1-2* (GABI_541D11) is a GABI-KAT line with the T-DNA inserted near the end of the first exon, interrupting the 124th codon, leaving intact the phospholipid binding domain and the conserved domain in the C-terminal portion [32]. *cci1-2* homozygous mutant plants had no identifiable phenotype. *cci1-3* (GABI_102G06) is also a GABI-KAT line inserted into the intron between the first and second exons. Homozygous *cci1-3* plants could not be identified in segregating populations from heterozygous parent plants. Sequencing the right border of the T-DNA insertion indicated centromeric satellite sequences, suggesting a possible chromosomal aberration. Analysis of progeny of *cci1-3*

heterozygotes indicated a 1:1 ratio of wild-type to heterozygous plants (32:30), consistent with lethality due to chromosomal abnormalities. To test this hypothesis, reciprocal crosses were performed between wild-type and *cci1-3* heterozygous plants. Among the F1 progeny, we observed transmission of the *cci1-3* allele through both the male and female gametes. Thus, the failure to observe *cci1-3* homozygous progeny is readily explained by the chromosomal rearrangement associated with the T-DNA insertion, although we cannot rule out the possibility that the *cci1-3* homozygous plants are inviable due to the loss of *CCI1* function.

DISCUSSION

In this study, we have identified CCI1, a novel CLV1 and BAM1 interacting partner. CCI1 localized to membranes apparently as a result of phospholipid binding activity. CCI1 partitioned to the plasma membrane, where a significant portion was detected in detergent-resistant microdomains. Consistent with this, CLV signaling components also partitioned to lipid rafts in Arabidopsis. CCI1 not only co-immunoprecipitated with CLV1 and BAM1, but also with other CLV pathway components in a manner dependent on co-localization to the DRM, suggesting a role for CCI1 in signaling complexes located in membrane microdomains.

CCI1 is the first protein identified to interact with both the CLV1 and BAM1 kinase domains. CCI1 is a protein with no identifiable domains or motifs.

Because prediction programs do not identify any transmembrane domains or lipid modification sites within CCI1, it is likely that the phospholipid binding activity of CCI1 is responsible for its localization. Other studies have shown polybasic regions are sufficient for PIP binding and plasma membrane localization [24]. For example, the C2 domain binds to PIPs by forming a positively charged pocket that interacts with the negatively charged inositol head group [33]. Interestingly, CCI1 has a very similar *in vitro* binding profile as the C2 domain of yeast Rsp5p, which is sufficient to drive membrane association [34]. The CCI1 N-terminal PIP-binding domain contains several such basic-rich regions. Although deletion constructs were unable to abolish phospholipid binding activity, it is possible that the multiple, positively charged basic rich regions contribute to electrostatic interactions with the negatively charged phosphate groups.

Full-length CCI1 binds to all three PI-monophosphates and PI(3,5)P_2. In plant cells, PI(3)P is found in endosomal compartments, as well as prevacuolar vesicles and vacuolar membranes as demonstrated by the localization of the FYVE domain which binds specifically to PI(3)P [35]. Using the PH domain as a marker, PI(4)P was found in pools at the plasma membrane and in the Golgi [36]. ATX1, an Arabidopsis chromatin modifying protein with a PHD domain conferring high specificity for PI(5)P, is found in several subcellular compartments showing plasma membrane, cytosolic/perinuclear, and nuclear localization. ATX1 nuclear localization is diminished and becomes more cytosolic upon exogenous PI(5)P addition, suggesting ATX1 localization responds to external stimuli as PI(5)P levels fluctuate in response to osmotic stress [37]. As with PI(5)P, PI(3,5)P_2

levels are also affected by osmotic stress, although the specific role $PI(3,5)P_2$ plays is unclear [38]. It has been implicated in vacuolar rearrangement in pollen grain development in Arabidopsis as mutations in PIKfyve/Fab1 proteins, which synthesize $PI(3,5)P_2$ from PI(3)P, result in abnormally large vacuoles in developing pollen grains [39]. In yeast cells, $PI(3,5)P_2$ is involved in protein trafficking and movement through endolysosomes [40]. Because PI(4)P is the only phosphatidylinositol isomer CCI1 binds that is found at significant concentration at the plasma membrane, this is likely to be the PIP CCI1 is binding *in vivo*. PI(4)P is the most abundant phosphatidylinositol monosphosphate found in plants [41]. PI(4)P is important for $PI(4,5)P_2$ synthesis, serving as the substrate for PI(4)P 5-kinase. In plants, $PI(4,5)P_2$ accumulates at much lower levels compared to animals because of product inhibition of the PI(4)P 5-kinase [42]. PI(4)P has been described as important for polarized membrane trafficking in pollen, root hair elongation, membrane formation in autophagy and establishment of cell polarity [43-45]. The POL/PLL1 phosphatases, which act as CLV signaling intermediates, are also plasma-membrane localized and bind PI(4)P, suggesting an important regulatory role for this phospholipid.

The DRM partitioning of CCI1 could be driven by its PI-binding activity and/or protei-proteinn interactions. DRMs are enriched in sphingolipids, sterols, GPI-anchored proteins and glycerophospholipids, including PIPs, compared to the plasma membrane as a whole [46]. DRMs isolated from *Nicotiana tabacum* plasma membrane are enriched for PIPs when compared to total plasma

membrane fractions [29]. Although PI(4)P is found in both plasma membrane and Golgi pools, CCI1 is only detectable in the plasma membrane fraction. In addition, CCI1 is found in both the soluble membrane and the detergent-insoluble membrane fractions. This suggests that CCI1 has specificity determinates beyond simply PI(4)P. In addition, CCI1 may traffic between microdomains of the plasma membrane.

Cells use these raft microdomains in pathogen response and protein trafficking, and they are the site of signaling hubs in the plasma membrane. Lipid rafts can both concentrate signaling components while at the same time insulating the raft members from negative signaling regulators such as phosphatases [25]. Signal transduction pathways utilizing membrane rafts have been well-characterized in animal immune response and G-protein signaling [25,47]. Membrane rafts in plants are enriched in proteins associated with signaling including LRR receptor kinases [48]. Auxin signaling and redox systems in membrane rafts in plants have also been characterized [49,50].

Although the specifics of lipid rafts are still being heavily studied, what is clear is that lipid rafts are vital for many signal transduction pathways. There are several overlapping models of the role of lipid rafts in signal transduction [25]. In the first, receptors are pre-assembled into signaling complexes in rafts where they are primed for ligand binding and signaling. In the second, ligand binding leads to mobilization of the receptors and the recruitment of signal transduction components into the lipid raft microdomain to build the signaling complex. Recruitment of proteins with affinity for lipid rafts can trigger the coalescence of a

larger lipid raft and signal transduction hub as in the case of cholera toxin binding to its receptor GM1 [51]. In T-cell receptor signaling, the lipid raft-localized Src tyrosine kinase, Lck, is responsible for transducing the T-cell receptor cascade. A mutant of Lck lacking lipid raft localization is unable to phosphorylate the T-cell receptor and trigger the T-cell receptor response [52]. Annexin is a PIP-binding protein with preference for $PI(4,5)P_2$ and has been identified in $PI(4,5)P_2$ clustering and membrane microdomain organization in giant unimellar vesicles [53]. Another proposed role for lipid rafts is in plasma membrane protein turnover [54].

Targeting to raft microdomains is poorly understood. Double-acylation is an indication of raft targeting; however, relatively short stretches of amino acids have also been implicated in lipid-raft targeting [55]. The CD4 receptor localizes to lipid rafts, yet this localization is abolished by alanine substitution of a basic-rich, positively charged RHRRR motif. Its raft localization is not dependent on glycosylation, palmitoylation or the transmembrane domain [56]. In another example, the lipid raft localization of the tyrosine phosphatases SHP-1 involved in T-cell response is conferred by the 6 amino acid stretch SKHKED. The PI(4)P binding activity of SHP-1 is also dependent on this motif, implicating PI(4)P binding in raft partitioning [57].

Supporting a physiological role for CCI1 in meristem homeostasis, expression profile mapping of the SAM niche identifies CCI1 as differentially upregulated in cells of the central zone of the meristem, correlating with expression of CLV3 [58]. Additionally, microarray data confirmed by qRT-PCR

identified CCI1 as one of 49 genes isolated directly upregulated by WUS in a Dex-inducible system [59].

Although the specific physiological role of CCI1 remains unclear, we have presented evidence supporting DRM partitioning and possible lipid raft association for several CLV pathway components, including CCI1. In addition, CLE binding to CLV2, BAM and CLV1 extracellular domains can only be detected in DRM fractions, suggesting CLV signaling depends on receptor localization to membrane microdomains [11]. The expression profiling data previously published and the direct interaction of CCI1 with the partially raft-associated kinases CLV1 and BAM1 combined with the co-immunoprecipitation of CCI1 with DRM-associated proteins suggest a role for CCI1 in lipid-raft based signal transduction in the shoot meristem.

METHODS

Lipid Binding

Sequences encoding CCI1, CCI2 and the last 70 amino acids of CCI1 (C-term CCI1) were amplified from cDNA and inserted into pGEX5X-1 with BamHI and NotI sites. The sequence encoding the first 83 amino acids of CCI1 (N-term CCI1) was inserted using BamHI and SalI sites. The N-terminus GST fusion proteins were expressed in *E. coli* protein expression strain BL21 CodonPlus (Stratagene). The GST-hFAPP expression construct was kindly provided by Erik

Nielsen. The expressed proteins were purified using glutathione sepharose (GE Healthcare).

PIP strips and membrane lipid strips were obtained from Echelon Biosciences. The strips were blocked with 3% fatty acid free BSA in PBS-T for 1 hour at room temperature. The expressed proteins were incubated with the blots at a concentration of 1nM for 1 hour at room temperature. Lipid-protein interactions were detected using a 1:10,000 dilution of an anti-GST HRP-conjugated antibody (Genscript).

For deletion construct blots, nitrocellulose membrane was blotted with PI(4)P and PE from Echelon biosciences.

Co-immunoprecipitation and fractionation of transiently expressed and Arabidopsis proteins

Binary vectors containing 35S:BRI1, CLV1, BAM1, BAM2, CLV2, CRN C-terminal GFP and CLV1 and BAM1 C-terminal fusion constructs, as well as BAM1-FLAG, BAM2-FLAG and CLV2-MYC have been previously described [6,11,58]. CCI1-GFP was generated by replacement of the CLV1 coding sequence in the 35S:CLV1-GFP construct. To generate the 35S:FLAG-CCI1 cassette, the CCI1 coding sequence was amplified and cloned into pENTR/D-TOPO to create entry vectors for subcloning into pEarleyGate 202 via LR clonase reaction.

For transient expression, binary vector constructs were transformed into *Agrobacterium tumefaciens* strain GV3101 and infiltrated along with P19, a viral silencing suppressor [18], into *Nicotiana benthamiana* leaves. After 48 hours, proteins were extracted in buffer (50 mM Tris-HCl, 150 mM NaCl, 10 mM EDTA, 10% glycerol, 10 mM NaF, 10 mM NaVO3, 2% plant specific protease inhibitor cocktail (Sigma), 10 ug/ml chymostatin and 2 ug/ml aprotinin). For stable expression lines, 8-10 Arabidopsis meristems were used for protein extraction. Extracts were centrifuged twice at 5,000 *g* for 10 minutes at 4°C to remove flocculate. Supernatants were centrifuged at 100,000 *g* for 1 hour at 4°C to separate soluble microsomal fractions. The microsomal fractions were then solubilized using 1% Triton X-100 with gentle agitation at 4°C.

When immunoprecipitation was performed with anti-GFP antibodies, the antibody was incubated with the solubilized membrane fraction at 4°C for 2 hours, then protein A agarose was added and incubated for an additional two hours. When immunoprecipitation was performed with anti-FLAG antibodies, anti-FLAG M2-Agarose was incubated with the solubilized membrane fractions for 4 hours at 4°C. Agarose was pelleted at 100 *g*, washed three times, and boiled in SDS buffer containing β-ME.

Sucrose Gradients

Tissue from 10 apices each of BAM1-FLAG, BAM2-FLAG, CLV1-GFP, and CLV2-myc were collected, placed in tubes containing 200 µL of detergent-

and glycerol-free extraction buffer (50 mM Tris pH 8.0, 10 mM EDTA, 100 mM NaCl, 5% protease inhibitor cocktail [Sigma, P9599]) on ice, and homogenized as previously described [6]. Homogenized tissue was centrifuged at 2400 *g* for 10 minutes at 4°C. The supernatants were pooled and centrifuged again at 2400 *g* for 10 minutes at 4°C. SDS sample buffer was added to a portion of the supernatant and boiled for 5 minutes. The remaining supernatant was centrifuged at 100,000 *g* for 1 hour at 4°C. SDS sample buffer was added to the 100,000 *g* supernatant and boiled for 5 minutes. The 100,000 *g* pellet was washed with extraction buffer, then resuspended in extraction buffer with 1% Triton X-100 and incubated on ice for 30 minutes and mixed by briefly vortexing every 10 minutes. Sucrose was added to 1.8 M, bringing the volume to 500 µL. Equal volumes of 1.6 M, 1.4 M, and 0.15 M sucrose solutions were layered on top of the 1.8 M sucrose layer containing the isolated detergent resistant membranes. This sucrose step gradient was centrifuged at 100,000 *g* for 15 hours at 4°C. 250 µL fractions were collected from top down (least dense to most dense) and diluted 14-fold with detergent and glycerol-free extraction buffer. Samples were centrifuged at 100,000 *g* for 2 hours at 4°C. The pellet from each fraction was resuspended in extraction buffer with 0.1% Triton X-100 and the samples were boiled for 5 minutes.

Two-phase Partitioning

The membrane fraction from tobacco leaves transiently expressing FLAG-CCI1 was isolated as described above and resuspended in microsome resuspension buffer containing 330 mM sucrose, 2 mM DTT, 5 mM KH_2PO_4, 10 mM EDTA, 10 mM NaF, 10 mM $NaVO_3$, 2% plant specific protease inhibitor cocktail (Sigma), 10 ug/ml chymostatin and 2 ug/ml aprotinin, pH 7.8. The plasma membrane fraction was extracted using PEG-dextran phases containing 6.4% (w/w) PEG 3350 and 6.4% dextran (w/w) [21]. Antibodies against plasma membrane marker PMA2 [59] and endoplasmic reticulum marker BiP2 (SPA-818; Stressgen) were used as controls.

E. coli expressed protein co-immunoprecipitation

The coding sequence for the CLV1 kinase domain and C-terminal GFP tag was cloned into pDEST42 and expressed in BL21 codon plus cells. Soluble sonicate from GST-CCI1 or GST-CCI2 and CLV1 KD-GFP were combined, then incubated with glutathione sepharose (GE Healthcare) 30 minutes at room temperature. The sepharose was washed 3 times and eluted. The co-immunoprecipitation was detected with anti-GFP ab6556 (Abcam).

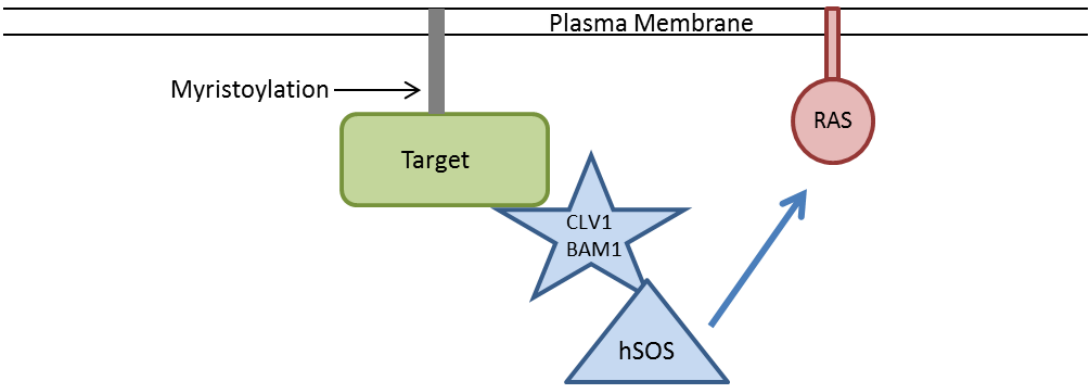

Figure 2.1 The Cytotrap system

The Cytotrap system uses a temperature sensitive mutant in the yeast Ras pathway activator homologue of hSos. In a protein-protein interaction, hSOS is recruited to the plasma membrane to activate the RAS pathway.

Figure 2.2 Alignment of CCI1-related proteins from land plants

An alignment of *Arabidopsis thaliana* CCI1, CCI2 and related proteins from various plant species is shown. Conserved residues are shaded at 75%. Basic-rich regions are underlined. The top and bottom segments of CCI1 sequence correspond to the N and C-terminal half constructs used in the lipid-binding assays. Alignment was performed with ClustalW using the BLOSUM scoring matrix. Identitical residues are shaded black, similar residues are shaded grey. Accession numbers: CCI1- NP_201351, CCI2- NP_195519, *G. max*- XP_003517377, O. sativa- NP_001061802, P. trichocarpa- XP_002301098, *R. communis*- XP_002534923, *S. bicolor*- XP_002444327, *V. vinifera*- XP_003635478, *Z. mays*- NP_001143419, *T. aestivum*- 25547580

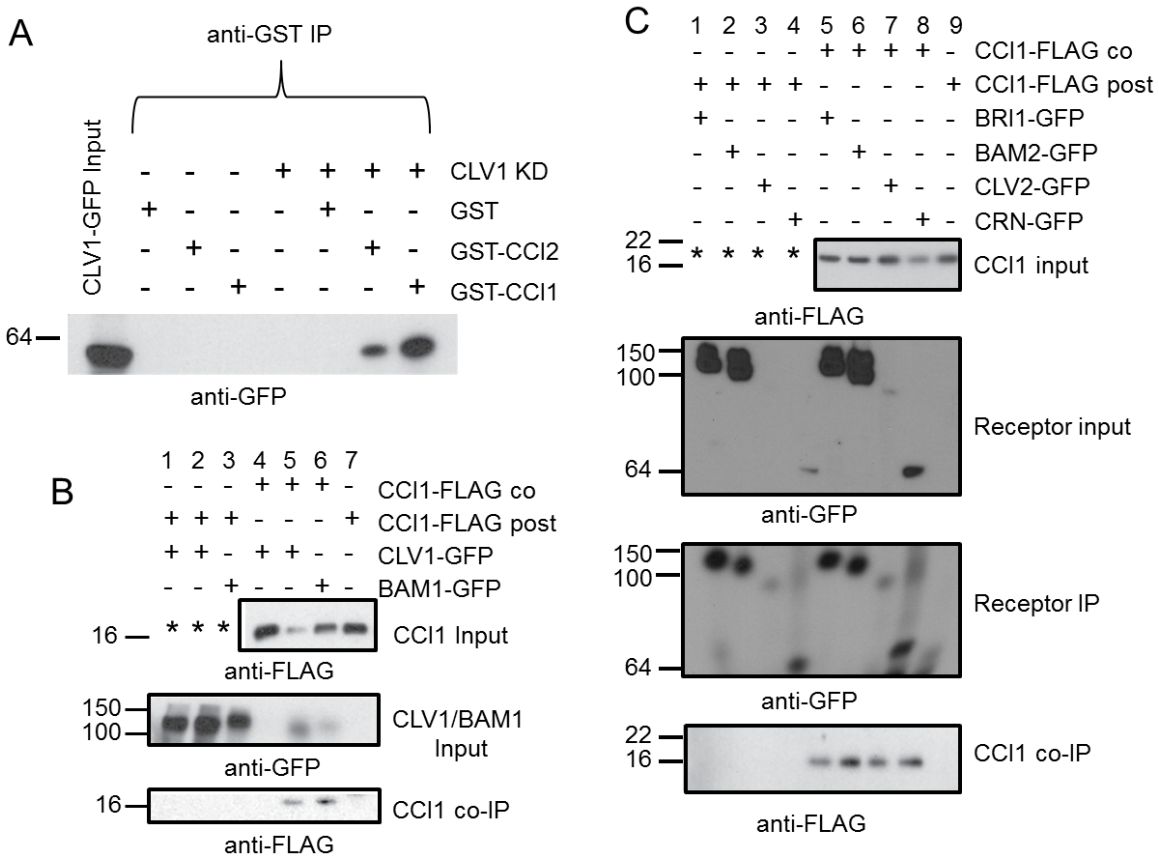
A
anti-GST IP
CLV1-GFP Input
CLV1 KD
GST
GST-CCI2
GST-CCI1
64
anti-GFP
B
1 2 3 4 5 6 7
CCI1-FLAG co
CCI1-FLAG post
CLV1-GFP
BAM1-GFP
16
CCI1 Input
anti-FLAG
150
100
CLV1/BAM1
Input
anti-GFP
16
CCI1 co-IP
anti-FLAG
C
1 2 3 4 5 6 7 8 9
CCI1-FLAG co
CCI1-FLAG post
BRI1-GFP
BAM2-GFP
CLV2-GFP
CRN-GFP
22
16
CCI1 input
anti-FLAG
150
100
64
Receptor input
anti-GFP
150
100
64
Receptor IP
anti-GFP
22
16
CCI1 co-IP
anti-FLAG

Figure 2.3 CCI1 interactions with CLV signaling components *in vitro* and in transient expression

A. Purified CLV1KD-GFP, GST, GST-CCI1 and GST-CCI2 proteins were mixed in various combinations, immunoprecipitated (IPd) with anti-GST antibodies, and the resulting immunoprecipitates were assayed on a protein gel blot probed with anti-GFP. The first lane shows CLV1KD-GFP input.

B. Total membrane extracts from *N. benthamiana* leaves expressing CCI1-FLAG and full-length CLV1-GFP and BAM1-GFP IPd with anti-GFP antibodies and co-IP detected with anti-FLAG antibodies. Lanes 1, 2 and lanes 4, 5 are replicates. Note, CLV1-GFP did not express detectably in the lane 4 replicate, nor was there co-IP detected. Experiments represented by lanes 1-3 used an aliquot from the lane 7 expression of CCI1-FLAG alone (*). Co-IP was detected when both CCI1 and BAM1 were co-expressed in the same leaf (CCI1 co), but not when mixed post expression (CCI1 post).

C. Total membrane extracts from *N. benthamiana* leaves expressing CCI1-FLAG and full-length BRI1-GFP, BAM2-GFP, CLV2-GFP and CRN-GFP IPd with anti-GFP antibodies and co-IP detected with anti-FLAG antibodies. Experiments represented by lanes 1-4 used an aliquot from the lane 9 expression of CCI1-FLAG alone (*). CoIP was detected when CCI1 and the receptors were co-expressed in the same leaf (CCI1 co), but not when mixed post expression (CCI1 post).

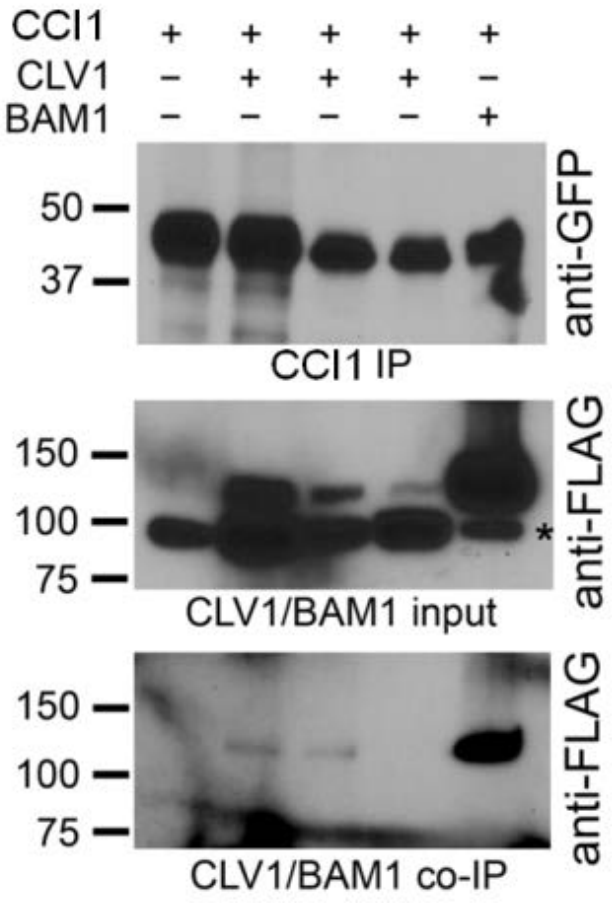

Figure 2.4 CCI1 CLV1 and BAM1 co-IP

Solubilized membrane extracts from *N. benthamiana* leaves expressing CCI1-GFP and full-length BAM1-FLAG and CLV1-FLAG (three replicates in lanes 2-4) IPd with anti-GFP antibody and co-IP detected with anti-FLAG antibody.

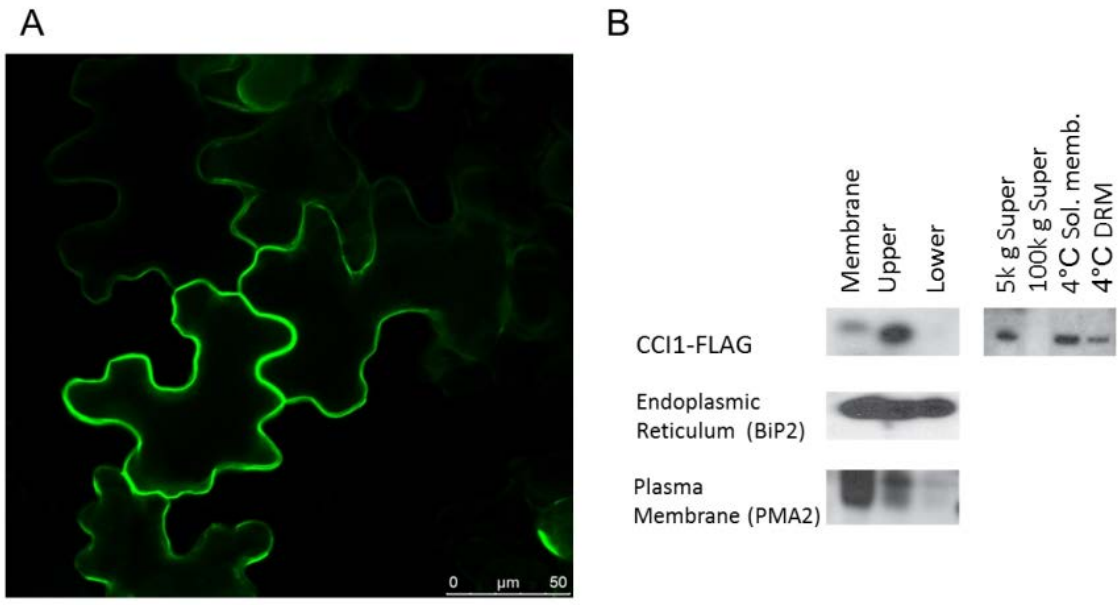

Figure 2.5 CCI1 is plasma membrane localized.

A. Confocal image of CCI1-GFP transiently expressed in *N. benthamiana* leaves 48 hours after infiltration. Signal is detected at the cell periphery.

B. Membrane partitioning of CCI1-FLAG transiently expressed in *N. benthamiana* leaves. Endoplasmic reticulum marker BiP2 and plasma membrane marker PMA2 are used to mark the lower and upper phases, respectively.

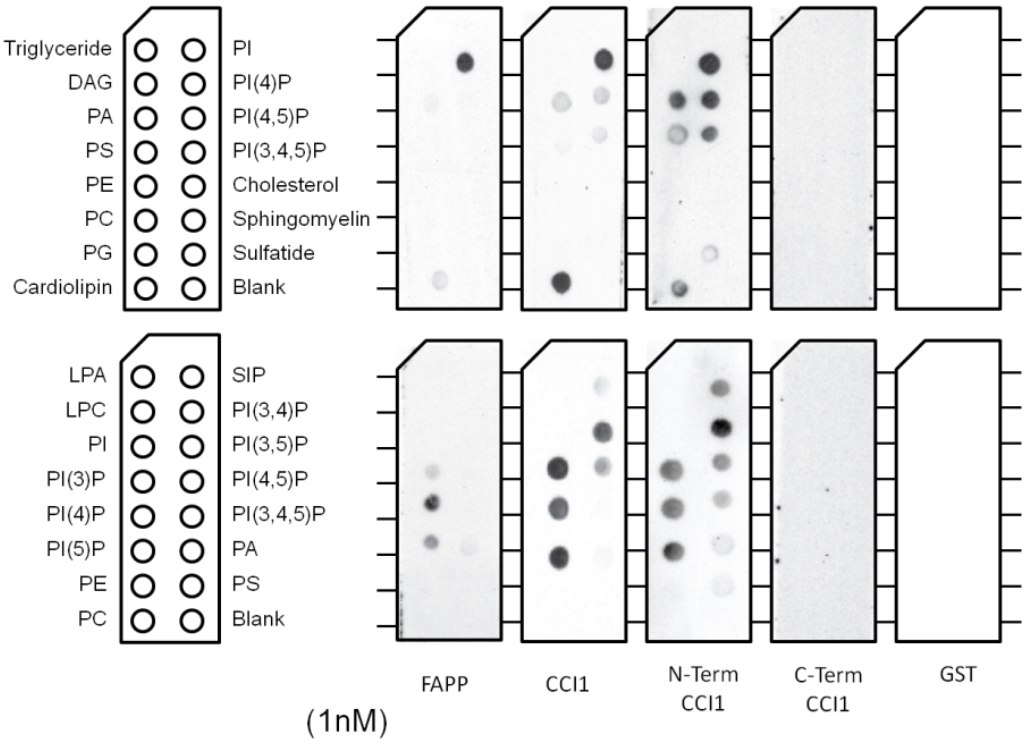

Figure 2.6 The N-terminal portion of CCI1 binds phospholipids.

Echelon membrane lipid strips and PIP strips probed with purified N-terminal GST tagged proteins at a concentration of 1nM. The PH domain of the human FAPP protein which specifically binds PI(4)P was used as a positive control. The GST tag alone was used as a negative control. N-terminal CCI1 corresponds to the first 83 amino acids of the protein and C-terminal CCI1 corresponds to the remaining 70 (see Figure 2.1).

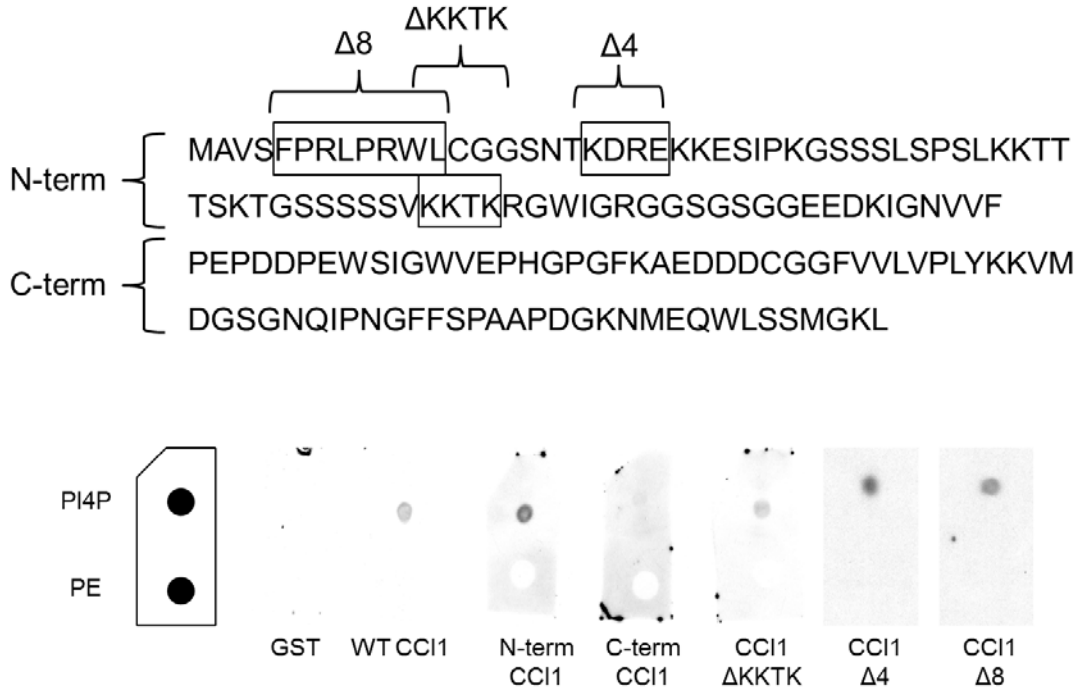

Figure 2.7 CCI1 deletion construct lipid binding.

Deletion of several regions of N-terminal CCI1 did not abolish lipid binding activity.

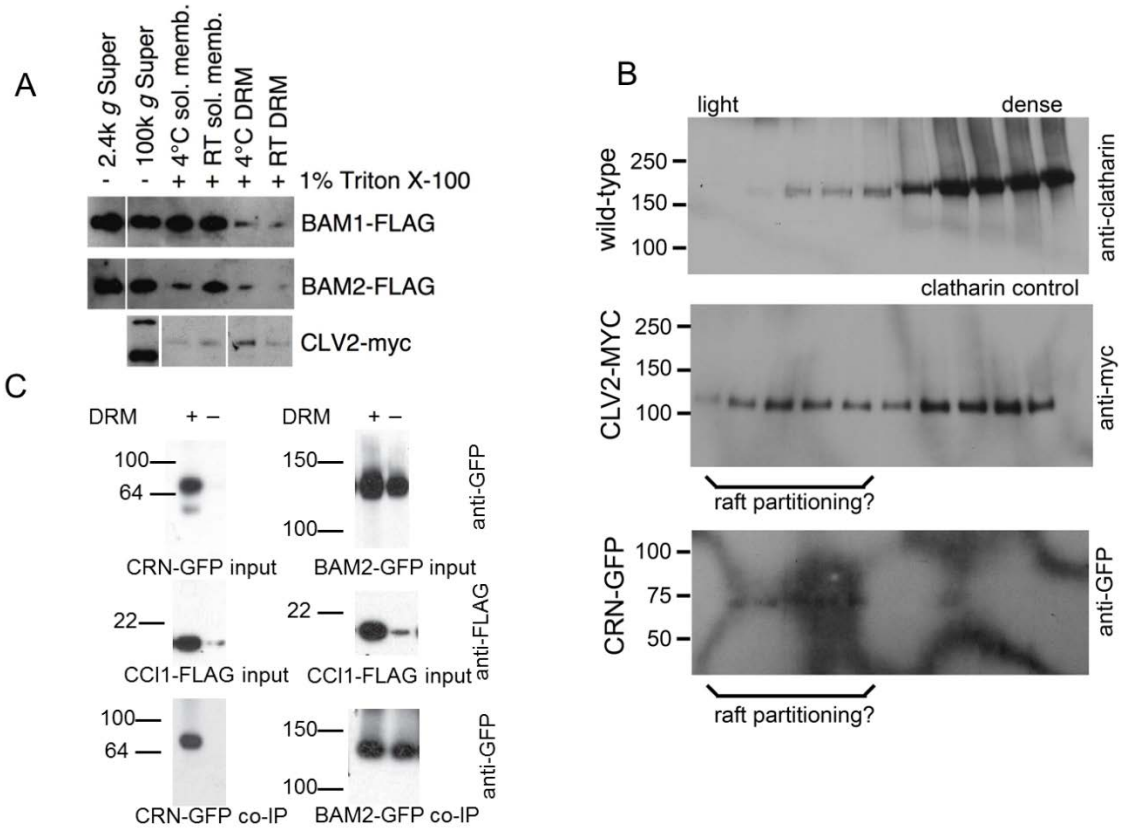

Figure 2.8 CLV pathway components partition to DRM/raft fractions.

A. Partitioning of BAM1-FLAG, BAM2-FLAG and CLV2-MYC proteins in stable Arabidopsis transgenic lines into soluble membrane and DRM fractions is shown.

B. Sucrose gradient sedimentation of solubilized membrane extracts of clatharin (as a control), CLV2-MYC and CRN-GFP from stable transgenic Arabidopsis meristem tissue. Lipid-associated proteins will float to the lighter fractions.

C. Co-IP of transiently expressed BAM2-GFP and CCI1-FLAG was detected in both total membrane fraction (+) and membrane fraction after DRM depletion (-). Co-IP of transiently expressed CRN-GFP and CCI1-FLAG depended on the presence of DRMs.

Panels A and B courtesy of Brody DeYoung and Linqu Han, respectively.

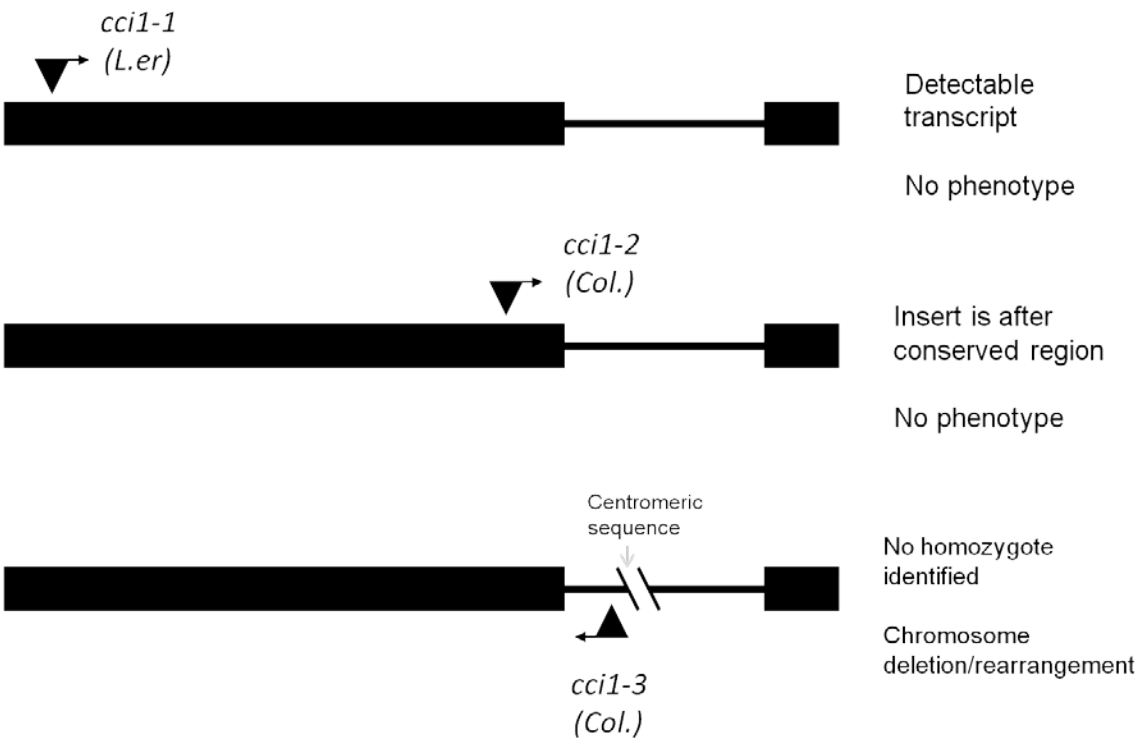

Figure 2.9 Three insertional lines of *CCI1*

Three insertional alleles for *CCI1* are diagramed. *cci1-1* is a JIC SM transposon line. *cci1-2* and *cci1-3* are GABI KAT T-DNA lines.

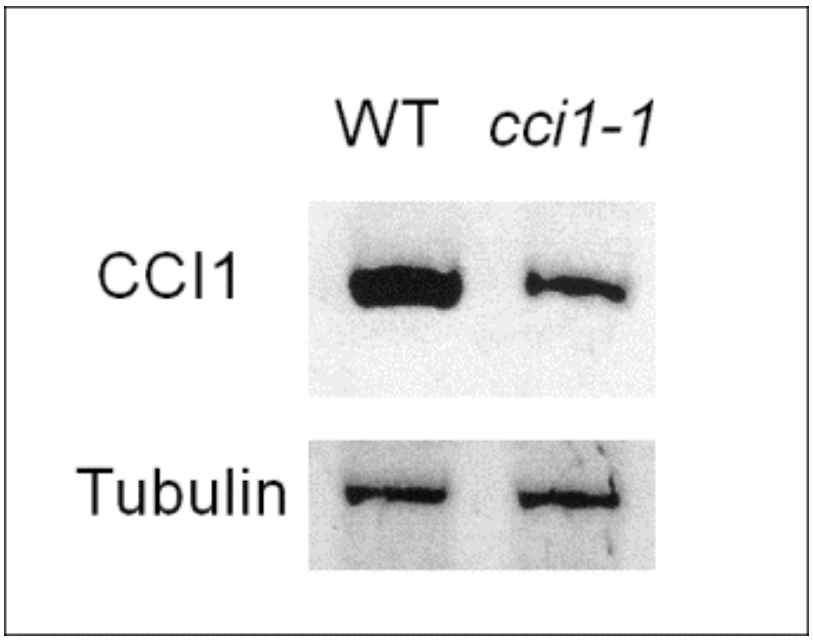

Figure 2.10 *CCI1* transcript detectable in *cci1-1.*

Reverse transcriptase PCR detected CCI1 transcript in the *cci1-1* allele. Tubulin was used as a control.

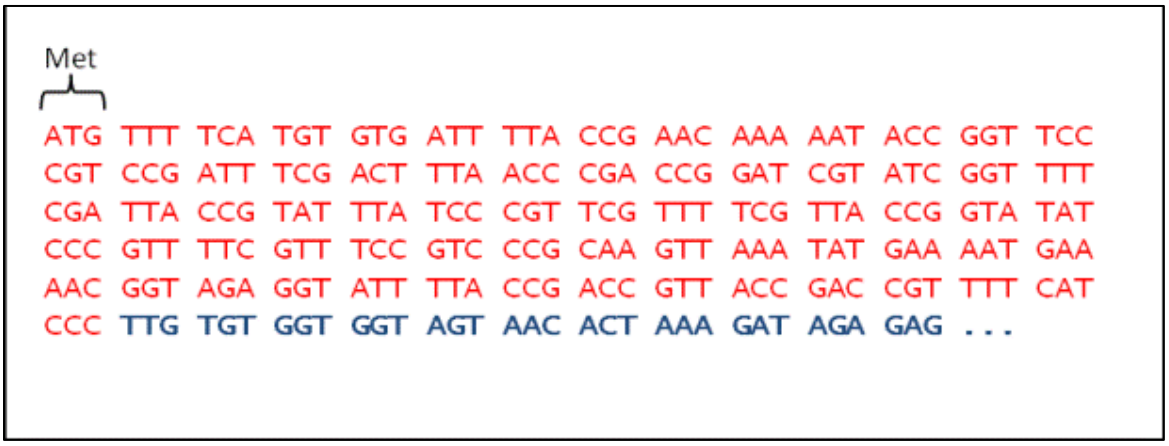

Figure 2.11 The *cci1-1* insertion allele in-frame methionine

The *cci1-1* insertion allele contains an upstream in-frame methionine. The junction of insertion sequence and CCI1 coding sequence leads to an intact ORF. *CCI1* coding sequence is in blue. Ds insertion sequence is in red.

Table 2.1 Positives from Cytotrap protein-protein interaction screen with the BAM1 kinase domain.

clones	Locus Tag	Description
5	AT5G38420	ribulose bisphosphate carboxylase small chain 2B
5	AT5G65480	CCI1
4	AT1G20823	RING-H2 finger protein ATL80
4	AT4G34870	Peptidyl-prolyl cis-trans isomerase CYP18-4
3	AT1G49970	ATP-dependent Clp protease proteolytic subunit-related protein 1
3	AT1G52230	photosystem I reaction center subunit VI-2
3	AT2G05100	photosystem II light harvesting complex protein 2.
3	AT4G09160	patellin-5
3	AT5G48480	Lactoylglutathione lyase / glyoxalase I-like protein
3	AT5G59310	non-specific lipid-transfer protein 4
2	AT1G31330	photosystem I reaction center subunit III
1	AT1G07940	elongation factor 1-alpha
1	AT1G09140	ATSRP30 splicing factor
1	AT1G21830	hypothetical protein
1	AT1G55540	emb1011 Nuclear pore complex protein
1	*AT2G39730*	ribulose bisphosphate carboxylase/oxygenase activase
1	AT3G02690	nodulin MtN21 /EamA-like transporter protein
1	AT3G05900	neurofilament protein-related protein
1	AT3G08580	ADP,ATP carrier protein 1
1	AT3G19820	DWF1 cell elongation protein DIMINUTO
1	AT3G53430	60S ribosomal protein L12-2
1	AT4G25050	ACP4 acyl carrier protein 4
1	AT5G17920	5-methyltetrahydropteroyltriglutamate--homocysteine methyltransferase
1	AT5G46550	DNA-binding bromodomain-containing protein
1	AT5G54270	LHCB3 light-harvesting chlorophyll B-binding protein 3

Table 2.2 Positives from Cytotrap protein-protein interaction screen with the CLV1 kinase domain.

clones	Locus tag	Description
7	AT1G08200	UDP-apiose/xylose synthase
4	AT5G17770	cytochrome-b5 reductase
4	AT5G65480	CCI1
3	AT1G13440	glyceraldehyde 3-phosphate dehydrogenase
2	AT2G27020	proteasome subunit alpha type-3
2	AT2G41090	calmodulin-like protein 10
2	AT4G29040	26S proteasome regulatory subunit 4-A
1	AT1G21460	Nodulin MtN3-like protein
1	AT1G29930	chlorophyll a-b binding protein 1
1	AT2G07340	prefoldin 1
1	AT2G38450	hypothetical protein
1	AT4G28750	photosystem I reaction center subunit IV A
1	AT4G38770	proline-rich protein 4
1	AT5G48480	Lactoylglutathione lyase / glyoxalase I-like protein
1	AT5G51545	LPA2 low psii accumulation2 protein

References

1. Steeves TA, Sussex IM (1989) Patterns in Plant Development. New York: Cambridge University Press.

2. Mayer KF, Schoof H, Haecker A, Lenhard M, Jurgens G, et al. (1998) Role of *WUSCHEL* in regulating stem cell fate in the *Arabidopsis* shoot meristem. Cell 95: 805-815.

3. Yadav RK, Perales M, Gruel J, Girke T, Jonsson H, et al. (2011) WUSCHEL protein movement mediates stem cell homeostasis in the Arabidopsis shoot apex. Genes Dev 25: 2025-2030.

4. Yadav RK, Tavakkoli M, Reddy GV (2010) WUSCHEL mediates stem cell homeostasis by regulating stem cell number and patterns of cell division and differentiation of stem cell progenitors. Development 137: 3581-3589.

5. Schoof H, Lenhard M, Haecker A, Mayer KF, Jurgens G, et al. (2000) The stem cell population of *Arabidopsis* shoot meristems in maintained by a regulatory loop between the *CLAVATA* and *WUSCHEL* genes. Cell 100: 635-644.

6. DeYoung BJ, Bickle KL, Schrage KJ, Muskett P, Patel K, et al. (2006) The CLAVATA1-related BAM1, BAM2 and BAM3 receptor kinase-like proteins are required for meristem function in Arabidopsis. Plant J 45: 1-16.

7. DeYoung BJ, Clark SE (2008) BAM receptors regulate stem cell specification and organ development through complex interactions with CLAVATA signaling. Genetics 180: 895-904.

8. Hord CL, Chen C, Deyoung BJ, Clark SE, Ma H (2006) The BAM1/BAM2 receptor-like kinases are important regulators of Arabidopsis early anther development. Plant Cell 18: 1667-1680.

9. Bleckmann A, Weidtkamp-Peters S, Seidel CA, Simon R (2010) Stem cell signaling in Arabidopsis requires CRN to localize CLV2 to the plasma membrane. Plant Physiol 152: 166-176.

10. Zhu Y, Wang Y, Li R, Song X, Wang Q, et al. (2010) Analysis of interactions among the CLAVATA3 receptors reveals a direct interaction between CLAVATA2 and CORYNE in Arabidopsis. Plant J 61: 223-233.

11. Guo Y, Han L, Hymes M, Denver R, Clark SE (2010) CLAVATA2 forms a distinct CLE-binding receptor complex regulating Arabidopsis stem cell specification. Plant J 63: 899-900.

12. Ogawa M, Shinohara H, Sakagami Y, Matsubayashi Y (2008) Arabidopsis CLV3 peptide directly binds CLV1 ectodomain. Science 319: 294.

13. Yu LP, Simon EJ, Trotochaud AE, Clark SE (2000) *POLTERGEIST* functions to regulate meristem development downstream of the *CLAVATA* loci. Development 127: 1661-1670.

14. Song SK, Clark SE (2005) POL and related phosphatases are dosage-sensitive regulators of meristem and organ development in Arabidopsis. Dev Biol 285: 272-284.

15. Song SK, Lee MM, Clark SE (2006) POL and PLL1 phosphatases are CLAVATA1 signaling intermediates required for Arabidopsis shoot and floral stem cells. Development 133: 4691-4698.

16. Gagne JM, Clark SE (2010) The Arabidopsis stem sell factor POLTERGEIST is membrane localized and phospholipid stimulated. Plant Cell 22: 729-743.

17. Aronheim A, Zandi E, Hennemann H, Elledge SJ, Karin M (1997) Isolation of an AP-1 repressor by a novel method for detecting protein-protein interactions. Mol Cell Biol 17: 3094-3102.

18. Voinnet O, Rivas S, Mestre P, Baulcombe D (2003) An enhanced transient expression system in plants based on suppression of gene silencing by the p19 protein of tomato bushy stunt virus. Plant J 33: 949-956.

19. Guo Y, Clark SE (2010) Membrane distributions of two ligand-binding receptor complexes in the CLAVATA pathway. Plant Signal Behav 5: 1442-1445.

20. Nimchuk ZL, Tarr PT, Ohno C, Qu X, Meyerowitz EM (2011) Plant stem cell signaling involves ligand-dependent trafficking of the CLAVATA1 receptor kinase. Curr Biol 21: 345-352.

21. Marmagne A, Salvi D, Rolland N, Ephritikhine G, Joyard J, et al. (2006) Purification and fractionation of membranes for proteomic analyses. Methods Mol Biol 323: 403-420.

22. Santagata S, Boggon TJ, Baird CL, Gomez CA, Zhao J, et al. (2001) G-protein signaling through tubby proteins. Science 292: 2041-2050.

23. Dowler S, Currie RA, Campbell DG, Deak M, Kular G, et al. (2000) Identification of pleckstrin-homology-domain-containing proteins with novel phosphoinositide-binding specificities. Biochem J 351: 19-31.

24. Heo WD, Inoue T, Park WS, Kim ML, Park BO, et al. (2006) PI(3,4,5)P3 and PI(4,5)P2 lipids target proteins with polybasic clusters to the plasma membrane. Science 314: 1458-1461.

25. Simons K, Toomre D (2000) Lipid rafts and signal transduction. Nat Rev Mol Cell Biol 1: 31-39.

26. Brown DA, London E (1998) Functions of lipid rafts in biological membranes. Annu Rev Cell Dev Biol 14: 111-136.

27. Brown DA (2006) Lipid rafts, detergent-resistant membranes, and raft targeting signals. Physiology (Bethesda) 21: 430-439.

28. Borner GH, Sherrier DJ, Weimar T, Michaelson LV, Hawkins ND, et al. (2005) Analysis of detergent-resistant membranes in Arabidopsis. Evidence for plasma membrane lipid rafts. Plant Physiol 137: 104-116.

29. Furt F, Konig S, Bessoule JJ, Sargueil F, Zallot R, et al. (2010) Polyphosphoinositides are enriched in plant membrane rafts and form microdomains in the plasma membrane. Plant Physiol 152: 2173-2187.

30. Krugel U, He HX, Gier K, Reins J, Chincinska I, et al. (2012) The potato sucrose transporter StSUT1 interacts with a DRM-associated protein disulfide isomerase. Mol Plant 5: 43-62.

31. Tissier AF, Marillonnet S, Klimyuk V, Patel K, Torres MA, et al. (1999) Multiple Independent Defective *Suppressor-mutator* Transposon Insertions in Arabidopsis: A Tool for Functional Genomics. Plant Cell 11: 1841-1852.

32. Kleinboelting N, Huep G, Kloetgen A, Viehoever P, Weisshaar B (2012) GABI-Kat SimpleSearch: new features of the Arabidopsis thaliana T-DNA mutant database. Nucleic Acids Res 40: D1211-1215.

33. Premkumar L, Bobkov AA, Patel M, Jaroszewski L, Bankston LA, et al. Structural basis of membrane targeting by the Dock180 family of Rho family guanine exchange factors (Rho-GEFs). J Biol Chem 285: 13211-13222.

34. Dunn R, Klos DA, Adler AS, Hicke L (2004) The C2 domain of the Rsp5 ubiquitin ligase binds membrane phosphoinositides and directs ubiquitination of endosomal cargo. J Cell Biol 165: 135-144.

35. Vermeer JE, van Leeuwen W, Tobena-Santamaria R, Laxalt AM, Jones DR, et al. (2006) Visualization of PtdIns3P dynamics in living plant cells. Plant J 47: 687-700.

36. Vermeer JE, Thole JM, Goedhart J, Nielsen E, Munnik T, et al. (2009) Imaging phosphatidylinositol 4-phosphate dynamics in living plant cells. Plant J 57: 356-372.

37. Alvarez-Venegas R, Sadder M, Hlavacka A, Baluska F, Xia Y, et al. (2006) The Arabidopsis homolog of trithorax, ATX1, binds phosphatidylinositol 5-phosphate, and the two regulate a common set of target genes. Proc Natl Acad Sci U S A 103: 6049-6054.

38. Meijer HJ, Divecha, N, Van den Ende, H, Musgrave, A, Munnik, T (1999) Hyperosmotic stress induces rapid synthesis of phosphatidyl-D-inositol 3,5-bisphosphate in plant cells. Planta 208: 294-298.

39. Whitley P, Hinz S, Doughty J (2009) Arabidopsis FAB1/PIKfyve proteins are essential for development of viable pollen. Plant Physiol 151: 1812-1822.

40. Dove SK, Dong K, Kobayashi T, Williams FK, Michell RH (2009) Phosphatidylinositol 3,5-bisphosphate and Fab1p/PIKfyve underPPIn endo-lysosome function. Biochem J 419: 1-13.

41. Meijer HJ, Munnik T (2003) Phospholipid-based signaling in plants. Annu Rev Plant Biol 54: 265-306.

42. Perera IY, Davis AJ, Galanopoulou D, Im YJ, Boss WF (2005) Characterization and comparative analysis of Arabidopsis phosphatidylinositol phosphate 5-kinase 10 reveals differences in Arabidopsis and human phosphatidylinositol phosphate kinases. FEBS Lett 579: 3427-3432.

43. Yamashita S, Oku M, Wasada Y, Ano Y, Sakai Y (2006) PI4P-signaling pathway for the synthesis of a nascent membrane structure in selective autophagy. J Cell Biol 173: 709-717.

44. Hammond GR, Fischer MJ, Anderson KE, Holdich J, Koteci A, et al. (2012) PI4P and PI(4,5)P2 are essential but independent lipid determinants of membrane identity. Science 337: 727-730.

45. Thole JM, Nielsen E (2008) Phosphoinositides in plants: novel functions in membrane trafficking. Curr Opin Plant Biol 11: 620-631.

46. Peskan T, Westermann M, Oelmuller R (2000) Identification of low-density Triton X-100-insoluble plasma membrane microdomains in higher plants. Eur J Biochem 267: 6989-6995.

47. Ostrom RS, Insel PA (2004) The evolving role of lipid rafts and caveolae in G protein-coupled receptor signaling: implications for molecular pharmacology. Br J Pharmacol 143: 235-245.

48. Shahollari B, Peskan-Berghöfer T, Oelmüller R (2004) Receptor kinases with leucine-rich repeats are enriched in Triton X-100 insoluble plasma membrane microdomains from plants. Physiologia Plantarum 122: 397-403.

49. Titapiwatanakun B, Blakeslee JJ, Bandyopadhyay A, Yang H, Mravec J, et al. (2009) ABCB19/PGP19 stabilises PIN1 in membrane microdomains in Arabidopsis. Plant J 57: 27-44.

50. Furt F, Lefebvre B, Cullimore J, Bessoule JJ, Mongrand S (2007) Plant lipid rafts: fluctuat nec mergitur. Plant Signal Behav 2: 508-511.

51. Hammond AT, Heberle FA, Baumgart T, Holowka D, Baird B, et al. (2005) Crosslinking a lipid raft component triggers liquid ordered-liquid disordered phase separation in model plasma membranes. Proc Natl Acad Sci U S A 102: 6320-6325.

52. Kabouridis PS (2006) Lipid rafts in T cell receptor signalling. Mol Membr Biol 23: 49-57.

53. Gokhale NA, Abraham A, Digman MA, Gratton E, Cho W (2005) Phosphoinositide specificity of and mechanism of lipid domain formation by annexin A2-p11 heterotetramer. J Biol Chem 280: 42831-42840.

54. Grossmann G, Malinsky J, Stahlschmidt W, Loibl M, Weig-Meckl I, et al. (2008) Plasma membrane microdomains regulate turnover of transport proteins in yeast. J Cell Biol 183: 1075-1088.

55. Zaman SN, Resek ME, Robbins SM (2008) Dual acylation and lipid raft association of Src-family protein tyrosine kinases are required for SDF-1/CXCL12-mediated chemotaxis in the Jurkat human T cell lymphoma cell line. J Leukoc Biol 84: 1082-1091.

56. Popik W, Alce TM (2004) CD4 receptor localized to non-raft membrane microdomains supports HIV-1 entry. Identification of a novel raft localization marker in CD4. J Biol Chem 279: 704-712.

57. Sankarshanan M, Ma Z, Iype T, Lorenz U (2007) Identification of a novel lipid raft-targeting motif in Src homology 2-containing phosphatase 1. J Immunol 179: 483-490.

58. Yadav RK, Girke T, Pasala S, Xie M, Reddy GV (2009) Gene expression map of the Arabidopsis shoot apical meristem stem cell niche. Proc Natl Acad Sci U S A 106: 4941-4946.

59. Yadav RK, Perales M, Gruel J, Ohno C, Heisler M, et al. (2013) Plant stem cell maintenance involves direct transcriptional repression of differentiation program. Mol Syst Biol 9: 654.

60. Hong Z, Jin H, Tzfira T, Li J (2008) Multiple mechanism-mediated retention of a defective brassinosteroid receptor in the endoplasmic reticulum of Arabidopsis. Plant Cell 20: 3418-3429.

61. Morsomme P, Dambly S, Maudoux O, Boutry M (1998) Single point mutations distributed in 10 soluble and membrane regions of the Nicotiana plumbaginifolia plasma membrane PMA2 H+-ATPase activate the enzyme and modify the structure of the C-terminal region. J Biol Chem 273: 34837-34842.

Chapter Three

A novel mutation in the DNA contact helix of BELLRINGER leads to pleiotropic meristematic and flower defects

Abstract

The BELL class transcription factors together with members of the KNOX class transcription factors have been implicated in inflorescence patterning, meristem maintenance as well as in flower specification and floral organ identity. Mutations in BELL class gene *BELLRINGER* (*BLR*) cause defects in internode elongation leading to organ clustering. BLR related proteins have both overlapping and distinct functions. We have identified and characterized a mutation, *blr-7*, in the DNA contact helix III of the homeodomain of BLR. Plants harboring this mutation not only display organ clustering but also lack axillary meristem development. Additionally, aborted organs can be seen along the length of the inflorescence of *blr-7* plants. *blr-7* flowers form reduced number of organs and lack either carpels, petals, or, rarely, both. The stronger meristem phenotypes of *blr-7* compared to *blr* null alleles suggests that blr-7 protein is

dominantly interfering with interacting proteins. One candidate for a partner protein disrupted by *blr-7* protein is the KNOX-class transcription factor SHOOTMERISTEMLESS (STM), previous shown *in vitro* to bind DNA in complex with BLR. Loss of STM function mirrors the meristem loss in *blr-7*. Furthermore, genetic interactions of *blr-7* with mutants of the CLAVATA pathway are consistent with a loss of STM function. Using transient expression in *Nicotiana benthamiana*, I show that blr-7 retains the ability to interact with STM, facilitate STM nuclear import, but blocks STM binding to consensus DNA sequences. This suggests *blr-7* disrupts meristem development by loss of transcriptional targets for a complex of BLR and STM.

INTRODUCTION

Post-embryonic growth and development in plants is derived from stem cell populations known as meristems. Above-ground organs are derived from shoot meristems (SM). Stem cell populations within these meristems are homeostatically maintained by balancing proliferation and stem cell maintenance with differentiation of daughter cells. Mutations in the factors controlling meristem homeostasis leads to disruptions in stem cell populations and organogenesis.

WUSCHEL and SHOOTMERISTEMLESS are two homeodomain proteins known to be necessary for stem cell maintenance within the SM. WUS and STM function in two different pathways necessary for meristem regulation. WUS protein moves from the organizing center underlying the stem cells directly into the stem cells to specify stem cell identity [1]. STM, on the other hand, prevents

ectopic differentiation of stem cells by antagonizing the meristem center factors that drive differentiation on the meristem periphery [2]. Loss of either of these regulators leads to loss of stem cells and meristem termination.

WUS expression is regulated in part through the action of the CLAVATA signaling pathway [3,4]. The CLV family receptors act through the regulation of the activity of the related phosphatases POLTERGEIST (POL) and PLL1 to restrict *WUS* expression from the apical daughters of the stem cells in the third meristem layer (L3) [5]. POL and PLL1 are positive regulators of *WUS* expression – *pol pll1* double mutant plants are unable to maintain *WUS* expression and thus phenocopy *wus* mutants [6]. CLV signaling acts to repress POL/PLL1 and thus *WUS* transcriptional activation.

STM is a member of the KNOX class of TALE (Three Amino acid Loop Extension) homeodomain proteins [7]. The TALE family of homeodomain-containing transcription factors includes the KNOX and BELL class of transcription factors, many of which have also been implicated in meristem regulation [7]. The TALE family is named as such because of a three amino acid loop extension between the first and second helices of the homeodomain relative to the classical homeobox proteins [8]. STM has no known nuclear localization sequence. Several studies have shown that STM without a binding partner is excluded from the nucleus, [9,10]. STM mobilizes to the nucleus when expressed along with BELL family transcription factors such as BLR, ATH1, BLH3 and BEL1 [9,10]. BELL transcription factors expressed alone are found in both the nucleus and cytosol [9-11]. The KNOX class transcription factors

contain a MEINOX protein-protein interaction domain which binds the SKY/BELL protein-protein interaction domain of BELL class proteins.

Consistent with their roles in separate meristem pathways, *stm* and *wus* mutants have dramatically different phenotypic interactions with *clv* mutants. While *wus* is fully epistatic to the stem cell accumulation in *clv* mutants, *stm* and *clv* are mutually suppressive, with *stm clv* double mutants displaying severe loss of stem cell homeostasis characterized by meristems that both accumulate stem cells and terminate [12].

The BELL class homeodomain protein BLR (also known as PENNYWISE, BLH9, VANAMA, LARSON and REPLUMLESS) is essential for internode elongation and floral organ specification. *blr* null alleles display internode elongation defects causing organ clustering [13,14]. BLR has been shown to be partially required for STM activity and enhances the weak *stm* mutant phenotype [13]. BLR expression patterns within the meristem and protein-protein interaction data support BLR-STM interaction in meristem maintenance [15]. Additionally, although both KNOX and BELL class transcription factors can bind to target sequence TGAC with low affinity, *in vitro* experiments show the heterodimer binds with much higher affinity, indicating combinatorial transcriptional regulation [16].

A major challenge in studying the developmental role of BELL class transcription factors is the extensive overlap in gene function between the numerous homologues. We have identified a unique missense allele in *BLR* in

the coding sequence for the third helix of the DNA-binding domain that has striking dominant-negative effects. Plants with this *blr* mutation display premature floral meristem termination, irregular internode patterning and aberrant floral organ initiation and development. We describe the developmental insights provided by this allele, its genetic interactions with CLV pathway mutants, and examine the impact of this *blr* allele on STM function.

RESULTS

blr-7 identification and mapping

To obtain the *pol-6* mutation in a completely Columbia but *erecta (er-)* background, the original *pol-6* in Columbia was crossed to Columbia *er-2* [17] by Jennifer Gagne. The F1 progeny of this cross were phenotypically wild type. In the F2 population, a spontaneous mutation was identified which caused the phenotypically wild-type *pol-6* plants (Figure 3.1A) to occasionally form flowers with filamentous gynoecia instead of the normal silique fruit formed by two fused carpels (Figure 3.1B). We termed this phenotype in the F2 population Class I. In addition, a more severe phenotype was also observed among plants characterized by phyllotaxy disruption, reduced apical dominance and flower malformation that we termed Class II (Figure 3.2A). In addition, a third phenotypic class (Class III) of plants was observed with vegetative meristem termination and absent or limited inflorescence development (Figure 3.1D-F). The Class I and III phenotypes were dependent on *pol-6* homozygosity, while

Class II plants were all either wild-type for *POL* or heterozygous for the *pol-6* mutation. This range of phenotypes and their genotypes indicated that a novel mutation had occurred in the progenitor plants.

The mutation was mapped to *At5g02030* (Figure 3.3A) by Jennifer Gagne. This gene has been identified in many screens and termed *BELL-LIKE HOMEODOMAIN 9*, *REPLUMLESS*, *PENNYWISE*, *LARSON*, *VAAMANA* and *BELLRINGER* (*BLR*) [11,13-15,18-20]. We termed our allele *blr-7*, which has a T to G missense mutation at position 1191 in the coding sequence resulting in a N397K substitution (Figure 3.3B and D). N397 is located in the highly conserved third helix of the homeodomain responsible for DNA contact (see below). Prior studies of the *BLR* locus have revealed that *blr* insertion alleles, presumed nulls, have a dwarf phenotype, decreased apical dominance and irregular phyllotaxy leading to organ clustering (Figure 3.3C). *blr-4* and *blr-5* alleles with missense mutations in helix I lead to sepal to carpel transformation in flowers in senescing inflorescence meristems [18]. The *blr-7* allele is the only allele identified with a lesion in helix III of the homeodomain (Figure 3.3D). When the plants of the F2 population of the original cross that identified *blr-7* were genotyped, Class I plants were *pol*/*pol blr-7*/+, Class II plants were *POL*/*POL blr-7*/*blr-7* or *pol-6*/+ *blr-7*/*blr-7*, while Class III plants were *pol-6 blr-7* double mutants.

blr-7 mutants displayed a low frequency (2.7%, n=147) of vegetative meristem termination. The cauline leaves of the inflorescence are typically clustered with a lack of axillary meristem development, similar to that observed in *revoluta* mutants which is a homeodomain leucine-zipper protein involved in

meristem development [21] (Figure 3.2D). Internode elongation is irregular with significant organ clustering (Figure 3.2 A and E). Additionally, aborted organs can be seen along the inflorescence (Figure 3.2C). *blr-7* flowers exhibited reduced flower organ number and produced two types of flowers: those lacking petals, and those lacking stamens and carpels (Figure 3.2E,G, H). Specifically, only 21% of the flowers produced stamens and carpels and 94% of these lacked any petals. Those flowers that did not form gynoecia typically formed sepals and petals, but in reduced numbers (Table 3.1). Gynoecia that did form in *blr-7* flowers are characterized by a notable defect in fusion (Figure 3.2H). In addition, mosaic and filamentous organs were frequently observed. (Figure 3.2F)

Previous analyses of *blr* null alleles revealed that the meristem structure was overall similar to that of wild-type, although occasionally *blr* null mutants displayed abnormal sites of organ initiation [13]. Because the *blr-7* exhibited clear meristem defects, with phenotypes including phyllotaxy disruption as well as floral organ malformation, we used scanning electron microscopy (SEM) to examine the meristem structure of *blr-7*. Consistent with the phenotypes described above, the *blr-7* meristem structure showed significant and variable defects. We observed both evidence of shoot meristem termination and alteration of shoot meristem structure (Figure 3.4C-H). The organization of the meristem appeared to be characterized by organ initiation close to the meristem center. This phenotype is similar to that of weak alleles of *stm* [22]. Flower meristems displayed clear evidence of meristem termination similar to *wus* mutants, with sepals flanking a terminated structure lacking the full complement

of internal floral organs (Figure 3.4I, J and K) [3,23]. Furthermore, occasional pin-like structures were observed produced from the infloresence shoot meristem in the place of flowers (Figure 3.4D and G). This is also reminiscent of *revoluta* mutants, which display both terminated floral meristems as well as filaments in the place of flowers [21].

blr-7 genetic interactions

Mutations in *POL* do not result in a readily observable meristem phenotype [24]. The dominant-negative *pol-1* allele has a slightly smaller shoot meristem when large numbers of meristems were compared to wild type by SEM [24]. Plants homozygous mutant for *pol-6* and heterozygous for *blr-7* form flowers which occasionally terminate in a central filament, consistent with a reduction in meristem activity (Figure 3.1B). This incompletely expressive filamentous gynoecium phenotype was previous observed among other genetic combinations with flower meristem defects [24]. This suggests presence of a single copy of the *blr-7* mutation acts synergistically with the *pol-6* mutation. Significantly, the *blr-7* mutation makes the phenotypically wild-type *pol-6* mutation phenotypically visible [5,24].

Among *blr-7 pol-6* double mutant plants, 60% (n=25) displayed vegetative meristem termination, sometimes in a trumpet leaf (Figure 3.1D). The *blr-7 pol-6* plants rarely showed very limited inflorescence development (Figure 3.1E). *blr-7 pol-6* typically continued to form occasional leaves, presumably through adventitious shoots (Figure 3.1E). A *BLR* null allele, *blr-3*, was crossed to *pol-6*

(Figure 3.5). Interestingly, the resulting *blr-3 pol-6* plants do not display synergistic phenotypes, consistent with the proposed dominant-negative character of the *blr-7* allele.

The mutant analysis above examined the combinatorial effect of the *blr-7* mutation with a mutation in *CLV* pathway genes that positively regulates stem cell number. The next step then was to analyze the effects of the *blr-7* mutation on mutants in genes that negatively regulate stem cell number. To test this class of mutants, *blr-7* was crossed into the *clv3-2* background. The *clv3-2* null allele exhibits the most severe stem cell defects among the various *clv* mutants [25]

Individuals carrying various combinations of the *blr-7* and *clv3-2* mutant alleles were identified and analyzed phenotypically (Figures 3.6 and 3.7). Plants homozygous for the *clv3-2* mutation typically display stem fasciation and an increase in the numbers of carpels per flower because of the accumulation of stem cells at the shoot and flower meristems [25]. When *clv3-2* homozygous plants are also heterozygous for *blr-7* the plants undergo stem fasciation. However, the *blr-7* mutation partially suppresses the *clv3-2* mutation in that these plants are phenotypically closer to wild type with a decrease in the severity of the gynoecium defect (Figure 3.6B).

Plants homozygous for *blr-7* and heterozygous for the *clv3-2* mutation display the meristem termination and reduced apical dominance phenotypes observed in *blr-7* (Figure 3.6C). Interestingly, some of the secondary meristems displayed extreme fasciation. Additionally, aborted organs can be seen along the

stem as small outgrowths of tissue (Figure 3.6E). Additionally, a mass of meristematic cells and filaments are often seen at the apex (Figure 3.6D)

Plants homozygous for both *clv3-2* and *blr-7* are severely abnormal in appearance (Figure 3.7E, I). Initially they lack the enlarged apex of the *clv3-2* inflorescence meristem but have the clustered cauline leaves of *blr-7*. (Figure 3.7A, B, F). The inflorescence meristem produces flowers with organ complements consistent with the flowers of the *blr-7* mutation; however, these inflorescences also produce a mass of filaments (Figure 3.7I) Defective organ production is also seen along the inflorescence with the production of very tiny spikelet leaf organs that are covered in trichomes consistent with the *blr-7* mutation (Figure 3.7C).

Analysis of *blr-7* protein defects

Previous studies have shown BLR is autonomously nuclear localized, while STM is cytosolic unless co-expressed with a BELL class homeodomain protein [9,10]. Because *blr-7* is a missense allele with dominant-negative characteristics, we sought to determine the nature of the defect in BLR function caused by the N397K substitution. We considered that the mutation might alter blr-7 accumulation, nuclear localization, interaction with STM and/or DNA binding. To test these possibilities, we used transient expression in *N. benthaniama*. When we compared BLR-GFP and blr-7-GFP proteins, both showed similar levels of accumulation and subcellular localization (Figure 3.8B and C). Both fusion proteins were distributed both to the cytosol and nucleus,

consistent with previously published results [9]. Thus, the *blr-7* lesion did not appear to significantly alter protein stability or localization.

To address the possibility that the mutant protein is unable to interact with and/or mediate the translocation of STM into the nucleus, BLR and blr-7 proteins were co-expressed with STM. When STM-mCherry alone was introduced into *N. benthaniama* leaf cells, it was excluded from the nucleus (Figure 3.8A). Instead, the mCherry signal was detected at the periphery of the cell, consistent with cytosolic localization previously observed for STM expressed alone [9,10]. When co-expressed with either BLR-GFP or blr-7-GFP the STM-mCherry signal was also detected within the nucleus, along with both the GFP signal from BLR-GFP and blr-7-GFP (Figure 3.8D-I). This demonstrates that not only was the blr-7 protein able to interact with STM, but was also capable of facilitating the translocation of STM into the nucleus.

Because the blr-7 lesion is located in the highly conserved third helix of the homeodomain at position 47, which has shown to be in direct contact with DNA in the crystallized homedomain [26], it is likely that DNA binding of the mutant protein is affected. To test this, a tetra repeat of the TGAC STM and BLR binding site was infiltrated along with STM-mCherry in combination with BLR-GFP and blr-7-GFP and chIP'd. The target was amplified in the extracts with BLR-GFP but not blr-7-GFP (Figure 3.9). This indicates the DNA binding capacity of the blr-7 protein, and associated cofactor STM, is disrupted.

Discussion

The evidence presented here supports the hypothesis that the *blr-7* allele is dominant negative. The N397K substitution is in the predicted DNA contact helix III of the homeodomain. In transient expression, *blr-7* protein is not altered in accumulation, nuclear localization or the ability to interact with STM and mobilize it to the nucleus. The activity disrupted in *blr-7* transient expression is the. This would imply the activity of BLR binding partners, such as STM, is also disrupted. Thus, *blr-7* may block the ability of STM to regulate transcriptional targets. In addition, *blr-7* would also prevent redundant compensation by other BELL class factors, because STM is otherwise sequestered. Furthermore, this model is fully consistent with the phenotypes and genetic interactions observed in the *blr-7* plants.

The N397K *blr-7* mutation is in the highly conserved third helix of the homeodomain, which is necessary for DNA binding. In addition, it is located at residue 47 of the homeodomain, in the -1 position relative to the nearly invariably conserved WFXN motif observed in homeodomain proteins [27] (Figure 3.10). Typically, residue 47 of the homeodomain is a valine or isoleucine and is in contact with the major groove of the DNA [28]. Data show that the residue at position 47 is important for the DNA binding sequence specificity. The homeobox protein Antennapedia has an isoleucine at this position implicated in DNA contact/base specificity [29] (Figure 3.10). The presence of the asparagine seen in KNOX and BELL class transcription factors may be partly responsible for the TGAC recognition site for these proteins over the classic TAAT recognition

site observed in homeodomains with a valine or isoleucine at this position [30,31] [32]. The crystal structure of MATa1 shows that the valine is in contact with DNA [33]. Interestingly, the binding partner of MATa1, MATα2, has an asparagine at this position (Figure 3.10).

In a missense mutation of this valine to a glutamic acid in the *C. elegans* paired-like homeodomain protein UNC-42, axon guidance is disrupted by the elimination of expression of chemosensory and glutamate receptors [34]. The defects caused by this missense mutation are more severe than those observed in the null allele suggesting the mutation creates a dominant-negative mutant protein.

In the *gorgon* allele of *STM*, an arginine in a conserved motif within the third helix of the homedomain is disrupted by a missense mutation to a lysine (Figure 3.10) [35]. This residue has been shown to contact the DNA backbone [28]. A mutation to a histidine in this residue in the mouse HESX1 homeobox protein eliminates DNA binding activity (Figure 3.10) [36]. The *gorgon* phenotype is distinct from all other published *stm* alleles. Instead of terminated meristems, plants harboring the *gorgon* allele have significantly enlarged meristems in addition to barren axillary meristem positions, as in *blr-7*. The arginine to lysine mutation could be seen as relatively conserved with respect to residue chemical properties. It is possible this could alter or reduce DNA binding activity or change specificity.

The drastic change in the properties of position 47 in the *blr-7* mutation most likely disrupts the conformation and/or DNA binding properties of the third

helix. Therefore, it is likely that the *blr-7* phenotype is the result of altered DNA binding capacity of the mutated gene product. The data from ChIP experiments presented here demonstrate the blr-7 isoform is unable to bind the target sequence. Additionally, it is conceivable blr-7 also disrupts the ability of STM to bind DNA. The phenotypes observed in the mutant are consistent with a loss of STM activity. While both KNOX and BLR homedomains bind DNA with low affinity, the complex binds with much higher affinity demonstrating the biochemical importance of the interaction [16].

The meristem defects in the *blr-7 pol-6* double mutant are consistent with a combined reduction in both WUS and STM function. WUS and STM are required for meristem maintenance; however, they most likely operate in independent pathways, as ectopic expression activates meristem function synergistically [37]. As POL acts to maintain *WUS* expression and BLR acts together with STM in meristem maintenance it is not surprising that a *pol blr-7* double mutant is synergistic in the loss of meristem function. However, the *pol-6 blr-3* double mutant does not display synergistic interaction; again supporting the model that *blr-7* is dominant negative in the disruption of STM activity.

The severity and pleiotropic phenotypes caused by the *blr-7* mutation when compared to null alleles that the mutation not only disrupts BLR activity, but other gene function as well. There are several possible explanations for this. Because the *blr-7* protein is still able to bind STM, this would suggest it maintains interactions with other binding partners as well, disrupting the transcriptional regulation activity of multiple KNOX class I homedomain proteins in addition to

STM. Further complicating matters, the mutant *blr-7* protein could be competing for class I KNOX interaction partners with other members of the BELL class proteins.

In total there are 13 BELL class proteins that could potentially share STM-interacting meristem maintenance function with BLR. A potential candidate would be its paralogue POUNDFOOLISH (PNF or BLH8). The *pnf* single mutant is phenotypically wild type; however, *blr pnf* double mutant plants do not respond to floral inductive signals and continue to make only leaves, implicating redundant activity in promoting the floral transition [38,39]. Triple mutant combination of *blr blh8* and a third BELL protein *ath1* phenocopy partial-loss-of-function *stm* mutants [10]. Taken together, the pleiotropic effects of the *blr-7* mutation can be explained by a combination of defective gene function and misregulation of downstream targets of multiple transcriptional regulators.

Because the homeodomain is so strikingly conserved, the introduction of *blr-7* type of dominant negative mutation into other homeodomain proteins could aid in the identification of downstream transcriptional targets. These alleles could potentially bypass genetic redundancy that complicates and masked developmental and transcriptional control. In this way, these alleles could potentially be used as tools in the mapping of transcriptional regulation networks.

Methods

Plant Materials and Growth Conditions

Arabidopsis thaliana was grown at 21°C under continuous light after 4-days stratification in water at 4°C. Plants were grown on a mixture of 2 parts Metro-Mix 360 (Sun Gro), 1 part vermiculite and 1 part perlite supplemented with Osmocote (Scotts). Col-0, Col *er-2,* L*er, blr-3, clv3-2,* and *pol-6* are as described [13,17,25,40,41].

Mutant Identification and Mapping

The SSLP markers used for rough mapping were designed by prior studies and can be found in Table 3.2 [20,42,43]. The primers for the SSLP and CAPS markers used for the fine mapping can be found in Table 3.3. While a few of the fine mapping markers were from prior studies the majority were designed by hand using the Monsanto Arabidopsis Polymorphism Sequence Collection Database [20,43]. All restriction enzymes used were obtained from Promega or New England Biolabs and PCR amplication was done using GoTaq (Promega).

All other primers used for this study are listed in Table 3.4 including the primers used to sequence At5g02010 and At5g02030 and the primers used to track the *blr-3* and *pol-6* T-DNA insertions. A CAPs marker was used to track the *blr-7* mutation. The *blr-7* CAPs marker primers generate a product of 243 bp from genomic DNA. When this product is digested with Tsp509I (New England Biolabs), wild type DNA is cleaved resulting in two bands, while PCR from *blr-7* mutant DNA is not cleaved.

Transient Expression and ChIP

The coding sequence for *STM* was cloned into pSAT4a, containing a *35S* promoter and C-terminal mCherry tag. This cassette was then amplified with the addition of attB sites for entry into the Gateway system via a BP clonase reaction into pDONR 207. The cassette was inserted into pEarleyGate100 through an LR clonase reaction.

The coding sequence for *BLR* was amplified from cDNA. The mutation corresponding to *blr-7* was generated through PCR site-directed mutagenesis. Both sequences entered the Gateway system through pDONR207 and were inserted upstream of the GFP sequence in pEarleyGate 103 via an LR clonase reaction.

For the 4x repeat TGAC binding target construct, overlapping complementary primers with TGAC and 7 nucleotide spacers were designed with XhoI and XbaI overhangs to ligate into pEarleyGate100.

The STM-mCherry, BLR-GFP, blr-7-GFP and target constructs were transformed into GV3101 *Agrobacterium tumefaciens* and infiltrated into tobacco leaves along with theRNA silencing suppressor P19. Subcellular localization was examined 48 hours post infiltration using a LeicaSP5 laser scanning confocal microscope.

The ChIP protocol used was provided by the Wierzbicki lab. For nuclei isolation and ChIP, tobacco leaves were crosslinked in 0.5% formaldehyde vacuum infiltration approximately 8 minutes, quenched with glycine, ground in

liquid nitrogen, and suspended in nuclear isolation buffer. Isolated nuclei were resuspended and sonicated in nuclei lysis buffer for nuclear disruption and DNA shearing. Optimum 300bp size of sheared DNA was checked by gel electrophoresis. 2µL of 1% nuclear input was used for input PCR. 100µL of nuclear extract was diluted 10x and IP'd at 4°overnight with anti-GFP antibody (ab6556 Abcam) and Protein A agarose (Invitrogen) blocked with salmon sperm DNA (Invitrogen). Beads were washed 3 times with wash buffer containing 1% Triton X-100 and 0.1% SDS and twice with TE. Chromatin was eluted in TE with 1% SDS at 65° and samples for input Western were taken before Proteinase K digestion. DNA was phenol/chloroform extracted and precipitated with ethanol using carrier salmon sperm DNA. Primers used to detect target were specific to the pEarleyGate vector.

SEM

Samples for SEM were prepared as in Dievart et al., 2003 [44]. Briefly, tissue samples were fixed in 4% glueraldehyde in a sodium phosphate buffer at 4°C overnight then stained with 0.5% osmium for several days at 4°C. The tissue was then taken through an ethanol dehydration series and critical point dried before mounting with silver paste and gold coating. Images were collected using a Hitachi 3200N SEM.

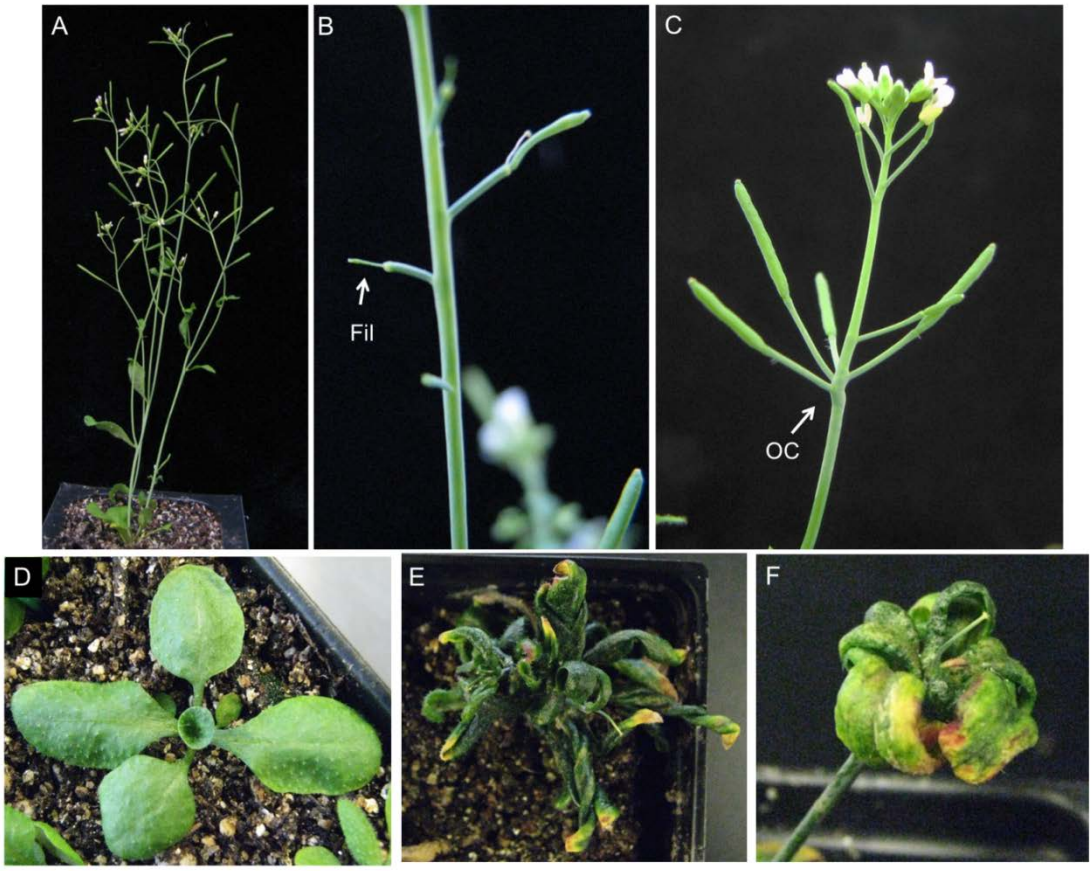

Figure 3.1 *blr-7* genetic interactions with *pol-6* (Class I and III)

A. *pol-6* plants were phenotypically wild type.
B. A Class I plant (*blr-7/+ pol-6*) with filamentous gynoecia (Fil).
C. A Class I plant with the organ clustering (OC) phenotype.
D. A Class III (*blr-7 pol-6*) vegetative meristem terminated with a trumpet leaf.
E. *blr-7 pol-6* plants have little to no transition to inflorescence development and continue to make leaves over a period of months.
F. A rare inflorescence of a *blr-7 pol-6* plant which terminates in a single, carpelloid organ.

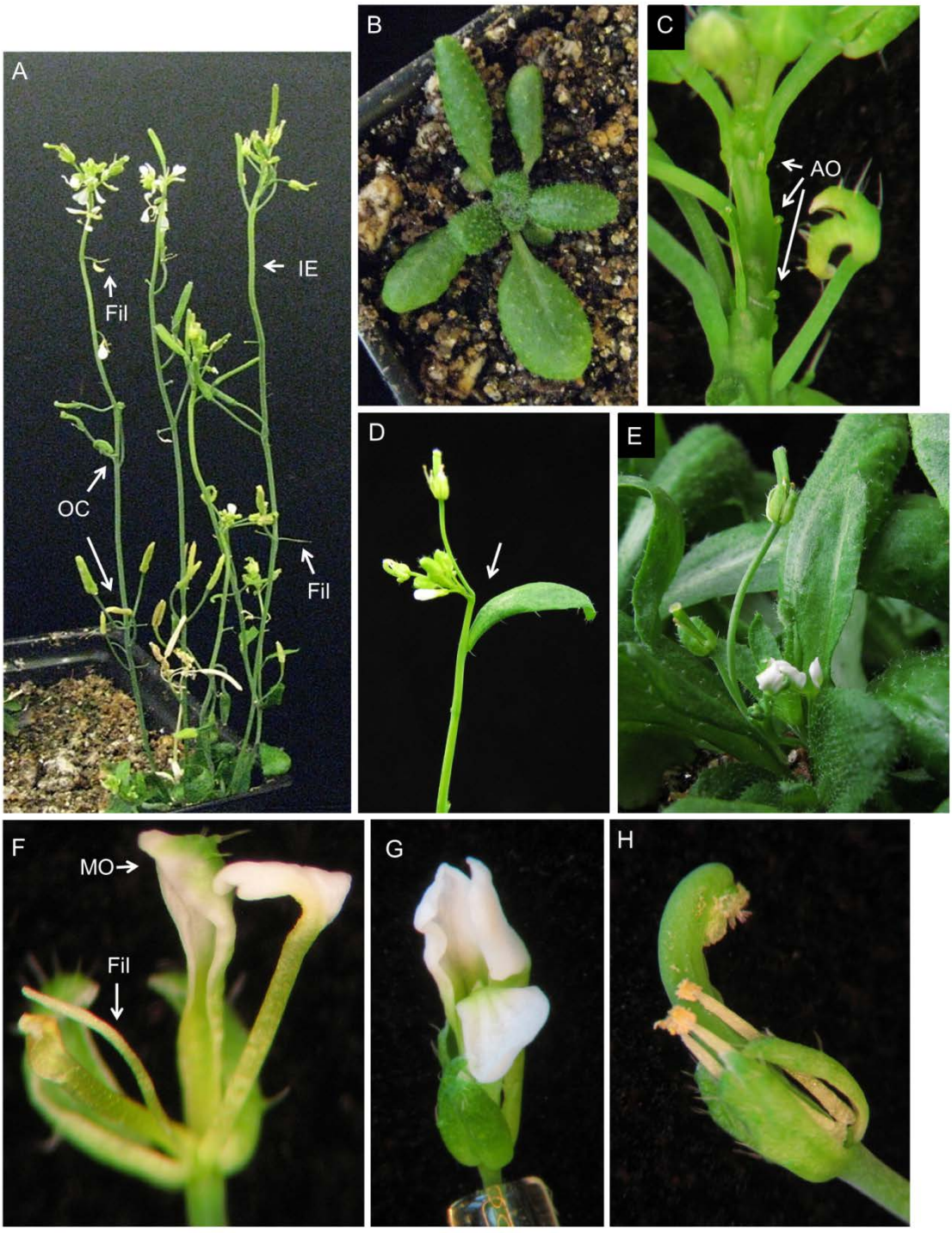
A
IE
Fil
OC
Fil
B
C
AO
D
E
F
MO
Fil
G
H

Figure 3.2 *blr-7* (Class II) mutant phenotypes

A. The inflorescence of *blr-7* plants showed reduced apical dominance as well as organ clustering (OC), aberrant internode elongation (IE) and flowers that formed filamentous gynecia (Fil).
B. A *blr-7* plant with normal vegetative growth.
C. Aborted organs (AO) can be seen along the inflorescence.
D. Arrow points to barren axillary meristem position.
E. Inflorescence with flowers with reduced floral organ complement. Two types of flowers are seen, those with sepals and petals, and flowers which lack petals.
F. Flower displaying sepal/petal mosaic organ (MO) and filamentous petal (Fil)
G. *blr-7* Flower with only sepals and petals.
H. *blr-7* Flower lacking petals. The gynoecium also has carpel fusion defects.

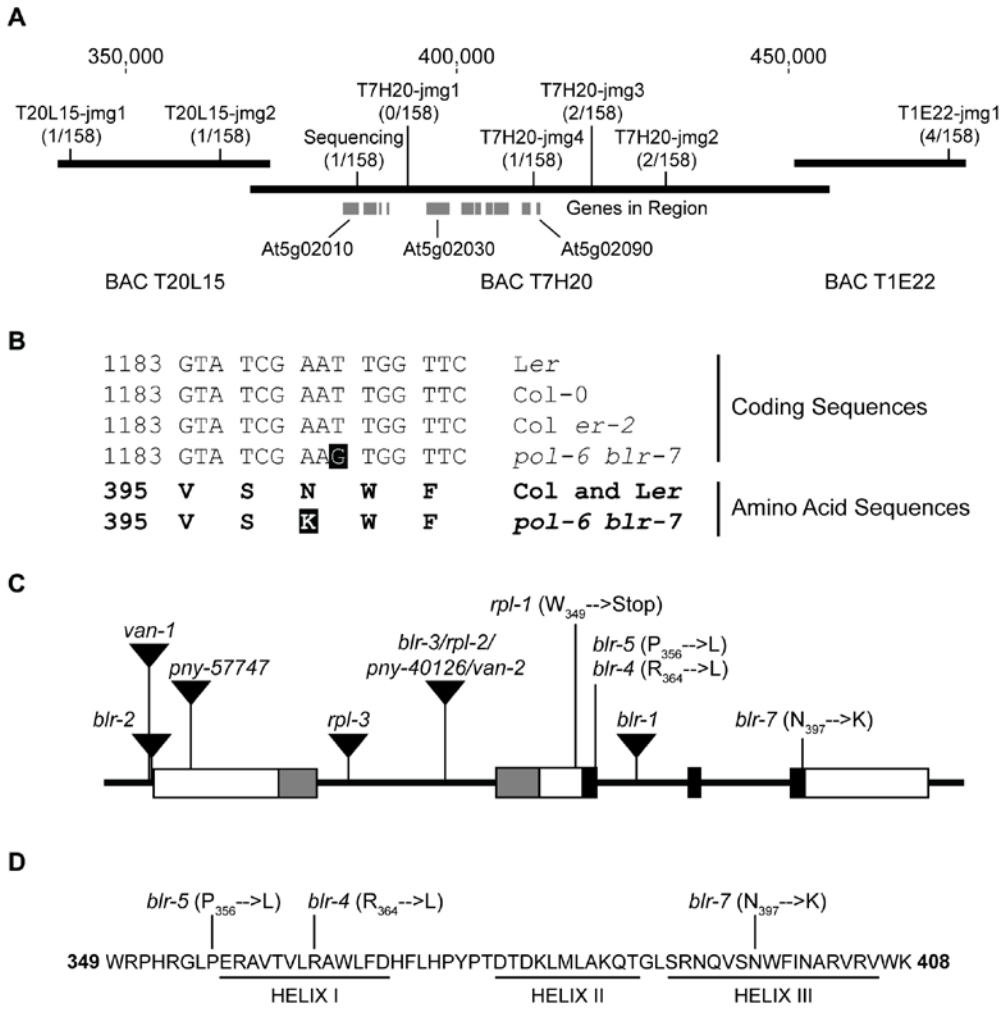

Figure 3.3 Mapping of *blr-7* mutation

A. The mutation mapped to the top of chromosome 5. Diagram indicates markers used for fine mapping. Recombinants detected in a mapping population for each marker are indicted.
B. The *blr-7* mutation is a T to G mutation resulting in a N397K substitution.
C. Gene diagram and location of previously published BLR alleles. The SKY/BELL domain is in grey, the homedomain is black.
D. Location of previously described mutant alleles *blr-4* and *blr-5* within helix I [18] and *blr-7* within helix III of the homeodomain.

Figure courtesy of Jennifer Gagne.

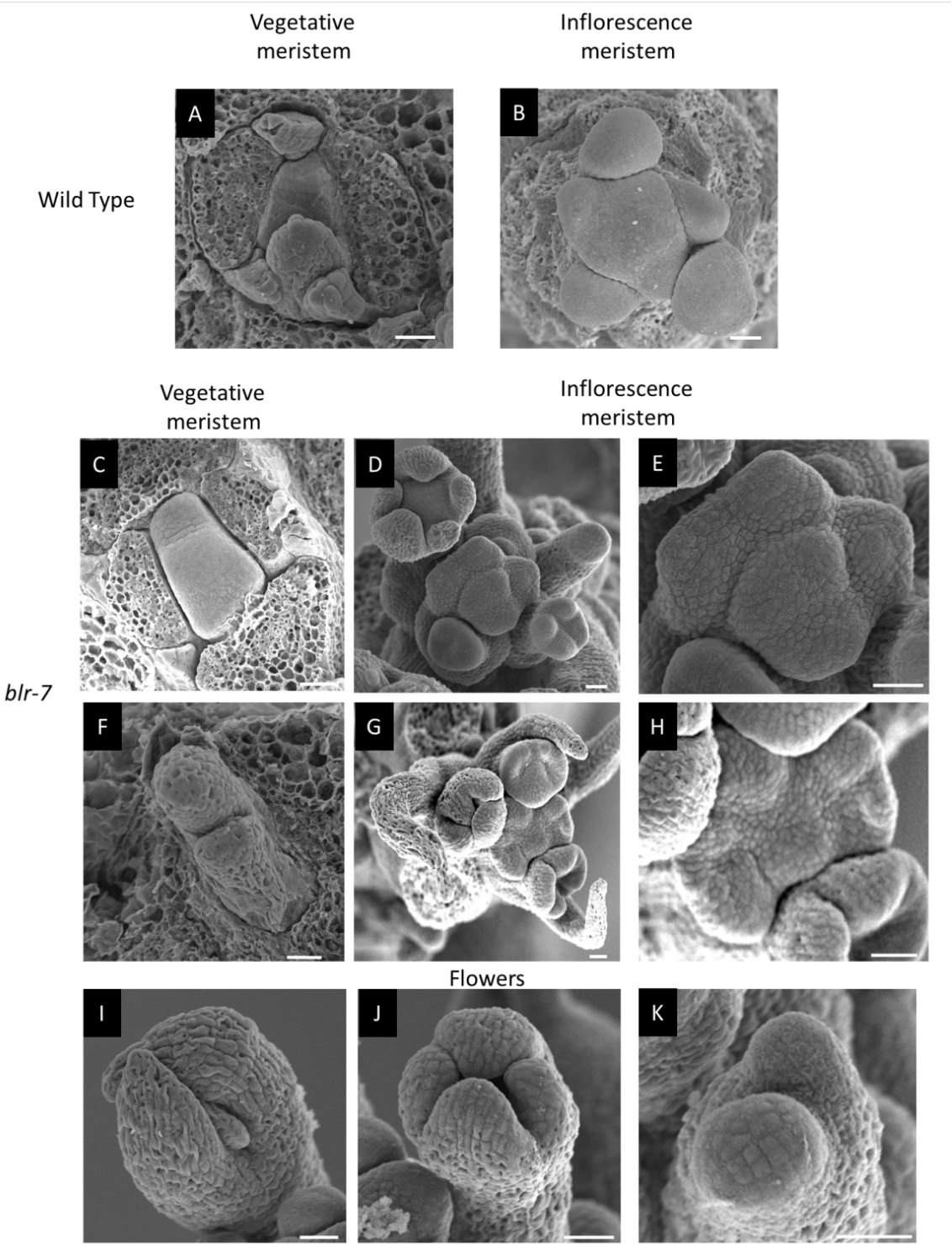

Scale bars = 20 µm

Figure 3.4 Scanning electron microscopy of *blr-7* meristems

A. Wild-type vegetative meristem.
B. Wild-ttype inflorescence meristem.
C. *blr-7* vegetative meristem.
D. Terminating inflorescence meristem. Aberrant and terminating flowers including pin-like structures can be seen along the flanks.
E. Inflorescence meristem from D is magnified. Note the alternate/perpendicular organ initiation sites contrasted with wild type phyllotactic organ initiation pattern.
F. Two leaves flanking a terminated vegetative meristem.
G. Inflorescence meristem with multiple pin-like organs and terminating flower meristems.
H. Meristem from G is magnified highlighting abnormal sites of organ initiation.
I, J, and K. *blr-7* flowers with sepals flanking pin structures or terminated flower meristem.

Figure 3.5 *pol-6* does not affect the phenotype of the *blr-3* null

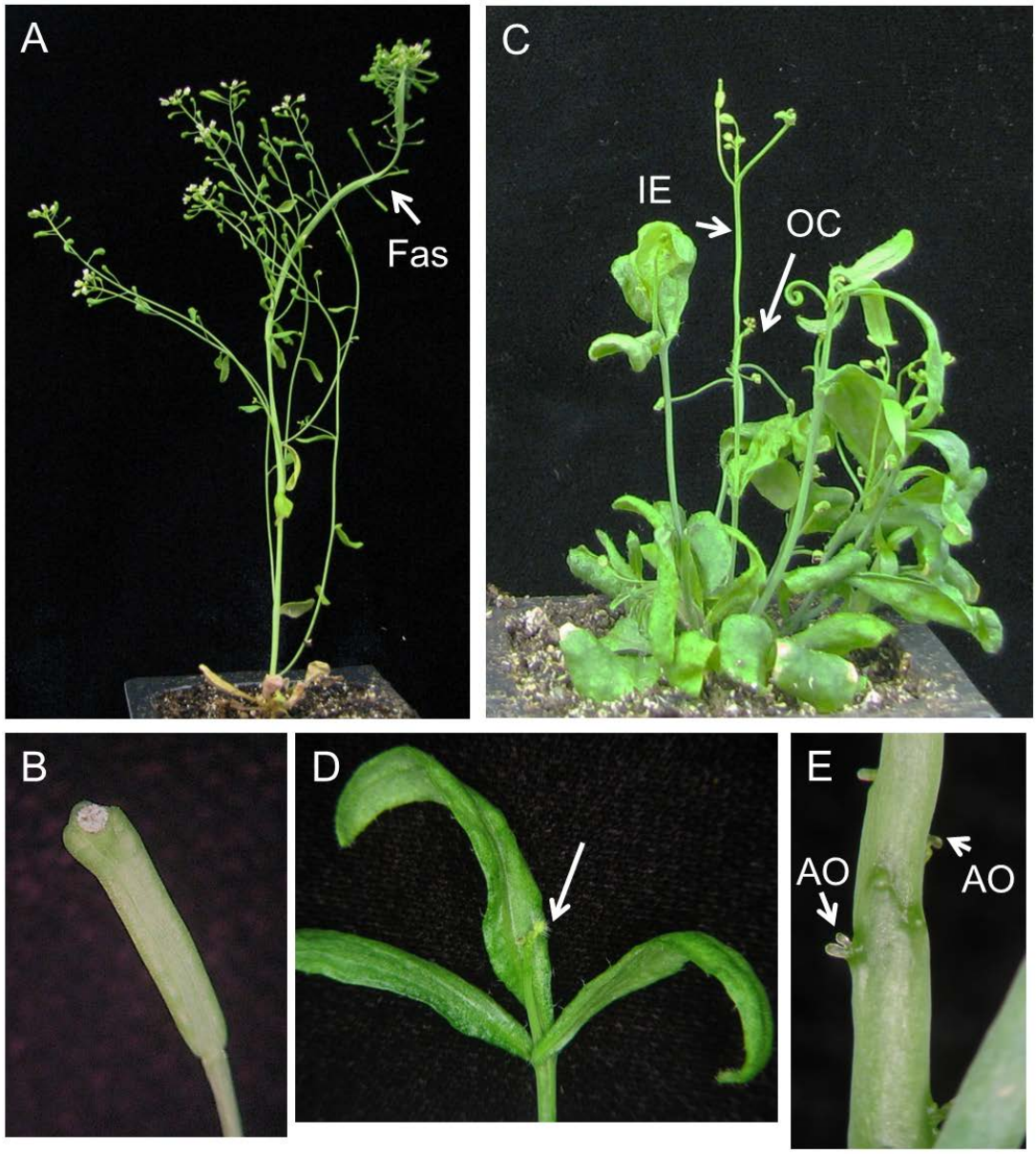

Figure 3.6 *blr-7 clv3-2* semi-dominant interactions

A. *blr-7*/+ *clv3-2* with stem fasciation (Fas)
B. *blr-7*/+ *clv3-2* silique. The *blr-7*/+ mutation partially suppresses the gynoecia defects seen in *clv3-2*
C. *blr-7 clv3-2*/+ plant with phenotypes consistent with the *blr-7* mutation, including organ clustering (OC) and reduced apical dominance.
D. *blr-7 clv3-2*/+ inflorescence with a mass of small filaments at tip (arrow).
E. Aborted organs (AO) emerge along the inflorescence of a *blr-7 clv3-2*/+ inflorescence.

Pictures for this figure courtesy of Jennifer Gagne.


A
B
CL
CL
C
D
E
Fil
Bif
Fas
BA
CO
F
I
Fil
G
H

Figure 3.7 *blr-7 clv3-2* double mutant phenotypes

A. *clv3-2* rosette with incipient inflorescence.
B. *blr-7 clv3-2* vegetative and inflorescence with enlarged cauline leaves (CL) and diminutive inflorescence.
C. Pin-like organ formation along a *blr-7 clv3-2* inflorescence.
D. *clv3-2* inflorescence.
E. *blr-7 clv3-2* inflorescence with fasciation (Fas), bifurcation (Bif), barren axils (BA), clustered organs (CO) and filaments (Fil) both in a mass at the apex and along the inflorescence.
F. *blr-7 clv3-2* cauline leaf cluster.
G. *clv3-2* silique.
H. *blr-7 clv3-2* silique.
I. *blr-7 clv3-2* inflorescence with mass of filaments (Fil) displaying flowers with organ complements similar to those of the *blr-7* single mutant.

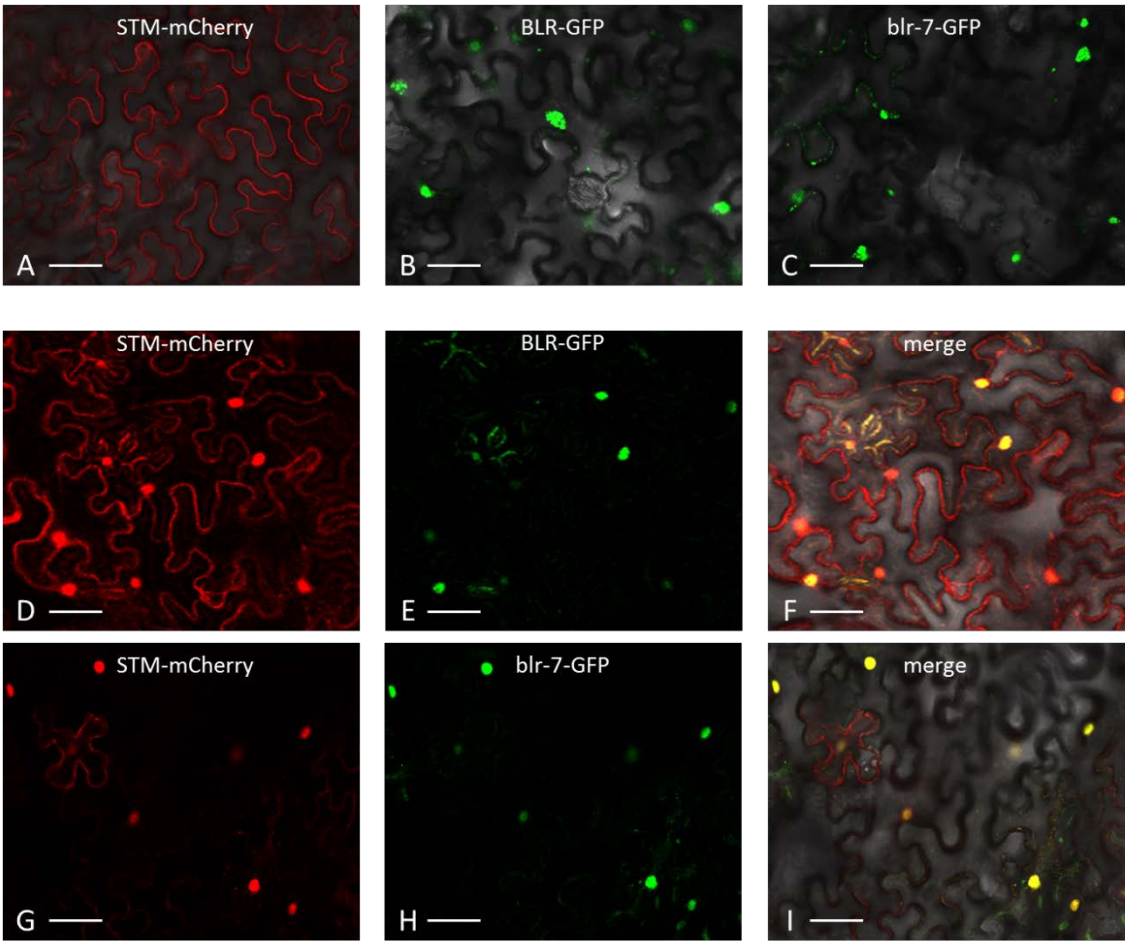

Scare bars = 50 µm

Figure 3.8 blr-7 remains capable of driving STM nuclear localization

STM-mCherry, BLR-GFP and blr-7-GFP were transiently expressed alone and in combination under the *35S* cis elements in *N. benthamiana* leaves.

A. STM-mCherry expressed alone was excluded from the nucleus.
B. BLR-GFP expressed alone was nuclear localized.
C. blr-7 expressed alone was nuclear localized.
D. STM-mCherry was detected in both cystosol and nucleus when co-expressed with BLR-GFP.
E. BLR-GFP was detected in the nucleus when co-expressed with STM-mCherry.
F. Merge of panels D and E.
G. STM-mCherry was detected in both cytosol and nucleus when co-expressed with blr-7-GFP.
H. blr-7-GFP was detected in the nucleus when co-expressed with STM-mCherry.
I. Merge of panels G and H.

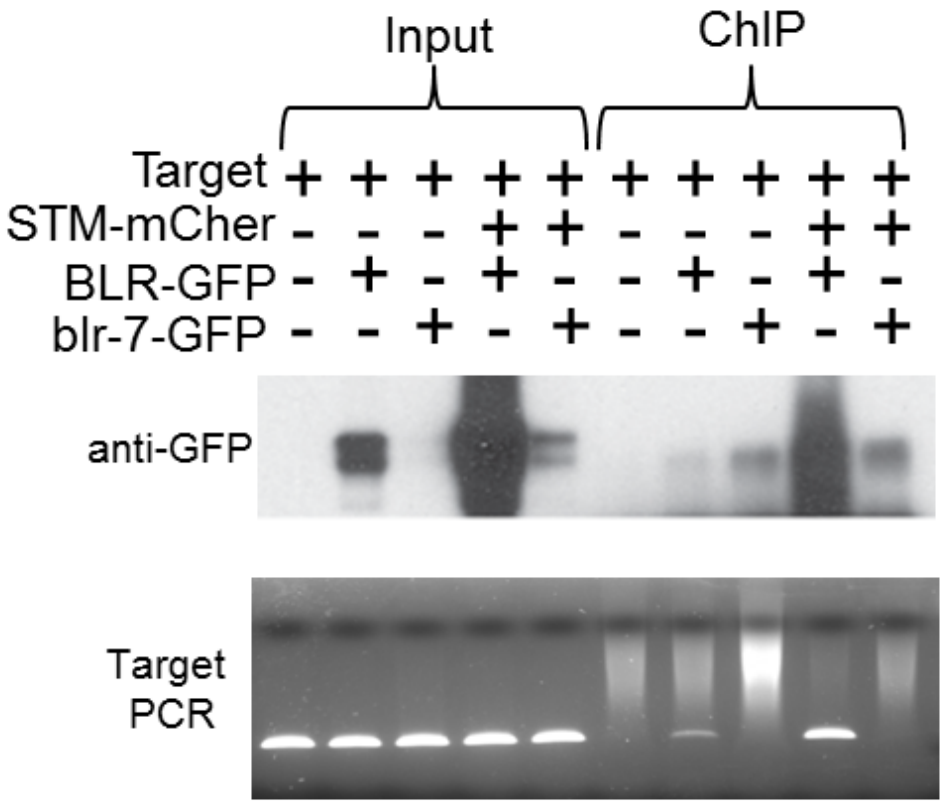

Figure 3.9 DNA binding is disrupted by blr-7 mutation.

Nuclear extracts containing tagged transcription factors and target sequence were ChIP'd with anti-GFP antibodies. Input nuclear extracts show presence of GFP fusion proteins (Input - top image). STM-mCherry expression was observed using confocal (data not shown). Input nuclear extract also contained the target sequence as detected by PCR (Input - bottom image). The GFP fusion proteins were detected in the IP (ChIP - top image). The target binding sequence was only detected in ChIP samples containing BLR-GFP (ChIP - bottom image). The ChIP sample for STM-mCher + BLR-GFP was diluted to account for differences in protein expression. The DNA smear size is consistent with that of salmon sperm carrier DNA used in DNA precipitation, not with that of sheared nuclear DNA observed after sonication.

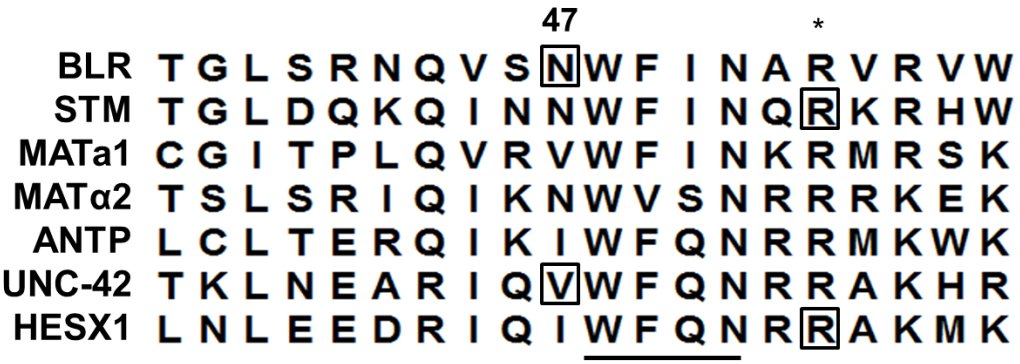

Figure 3.10 Alignment of third helix of the homeodomain.

The WFXN motif is underlined. Residue 47, site of the *blr-7* mutation, is indicated and boxed, as is the corresponding mutation identified in the *unc-42(e270)* mutation. * denotes the site of the *STM* gorgon allele resulting in R53K and the hesx1 R53H lesion, which are boxed.

Table 3.1 *blr-7* flower organ composition

blr-7 plants produce flowers with and without a gynoecium. Flowers with a gynoecium typically do not have petals, while flowers without gynoecia have a reduced number of all floral organs with few stamens produced.

	Sepals	Petals	Stamens	Carpels
Flowers w/ gynoecia (21%)	4.63	0.05	5.53	2.16
Flowers w/o gynoecia (79%)	2.76	2.26	0.44	0

Table 3.2 Rough mapping markers used to map *blr-7*

MARKER	Forward	Reverse	Col	Lan
Chromosome 1				
F3O9	GCCCTTCGTTTTTGTCGAT	TTGAGGAACTTACAATTCTTGTCG	163	130
SO392	TTTGGAGTTAGACACGGATCTG	GTTGATCGCAGCTTGATAAGC	142	156
nF5I14	CTGCCTGAAATTGTCGAAAC	GGCATCACAGTTCTGATTCC	195	290
nga111	GGGTTCGGTTACAATCGTGT	AGTTCCAGATTGAGCTTTGAGC	148	154
Chromosome 2				
F17L24	TTGAAAATGCTCAAAACGACAA	ACTGAATGTTTGCTTCCCAGAC	385	340
F26B6	CTCTATCTGCCCACGAACAAG	CAGGCGATAGAGATGGTAGACA	200	220
nga168	TCGTCTACTGCACTGCCG	GAGGACATGTATAGGAGCCTCG	151	135
Chromosome 3				
nga172	CTCTGTCACTCTTTTCCTCTGG	CATGCAATTTGCATCTGAGG	110	85
F2010	AAGAATTGAAATCCCGATGG	GTTGATAAAGCAACGCAGCA	190	215
ciw 11	CCCCGAGTTGAGGTATT	GAAGAAATTCCTAAAGCATTC	180	230
ciw 4	GTTCATTAAACTTGCGTGTGT	TACGGTCAGATTGAGTGATTC	190	215
nga6	TGGATTTCTTCCTCTCTTCAC	ATGGAGAAGCTTACACTGATC	143	123
Chromosome 4				
F2N1	CAACATGTTTGGGCTCCTCT	TCCCTTCTTGTTTTCACTTTTCA	216	249
ciw 6	CTCGTAGTGCACTTTCATCA	CACATGGTTAGGGAAACAATA	150	155
F4B14	TCTTCCACCAGTTCATGCTG	GCGTCTCAGGTGGTTTTAGC	512	357
nga1107b	GCGAAAAAAACAAAAAAATCCA	CGACGAATCGACAGAATTAGG	150	140
Chromosome 5				
nga151	GTTTTGGGAAGTTTTGCTGG	CAGTCTAAAAGCGAGAGTATGATG	150	120
AthPHYC	CTCAGAGAATTCCCAGAAAAATCT	AAACTCGAGAGTTTTGTCTAGATC	207	222
MNF13	CGTATTTCATATAAAGTCGTTCTTCGT	ATGTAAATTTGGTATAAGCCGAACA	130	104
MIO24	TGGTGGTGTACGATTTTACCAA	TGCATTTCTCGCCATAGTTG	288	231
K919	CTAATCAACTGCTAAAGTCTGTATTC	GTTTCGACAGCCACAAGAGA	178	166

Table 3.3 Fine mapping markers used to map *blr-7* mutation

MARKER	LOC.	GENE	5' PRIMER	3' PRIMER	Enzyme	L *er*	Col
F7J8-jmg1	23 kb	At5g01060	GTGGACCTTTTTTCAGAATGAAGC	CTTGAATATATGGAGAGAGTGACACG	EcoRV	989	200 & 789
F7A7-3ME	190 kb	At5g01490	CAATTGCAGCCGAAACCAA	TTATCATGATTGCCAGTTGACAGTTA	--	200	180
F7A7-1ME	209 kb	At5g01540	TAATCCGGACAATATAACAAAAATGA	ATAGCTAAAAGTTTCTGAAATGAATG	--	190	210
T20L15-1ME	325 kb	At5g01840	CTACTTTTGCGTCATCAATCATACTA	TGTCGGCATCGTAGGTCTAATA	--	185	220
T20L15-jmg1	341 kb	At5g01890	CCGAGAGATTATTGCCACTGAAATC	CGTTTCACTACTCTTCCTCTTCCTT	StyI	373	97 & 277
T20L15-jmg2	363 kb	At5g01940	AAGACACTAAACCCTTAATCTCTAGCCG	CGAGGTTATAGATAACGATTCTTCATGG	EcoRI	780	177 & 603
T7H20-jmg1	395 kb	At5g02025	CAAATGAAGAGGAGTTGTGCAAG	TAGTACCTAGCTAACGGACCTATTGC	--	114	103
T7H20-jmg4	410 kb	At5g02090	AAGAATGCGTAAATGACAAGAAC	GTCCATAATTTTGATGAAGAAAATAAAC	MseI	213	55 & 158
T7H20-jmg3	420 kb	At5g02130	ACCGTAATGTTCCTCAGTCTTTGTC	CGAGGACTTGAGAATCATGAAAGCT	MspI	157 & 299	456
T7H20-jmg2	434 kb	At5g02180	GTTGTTGTGGTACTTACTCGGCTATCTC	CTTCACTTACCAATCAACTTCTTCTCAC	Csp45I	297 & 401	698
T1E22-jmg1	480 kb	At5g02310	CTTGAACATATGATGGCTGCTG	CTTCATGGGGTTGATGATCTACAC	TaqI	77 & 858	935

Table 3.4 Additional primers used in BLR study

NAME	PRIMER SEQUENCE	USE
At5g02010 P1	AAAATAATCACCTGGTTACTGAGAG	5' Amp and Seq
At5g02010 P2	GGAAACAACCAGACAAGAGGAGGAA	Sequencing
At5g02010 P3	ATGTGGAATTGGAATTACTCACATG	Sequencing
At5g02010 P4	AAGAACAAGTGATCTCTTTTCGTCT	Sequencing
At5g02010 P5	CTTTTTTGGTATGTTTCAGAAAGGG	Sequencing
At5g02010 P6	TCCAATACAACAAGGTTACTACATG	Sequencing
At5g02010 P7	TGACAGCTTATGTAACAAAGAACGA	Sequencing
At5g02010 P8	TGTTGTTAATCTCAAAGTCAAAGCC	3' Amp and Seq
At5g02030 P1	TGTAATGCTCATACTAAATTCCTCC	5' Amp and Seq
At5g02030 P2	GAGATCATTCCTTTAACGCCGGACT	Sequencing
At5g02030 P3	ATGTTCACAGTTTTTGGTCGGTGTC	Sequencing
At5g02030 P4	CACCCATTTTATTATGTAAGTGGGG	Sequencing
At5g02030 P5	TACCCGAACGTGCTGTTACTGTTCT	Sequencing
At5g02030 P6	CAGTCTTCTTCTTTTTTCTCTTTCC	Sequencing
At5g02030 P7	CAGCAAAGACCTAACAACTCATCTC	Sequencing
At5g02030 P8	CATAGACAACTCTAAAGTCTAACCC	3' Amp and Seq
BLR 5' Primer	GAGATCATTCCTTTAACGCCGGACT	Genotyping
BLR 3' Primer	GAATTGAAGCTGGTCCGTTATAGCA	Genotyping
blr-7 CAPs Marker	CGCTTGAGGGTTATTAATATATTATGG	Genotyping
blr-7 CAPs Marker	GATGAGTTGTTAGGTCTTTGCTGTG	Genotyping
CLV3 5' Primer	CTCACTCAAGCTCATGCTCACG	Genotyping
CLV3 3' Primer	GGGAGCTGAAAGTTGTTTCTTGG	Genotyping
clv3-2 3' Inversion	TATGCGAGGATTATAAATGCC	Genotyping
erecta (Col *er-2*) CAPs	TTCTCTTGGACAAAGACTTAGAGGC	Genotyping
erecta (Col *er-2*) CAPs	CTGTAGACATCGGATTTCTCAGTGA	Genotyping
erecta (L*er*) CAPs	GAGTTTATTCTGTGCCAAGTCCCTG	Genotyping
erecta (L*er*) CAPs	CTAATGTAGTGATCTGCGAGGTAATC	Genotyping
PLL1 5' Primer	CTCGCTCTCTCTTTTTCTTTCTCTCTTTC	Genotyping
PLL1 3' Primer	ATATAAAACACCCCCACCTAATCTGACCC	Genotyping
POL 5' Primer	TGGTCCTGGCAAGAAAAGCATGAGA	Genotyping
POL 3' Primer	CTTTTTCAGGTGAGAAGACCTTCTAGCTC	Genotyping
SALK T-DNA Primer	TGGTTCACGTAGTGGGCCATCG	Genotyping
SAIL T-DNA Primer	GCCTTTTCAGAAATGGATAAATAGCCTTGCTTCC	Genotyping

Table courtesy of Jennifer Gagne

References

1. Yadav RK, Perales M, Gruel J, Girke T, Jonsson H, et al. (2011) WUSCHEL protein movement mediates stem cell homeostasis in the Arabidopsis shoot apex. Genes & Development 25: 2025-2030.

2. Lenhard M, Jurgens G, Laux T (2002) The *WUSCHEL* and *SHOOTMERISTEMLESS* genes fulfil complementary roles in *Arabidopsis* shoot meristem regulation. Development 129: 3195-3206.

3. Schoof H, Lenhard M, Haecker A, Mayer KF, Jurgens G, et al. (2000) The stem cell population of *Arabidopsis* shoot meristems in maintained by a regulatory loop between the *CLAVATA* and *WUSCHEL* genes. Cell 100: 635-644.

4. Brand U, Fletcher JC, Hobe M, Meyerowitz EM, Simon R (2000) Dependence of stem cell fate in *Arabidopsis* on a feedback loop regulated by *CLV3* activity. Science 289: 617-619.

5. Yu LP, Miller AK, Clark SE (2003) *POLTERGEIST* Encodes a Protein Phosphatase 2C that Regulates CLAVATA Pathways Controlling Stem Cell Identity at *Arabidopsis* Shoot and Flower Meristems. Curr Biol 13: 179-188.

6. Song SK, Clark SE (2005) POL and related phosphatases are dosage-sensitive regulators of meristem and organ development in Arabidopsis. Dev Biol 285: 272-284.

7. Hay A, Tsiantis M (2010) KNOX genes: versatile regulators of plant development and diversity. Development 137: 3153-3165.

8. Burglin TR (1997) Analysis of TALE superclass homeobox genes (MEIS, PBC, KNOX, Iroquois, TGIF) reveals a novel domain conserved between plants and animals. Nucleic Acids Res 25: 4173-4180.

9. Cole M, Nolte C, Werr W (2006) Nuclear import of the transcription factor SHOOT MERISTEMLESS depends on heterodimerization with BLH proteins expressed in discrete sub-domains of the shoot apical meristem of Arabidopsis thaliana. Nucleic Acids Res 34: 1281-1292.

10. Rutjens B, Bao D, van Eck-Stouten E, Brand M, Smeekens S, et al. (2009) Shoot apical meristem function in Arabidopsis requires the combined activities of three BEL1-like homeodomain proteins. Plant J 58: 641-654.

11. Hackbusch J, Richter K, Muller J, Salamini F, Uhrig JF (2005) A central role of Arabidopsis thaliana ovate family proteins in networking and subcellular localization of 3-aa loop extension homeodomain proteins. Proc Natl Acad Sci U S A 102: 4908-4912.

12. Clark SE, Jacobsen SE, Levin JZ, Meyerowitz EM (1996) The *CLAVATA* and *SHOOT MERISTEMLESS* loci competitively regulate meristem activity in Arabidopsis. Development 122: 1567-1575.

13. Byrne ME, Groover AT, Fontana JR, Martienssen RA (2003) Phyllotactic pattern and stem cell fate are determined by the Arabidopsis homeobox gene BELLRINGER. Development 130: 3941-3950.

14. Smith HM, Hake S (2003) The interaction of two homeobox genes, BREVIPEDICELLUS and PENNYWISE, regulates internode patterning in the Arabidopsis inflorescence. Plant Cell 15: 1717-1727.

15. Bhatt AM, Etchells JP, Canales C, Lagodienko A, Dickinson H (2004) VAAMANA--a BEL1-like homeodomain protein, interacts with KNOX proteins BP and STM and regulates inflorescence stem growth in Arabidopsis. Gene 328: 103-111.

16. Smith HM, Boschke I, Hake S (2002) Selective interaction of plant homeodomain proteins mediates high DNA-binding affinity. Proc Natl Acad Sci U S A 99: 9579-9584.

17. Prigge MJ, Otsuga D, Alonso JM, Ecker JR, Drews GN, et al. (2005) Class III Homeodomain-Leucine Zipper Gene Family Members Have Overlapping, Antagonistic, and Distinct Roles in Arabidopsis Development. Plant Cell 17: 61-76.

18. Bao X, Franks RG, Levin JZ, Liu Z (2004) Repression of AGAMOUS by BELLRINGER in floral and inflorescence meristems. Plant Cell 16: 1478-1489.

19. Roeder AH, Ferrandiz C, Yanofsky MF (2003) The role of the REPLUMLESS homeodomain protein in patterning the Arabidopsis fruit. Curr Biol 13: 1630-1635.

20. TAIR The Arabidopsis Information Resource , http://www.arabidopsis.org/.

21. Talbert PB, Adler HT, Parks DW, Comai L (1995) The REVOLUTA gene is necessary for apical meristem development and for limiting cell divisions in the leaves and stems of Arabidopsis thaliana. Development 121: 2723-2735.

22. Endrizzi K, Moussian B, Haecker A, Levin JZ, Laux T (1996) The *SHOOT MERISTEMLESS* gene is required for maintenance of undifferentiated cells in *Arabidopsis* shoot and floral meristems and acts at a different regulatory level than the meristem genes *WUSCHEL* and *ZWILLE*. Plant J 10: 967-979.

23. Laux T, Mayer KF, Berger J, Jurgens G (1996) The WUSCHEL gene is required for shoot and floral meristem integrity in Arabidopsis. Development 122: 87-96.

24. Yu LP, Simon EJ, Trotochaud AE, Clark SE (2000) *POLTERGEIST* functions to regulate meristem development downstream of the *CLAVATA* loci. Development 127: 1661-1670.

25. Clark SE, Running MP, Meyerowitz EM (1995) *CLAVATA3* is a specific regulator of shoot and floral meristem development affecting the same processes as *CLAVATA1*. Development 121: 2057-2067.

26. Li T, Jin Y, Vershon AK, Wolberger C (1998) Crystal structure of the MATa1/MATalpha2 homeodomain heterodimer in complex with DNA containing an A-tract. Nucleic Acids Res 26: 5707-5718.

27. Gehring WJ, Affolter M, Burglin T (1994) Homeodomain proteins. Annu Rev Biochem 63: 487-526.

28. Kissinger CR, Liu BS, Martin-Blanco E, Kornberg TB, Pabo CO (1990) Crystal structure of an engrailed homeodomain-DNA complex at 2.8 A resolution: a framework for understanding homeodomain-DNA interactions. Cell 63: 579-590.

29. Otting G, Qian YQ, Billeter M, Muller M, Affolter M, et al. (1990) Protein--DNA contacts in the structure of a homeodomain--DNA complex determined by nuclear magnetic resonance spectroscopy in solution. EMBO J 9: 3085-3092.

30. Kalionis B, O'Farrell PH (1993) A universal target sequence is bound in vitro by diverse homeodomains. Mech Dev 43: 57-70.

31. Shen WF, Rozenfeld S, Lawrence HJ, Largman C (1997) The Abd-B-like Hox homeodomain proteins can be subdivided by the ability to form complexes with Pbx1a on a novel DNA target. J Biol Chem 272: 8198-8206.

32. Tejada ML, Jia Z, May D, Deeley RG (1999) Determinants of the DNA-binding specificity of the Avian homeodomain protein, AKR. DNA Cell Biol 18: 791-804.

33. Li T, Stark MR, Johnson AD, Wolberger C (1995) Crystal structure of the MATa1/MAT alpha 2 homeodomain heterodimer bound to DNA. Science 270: 262-269.

34. Baran R, Aronoff R, Garriga G (1999) The C. elegans homeodomain gene unc-42 regulates chemosensory and glutamate receptor expression. Development 126: 2241-2251.

35. Takano S, Niihama M, Smith HM, Tasaka M, Aida M (2010) gorgon, a novel missense mutation in the SHOOT MERISTEMLESS gene, impairs shoot meristem homeostasis in Arabidopsis. Plant Cell Physiol 51: 621-634.

36. Dattani MT, Martinez-Barbera JP, Thomas PQ, Brickman JM, Gupta R, et al. (1998) Mutations in the homeobox gene HESX1/Hesx1 associated with septo-optic dysplasia in human and mouse. Nat Genet 19: 125-133.

37. Gallois JL, Woodward C, Reddy GV, Sablowski R (2002) Combined SHOOT MERISTEMLESS and WUSCHEL trigger ectopic organogenesis in *Arabidopsis*. Development 129: 3207-3217.

38. Ung N, Lal S, Smith HM (2011) The role of PENNYWISE and POUND-FOOLISH in the maintenance of the shoot apical meristem in Arabidopsis. Plant Physiol 156: 605-614.

39. Smith HM, Campbell BC, Hake S (2004) Competence to respond to floral inductive signals requires the homeobox genes PENNYWISE and POUND-FOOLISH. Curr Biol 14: 812-817.

40. Kayes JM, Clark SE (1998) *CLAVATA2*, a regulator of meristem and organ development in *Arabidopsis*. Development 125: 3843-3851.

41. Song SK, Clark SE (2005) POL and related phosphatases are dosage-sensitive regulators of meristem and organ development in Arabidopsis. Dev Biol 285: 272-284.

42. Bell CJ, Ecker JR (1994) Assignment of 30 microsatellite loci to the linkage map of Arabidopsis. Genomics 19: 137-144.

43. Jander G, Norris SR, Rounsley SD, Bush DF, Levin IM, et al. (2002) Arabidopsis map-based cloning in the post-genome era. Plant Physiol 129: 440-450.

44. Diévart A, Dalal M, Tax FE, Lacey AD, Huttly A, et al. (2003) *CLAVATA1* dominant-negative alleles reveal functional overlap between multiple receptor kinases that regulate meristem and organ development. Plant Cell 15: 1198-1211.

Chapter 4

Identification and mapping of two meristem mutants

Abstract

Traditional forward genetic screens have identified few signaling intermediates between the plasma membrane associated receptor proteins and the nuclear localized transcription factor WUS in the CLAVATA pathway. One possible cause of this gap is redundancy and robust pathway feedback regulation leading only to identification of non-redundant pathway components while components with dispensable function due to redundancy or other features of signaling remain undiscovered. In an attempt to overcome this shortcoming, an EMS mutagenesis screen of a mutant in the CLAVATA pathway signaling intermediate POLTERGEIST (POL) was analyzed for enhancement of phenotype. While *pol* single mutants do not display a noticeable phenotype, these mutants provide a genetically sensitive background in which to identify novel intermediates. In this work, two such enhancer lines were mapped and the causative mutation was identified. The two *pol* enhancer mutants corresponded to lesions in the small-RNA binding protein AGO10, of the Argonaute family

involved in RNA silencing, and TSK, a unique cell-cycle dependent protein involved in orienting proper plane of cell division.

Introduction

All post-embryonic above and below ground growth in plants arises from pools of stem cells maintained in two structures known as meristems. Meristems are formed in the plant embryo and are maintained throughout the life of the plant to maintain reiterative organ formation. The root apical meristem is located at tip of the root while the shoot apical meristem is located at the tip of the apical embryo between the cotyledons in dicotyledenous plants.

In order for the plant to maintain meristems, the pools of stem cells must not only give rise to differentiating cells, but must also replenish the pool. A signal transduction pathway responsible for meristem maintenance in *Arabidopsis thaliana* is known as the CLAVATA pathway. The CLV receptor proteins, CLV1, CLV2, CLV3 and CRN act through the phosphatases POL and PLL1 to negatively regulate the expression of the transcription factor WUS, which specifies the stem cell population.

pol-6 mutants do not have an identifiable mutant phenotype as a single mutant because of redundancy with the related PLL1 [1]. However this provides a genetically sensitized background in which to identify other components involved in meristem maintenance. Mutations in *POL* partially suppress the enlarged meristem phenotype of *clv* mutants.

Results

Chunghee Lee, a fellow graduate student, performed an EMS mutagenesis of *pol-6*, screening for enhancers with defective meristem phenotypes. He isolated several mutant lines. I mapped and identified the causative mutation in two lines, CL171 and CL33.

Mapping CL171

After germination, the mapping population of CL171 displayed seedling phenotypes ranging from a flat apex between the cotyledons and no organ formation, to a single pin-shaped organ, or a single leaf (Figure 4.1). These phenotypes are all consistent with early termination of the SAM. Adult plants were able to initiate adventitious shoot meristems which occasionally fasciated and resulted in flowers with extra floral organs.

Rough mapping of CL171 linked the mutant phenotype with the bottom of chromosome 5 (Figure 4.2). Based on phenotype, an obvious candidate that could cause the meristem phenotype was *AGO10*. *AGO10* is necessary for the embryonic development of the SAM and *ago10* mutations lead to meristems that terminate in a single leaf in addition to extra carpels later during inflorescence development [2]. As these mutant phenotypes are consistent with the mapping population, *AGO10* was sequenced in the CL171 isolate. A G→A mutation was found in the intron donor site after the 13th exon (Figure 4.3), presumably affecting splicing.

Mapping CL33

The mapping population for CL33 mutant plants displayed meristem termination, stem fasciation and bifurcation, as well as extra floral organs and unfused carpels (Figure 4.4). The mutation in line CL33 was roughly mapped to the top of chromosome 3 (Figure 4.5). Fine mapping narrowed the area of the mutation to a 2.4Mb region between markers nT204 and F16J14 (Figure 4.6). Using a candidate approach based on phenotype, the coding region for *TSO1* was sequenced. TSO1 is a CXC-domain-containing DNA-binding protein necessary for proper cell division in the developing flower. Plants mutant for *TSO1* display flowers with missing or malformed floral organs [3]. The CL33 isolate was wild-type for *TSO1* coding region.

Another candidate in the region, At3g18730 which encodes TONSOKU (TSK) was also considered. Plants mutant for *TSK* have bifurcated and fasciated meristems as well as terminated floral meristems and extra floral organs [4]. Sequencing the *TSK* coding region in the CL33 isolate revealed a nonsense mutation. The mutation is a C to T substitution in codon 131 in the second exon leading to a premature stop codon amidst the N-terminal LGN (Leu-Gly-Asn) repeats (Figure 4.6). This truncates the 1312 amino acid TSK protein to 130 residues. *tsk-4*, a T-DNA insertion allele at the end of the exon causes phenotypes similar to those observed in the mapping population [5]. In addition, most *tsk* alleles published thus far show similar phenotypes. The exception is *bru1-3* which is *tsk* allele in which the gene is disrupted by a T-DNA insertion in

the middle of the 6th exon between the LGN repeat and second NLS which results in severe dwarfing and low seed production [4].

Discussion

Several mutants with meristem development defects were identified in an EMS mutagenesis enhancer screen in the sensitized *pol-6* genetic background. Although the effects of the two meristem mutants mapped, AGO10 and TSK, are not dependent on the function POL, they nevertheless fulfill important roles in meristem development.

MicroRNAs have recently been identified as having important roles in gene regulatory networks. They are processed from larger pieces of precursor RNA by what are called Dicer proteins. miRNAs are not translated into protein but instead become a part of a silencing complex (RISC), along with Argonaute proteins, where they help target mRNA transcripts for repression. The precursor RNA are divided into families based on sequence similarity. miR165/166 are similar precursors that have been shown to play a pivotal role in plant development, including meristem development [6]. Many of the targets of miRNA degradation are transcription factors [7] and the targets of miR165/166 include the HD-ZIP III transcription factors PHV, REV, PHB, ATHB8 and ATHB15 that are involved in regulating the differentiation status of stem cells, promoting adaxial identity [8]. AGO10 associates specifically with miR165/166 as does AGO1 [9]. In the current model, HD ZIP III transcription factors are suppressed

in the abaxial side of the leaf because of targeting by the AGO1/miRNA165 in the RISC. In the adaxial side, AGO10 competes for miR165/166, sequestering it from AGO1 but not catalyzing HD ZIP III transcript degradation, resulting in the increased expression of the HD-ZIP III transcription factors and the maintenance of the adaxial-abaxial boundary [9].

Argonaute proteins contain several conserved motifs. The PAZ and MID domains are responsible for binding the miRNA while the C-terminal PIWI domain contains catalytic activity necessary for mRNA degradation. The mutation mapped at introns donor site after the 13th exon is in catalytic PIWI domain. It is identical to the *zll-8* mutation, which also changes this introns/exon border, resulting in a predicted translational stop after amino acid 773 [10].

TONSOKU/MGOUN3/BRUSHY1 (TSK) encodes a 1312 amino acid protein with two potential protein-protein interaction domains, leucine-glycine-asparagine (LGN) repeats at the N-terminus and LRR-repeats in the C-terminus [11]. It also contains a leucine zipper motif and 2 nuclear localization signals. It has been implicated in the orientation of the plane of cell division in and its expression and subcellular localization is cell cycle-dependent [5]. Mutations in TSK lead to shoot and root meristem malformation. These phenotypes most likely stem from abnormal cell divisions during embryogenesis. This results in the broadened expression of WUS and in some cases multiple areas of WUS expression. Presumably because of the negative control of CLV3 expression by WUS, tsk mutants also have a restricted zone of CLV3 expression. Often this results in meristem fasciation in the mutant [5].

tsk mutants are also hypersensitive to DNA damaging agents such as UV irradiation, bleomycin, an inducer of double strand breaks, and mitomycin C, a DNA-cross-linker as measured by 4x heightened sensitivity to MMS (methyl methane sulfonate) [4]. Generally a nuclear protein, TSK localization moves to the ends of spindle microtubules ahead of separating sister chromatids during mitosis along with its interaction partner, TSA1 [12]. Taken together, the role of TSK in genome maintenance, cell cycle progression and the plane of cell division along with meristem formation suggest a possible link between cell cycle processes and meristem development.

Methods

Plants were grown in a 2:1:1 MetroMix360: Vermiculite: Perlite mixture supplemented with 14-14-14 Osmocote under continuous light conditions. Leaf tissue was ground with a pestle in 200mM Tris-HCL (pH=7.5), 250mM NaCl, 25mM EDTA and 0.5% SDS. After centrifugation to removed cellular debris, DNA was precipitated with isopropanol and the subsequent pellet washed with 75% ethanol to remove salts before drying and dissolving in water or TE.

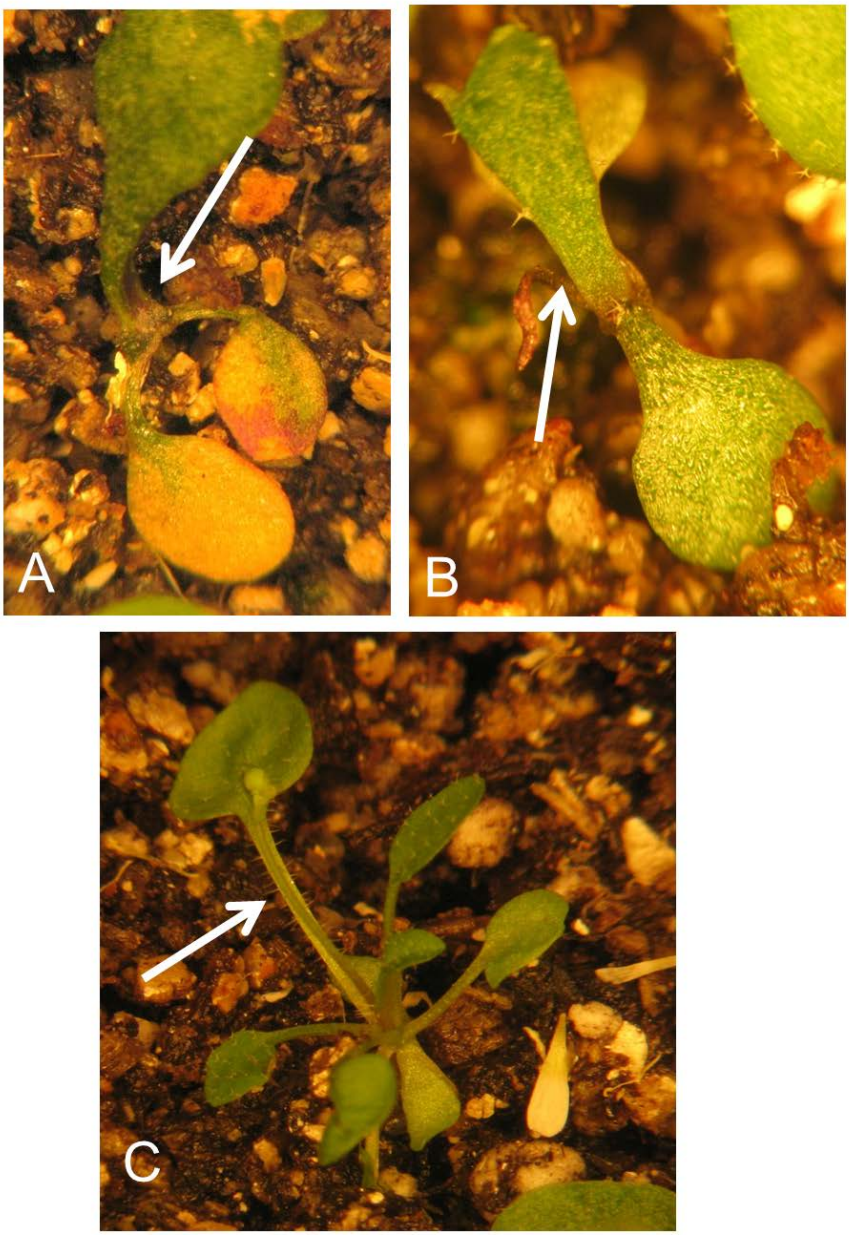

Figure 4.1 Phenotypes of the CL171 isolate

CL171 phenotypes indicate early meristem termination consistent with mutations in *AGO10*.

A. Arrow points to terminated apex
B. Arrow points to termination in central leaf
C. Arrow points to central pin-like structure.

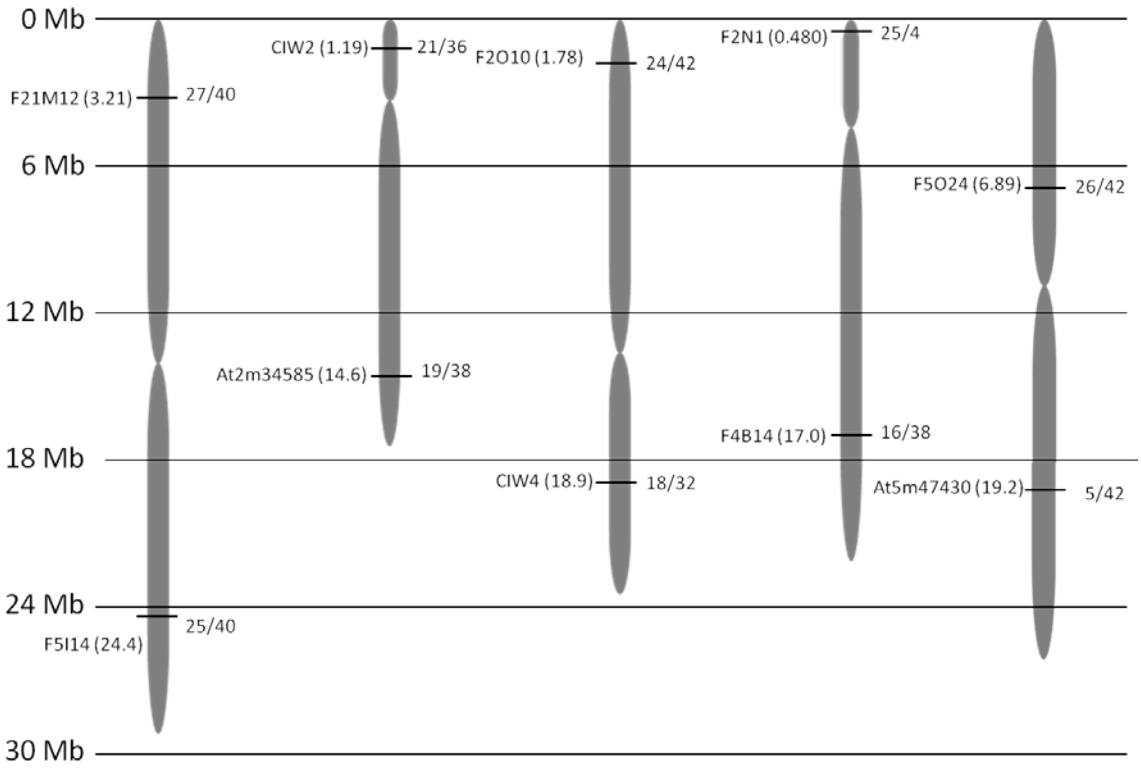

Figure 4.2 Rough mapping of CL171

CL171 maps to the bottom of chromosome 5. The markers used and number of recombinants are indicated.

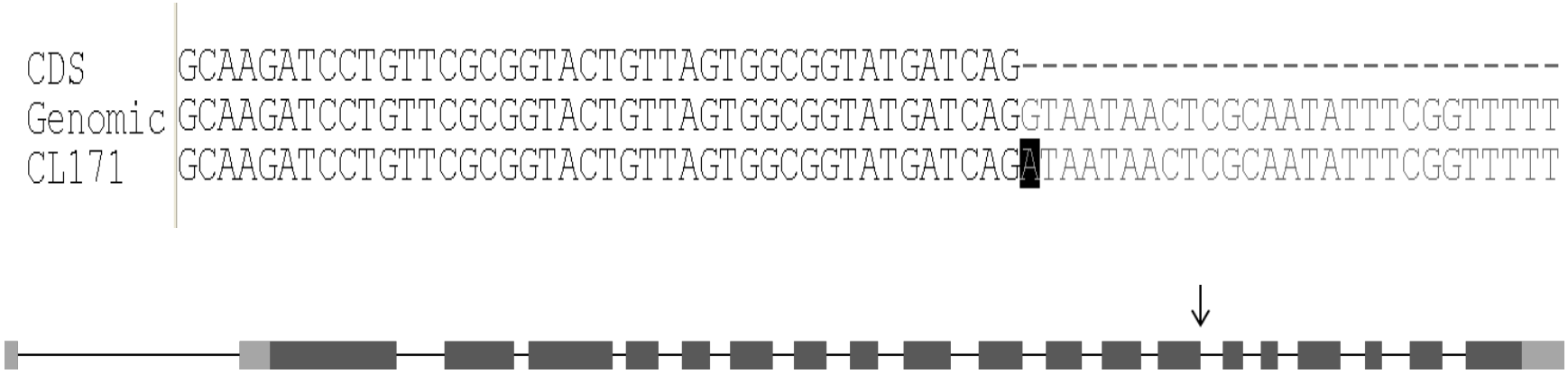

Figure 4.3 CL171 mapped to AGO10

The coding sequence (CDS) genomic and CL171 sequence are shown with the mutation highlighted in black. The CLV171 mutation is a G to A substitution in the intron donor site after the 13th exon. This is identical to the *zll-8* mutation [10]

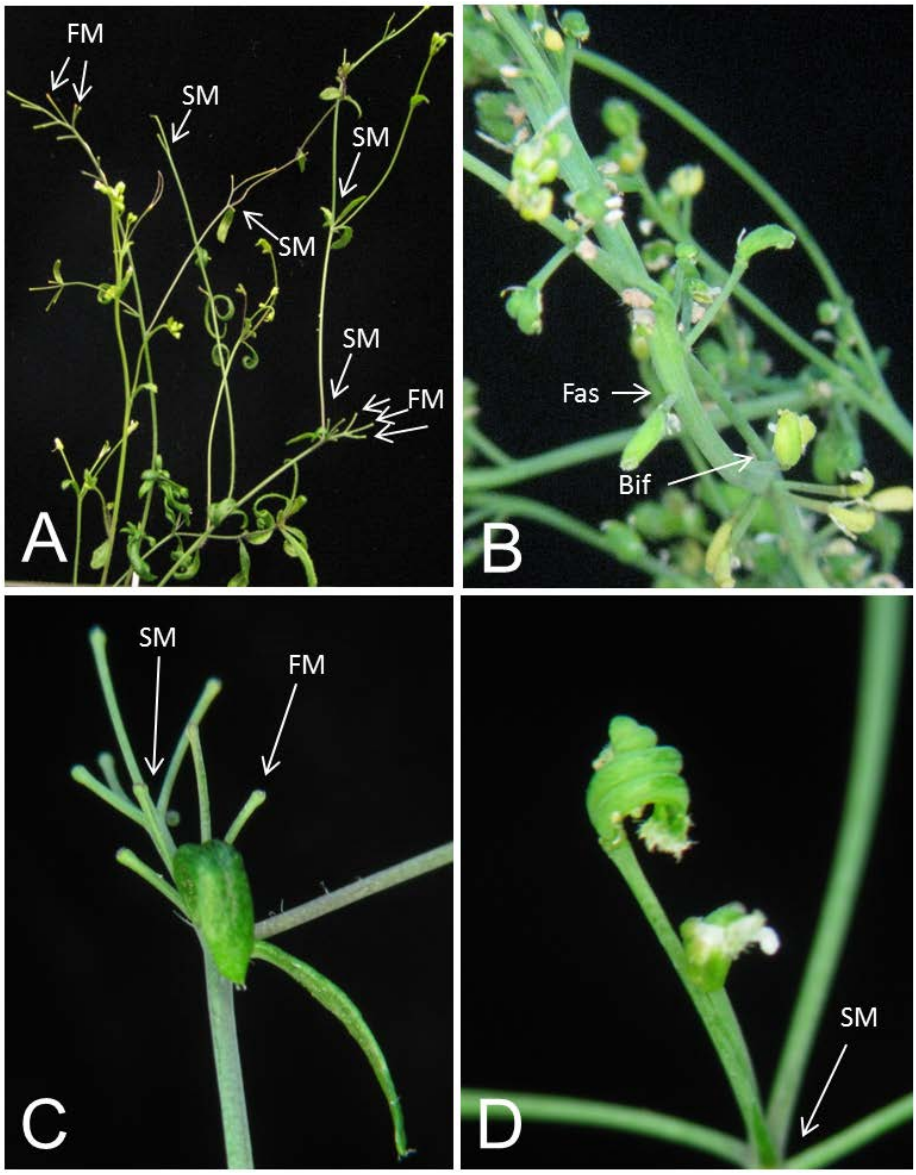

Figure 4.4 Phenotypes of the CL33 isolate

The CL33 mapping population displayed phenotypes consistent with mutations in *TSK*. Terminated shoot meristems (SM) and floral meristems (FM), as well as meristem fasciation (Fas) and meristem bifurcation (Bif) are indicated with arrows.

A. Extensive meristem termination in a CL33 inflorescence.
B. Meristem fasciation (Fas) and bifurcation (Bif) are indicated.
C. In addition to flowers with extra floral organs, CL33 floral meristems also terminated. The arrow points to a pedicel with no gynoecium.
D. CL33 produced flowers with extra and unfused carpels

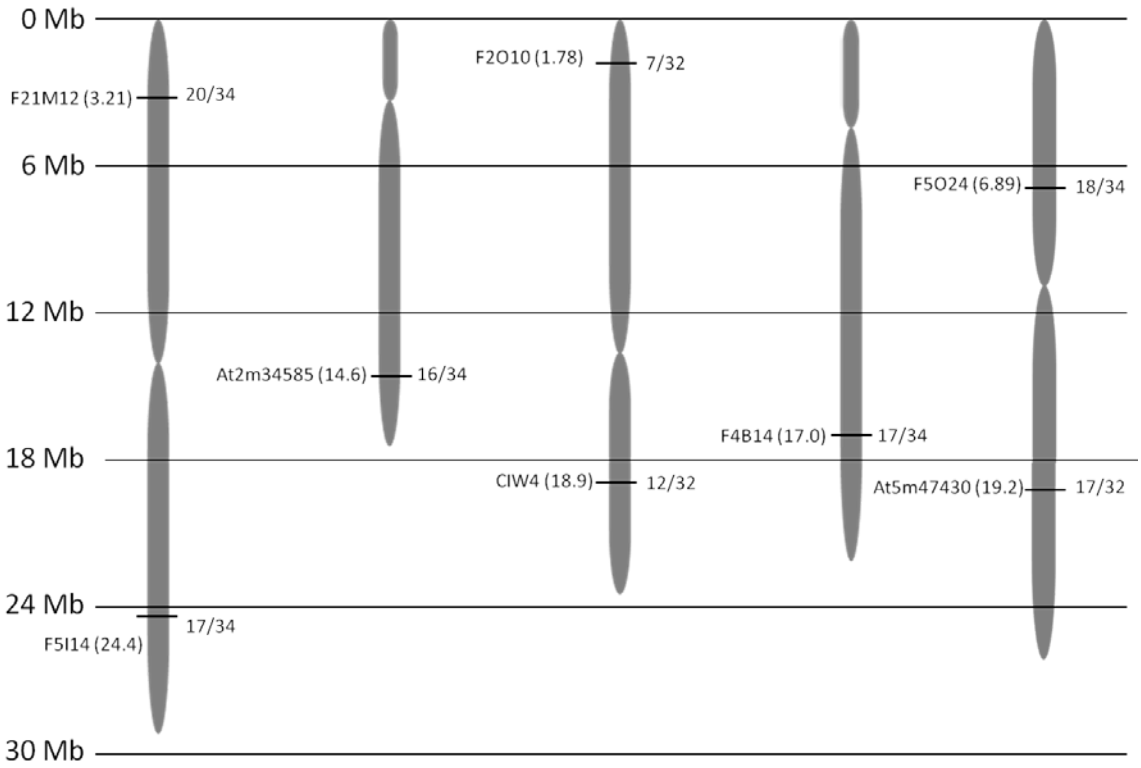

Figure 4.5 Rough mapping CL33

CL33 rough maps to the top of chromosome 3. The marker used and number of recombinants are indicated.

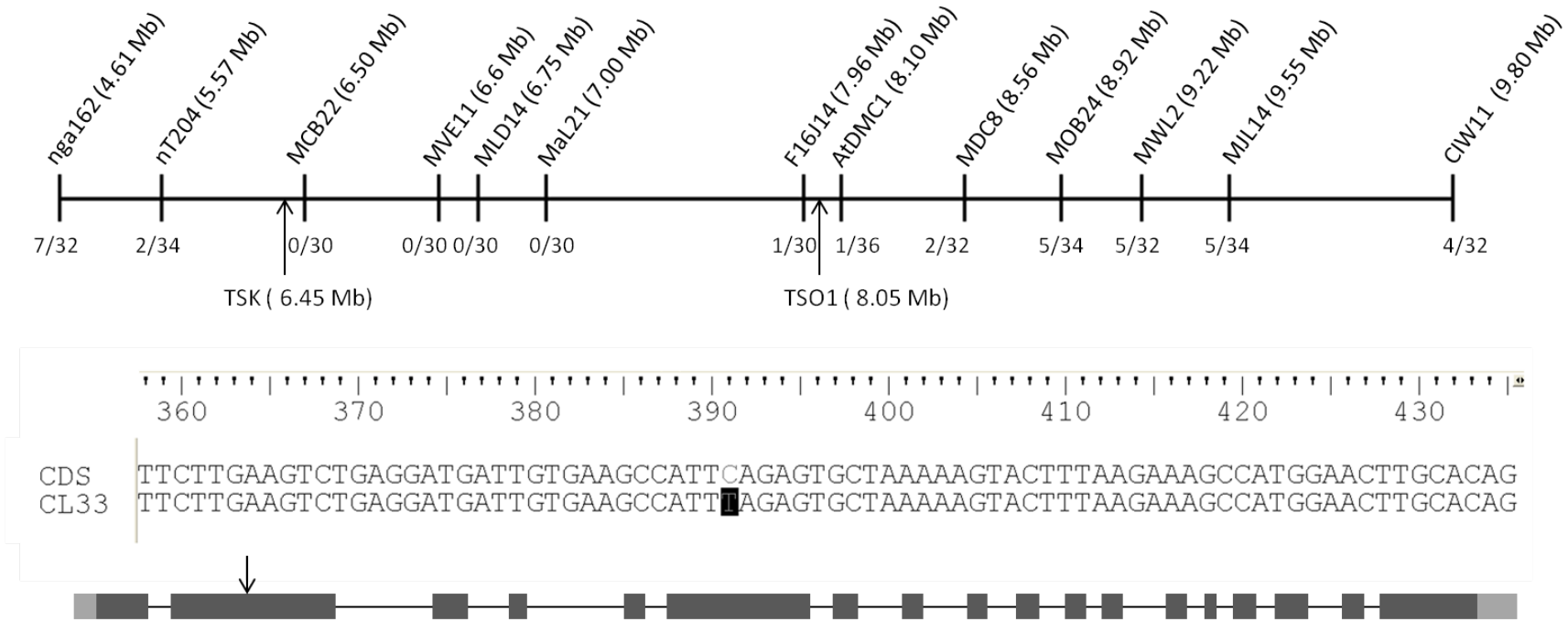

Figure 4.6 Fine mapping the mutation in CL33

The CL33 mutation was mapped to a 2.4Mb region of chromosome 3. The location of the two candidates sequenced, *TSO1* and *TSK* are indicated with arrows. The mutation was identified as a C391T in *TSK* which introduces a premature stop codon.

Table 4.1 Rough mapping primers

Chromo.	Position (Mb)	Marker	Forward primer	Reverse primer	Columbia (bp)	Landsberg (bp)
1 top	3.21	F21M12	GGCTTTCTCGAAATCTGTCC	TTACTTTTTGCCTCTTGTCATTG	200	160
1 bottom	24.4	F5I14	CTGCCTGAAATTGTCGAAAC	GGCATCACAGTTCTGATTCC	195	290
2 bottom	14.6	At2m34585	AGCGGTTTCACCACTTACTCA	ATGCCCCACTGTTCTTTTGA	129	119
3 top	1.78	F2O10	AAGAATTGAAATCCCGATGG	GTTGATAAAGCAACGCAGCA	190	215
3 bottom	18.9	CIW4	GTTCATTAAACTTGCGTGTGT	TACGGTCAGATTGAGTGATTC	190	215
4 bottom	17.0	F4B14	TCTTCCACCAGTTCATGCTG	GCGTCTCAGGTGGTTTTAGC	512	357
5 top	6.89	F5O24	TGGCCCTTGCAGAGAAAGTA	CCGATCTGGATAAGCTGGAA	196	175
5 bottom	19.2	At5m47430	GTATTAATAA GTGGAAGTCC	GACAGTAAATTGACTCGAAC	231	220

Table 4.2 CL33 fine mapping primers

Marker	Forward Primer	Reverse Primer	Columbia (bp)	Landsberg (bp)
nga162	CTCTGTCACTCTTTTCCTCTGG	CATGCAATTTGCATCTGAGG	110	85
NT204	TGGAAGCTCTAGAAACGATCG	ACCACCTAAACCGAGAATTGG	130	145
MCB22	GAACCCCCAGAATATCAACATC	GCTCTGATGGTGATTCTGGTAAC	229	203
MVE11	CCATTAAGGTTTGGGAAGATCATG	CCAGAAACTTGTCTGCCTG	244	225
MLD14	GCTACAGTTCTCAACCGGTAAATC	CATAAGCTTTTATGCTCCAAAATAGTCTC	150	132
MaL21	CTCCAACTTCAAGCAAAACGGATG	CTCTGTTTTTTGGGCTAGTGATGG	107	100
F16J14	GGTAAGCTTCAGGTCGTGCT	GTCAACACTTTGACCCGACA	224	202
AtDMC1	GCAACTGAATTTGTTTTCGTTTG	TTGATTAGTGGATCCGCAAACAA	2200	342
MDC8	GTGTATCGTACGCCCCACTC	TGTCGTCGTTTAGTGGATGTG	211	172
MOB24	CGACGACAAAGAAATAACCATTC	CGTTAACACCGGCTAGTTCC	292	206
MJL12	CTTGGGGCAGGTTATTTGTG	TCCTCGACGAAGAAGCCTTA	667	638
MWL2	CAGATACCGACCCTGATTCG	CCTAGCTGCCGAGATTTACG	492	460
MJL14	TGAGCAAACAGTCGGTCAAG	CCTAGGTCAACCCAATTTCG	479	438
MTC11	TCATTTTTCGCTAATTAACTTCGT	TTTTGAATCGTTTGGAAGTGG	451	429
CIW11	CCCCGAGTTGAGGTATT	GAAGAAATTCCTAAAGCATTC	180	230

References

1. Song SK, Clark SE (2005) POL and related phosphatases are dosage-sensitive regulators of meristem and organ development in Arabidopsis. Dev Biol 285: 272-284.

2. Lynn K, Fernandez A, Aida M, Sedbrook J, Tasaka M, et al. (1999) The PINHEAD/ZWILLE gene acts pleiotropically in Arabidopsis development and has overlapping functions with the ARGONAUTE1 gene. Development 126: 469-481.

3. Liu Z, Running MP, Meyerowitz EM (1997) TSO1 functions in cell division during Arabidopsis flower development. Development 124: 665-672.

4. Takeda S, Tadele Z, Hofmann I, Probst AV, Angelis KJ, et al. (2004) BRU1, a novel link between responses to DNA damage and epigenetic gene silencing in Arabidopsis. Genes Dev 18: 782-793.

5. Suzuki T, Inagaki S, Nakajima S, Akashi T, Ohto MA, et al. (2004) A novel Arabidopsis gene TONSOKU is required for proper cell arrangement in root and shoot apical meristems. Plant J 38: 673-684.

6. Jung JH, Park CM (2007) MIR166/165 genes exhibit dynamic expression patterns in regulating shoot apical meristem and floral development in Arabidopsis. Planta 225: 1327-1338.

7. Mallory AC, Vaucheret H (2006) Functions of microRNAs and related small RNAs in plants. Nat Genet 38 Suppl: S31-36.

8. Emery JF, Floyd SK, Alvarez J, Eshed Y, Hawker NP, et al. (2003) Radial patterning of Arabidopsis shoots by class III HD-ZIP and KANADI genes. Curr Biol 13: 1768-1774.

9. Zhu H, Hu F, Wang R, Zhou X, Sze SH, et al. (2011) Arabidopsis Argonaute10 specifically sequesters miR166/165 to regulate shoot apical meristem development. Cell 145: 242-256.

10. Moussian B, Schoof H, Haecker A, Jurgens G, Laux T (1998) Role of the ZWILLE gene in the regulation of central shoot meristem cell fate during Arabidopsis embryogenesis. EMBO J 17: 1799-1809.

11. Guyomarc'h S, Vernoux T, Traas J, Zhou DX, Delarue M (2004) MGOUN3, an Arabidopsis gene with TetratricoPeptide-Repeat-related motifs, regulates meristem cellular organization. J Exp Bot 55: 673-684.

12. Suzuki T, Nakajima S, Morikami A, Nakamura K (2005) An Arabidopsis protein with a novel calcium-binding repeat sequence interacts with TONSOKU/MGOUN3/BRUSHY1 involved in meristem maintenance. Plant Cell Physiol 46: 1452-1461.

Chapter Five

Final remarks

Finding new regulators necessary for meristem maintenance has proven challenging. Many gaps in the regulatory pathways controlling organogenesis remain despite research spanning several decades by a large number of labs. In my doctoral research, I have attempted to identify novel regulators of meristem maintenance using a variety of approaches.

Our understanding of the mechanisms of meristem maintenance has come a long way since the first meristem mutants were isolated, mapped and described. However there are still facets that require further research and explanation [1-5]. The identification of the regulatory loop between CLAVATA pathway factors and transcriptional regulator WUS, as well as the function of SHOOTMERISTEMLESS, inevitably bring about questions of mechanistic interactions and pathway intermediates. To date, we are unaware of how CLV components specifically suppress POL/PLL1 function and how, in turn, POL/PLL1 act to maintain WUS expression within the meristem. Given the lack of detected direct interactions between these components and their distinct subcellular localization, key signaling intermediates likely remain unidentified.

Very little is known about WUS or STM direct targets, nor regulators upstream of STM.

Using straight forward genetic screens for specific defects in meristem function, researchers identified CLV1/CLV2/CLV3 as well as WUS and STM as meristem regulators. It took many approaches to move beyond this core group of regulators [4-8]. CRN was found in a screen for resistance to exogenous CLV3 application and in a screen for CLV3 overexpression phenotype suppression [9,10]. POL/PLL1 were found as suppressors of partial-loss-of-function *clv* mutants [11,12]. BAM receptors were characterized through reverse genetic analyses [13]. KNATs and BELLs were found largely through their phenotypes outside of the meristem [14-22]. The various roles of HD-zip III proteins in meristem formation and maintenance were not known until a comprehensive genetic analysis encompassing triple, quadruple and even quintuple mutants was performed [23-27].

Why are so many of the factors controlling meristem development hard to identify? Why are there so many missing steps in the known regulatory pathways? The most important answer appears to be genetic redundancy. CLV1, POL, CRN, BAM, BELL, KNAT, HD-zip III activities in the meristem are all redundantly encoded. Thus, mutants in many components have no phenotypes on their own.

Sensitized genetic backgrounds are an essential starting point to identify redundantly encoded factors. This was the rationale behind the *pol* enhancer

mutant screen to which I contributed. *pol* single mutants have a barely detectable reduction in meristem size, but are sensitized to other changes in meristem function as a result. As part of a larger screen by Chunghee Lee, I mapped and identified the lesion for two putative *pol* enhancer mutants. When these mutants were mapped, they corresponded to the previously identified *AGO10* and *TSK*. AGO10 is interesting because it is known to specifically regulate HD-zip III gene function by modulating the activity of miRNAs that target these genes. Chunghee Lee also identified an *ago10* mutant from another *pol* enhancer mutant which suggests a synergistic interaction between the two and is currently pursuing this line of investigation. The synergistic interaction between *ago10* and *pol* mutants suggests they may act in parallel. The significance of TSK is difficult to interpret because of the *tsk* pleiotropic phenotypes. The mutant does contain defects in meristem function, but they are not dependent on *pol* and could be an indirect consequence of the apparent loss of proper orientation of division planes.

Another *pol* enhancer that appeared in a fortuitous manner was the spontaneous *blr-7* mutation that appeared in a cross with *pol*, revealing the strong phenotypes characteristic of the *blr-7 pol* double mutants. Like *ago10*, the *blr-7* synergism with *pol* suggests the two mutations reflect parallel pathways controlling meristem development. *blr-7* is similar to many of the meristem mutants identified in genetic screens; namely, that it is a dominant-negative allele. Most *clv1* alleles, all *crn* alleles, the first *pol* allele are all dominant-

negative [10,28,29]. The dominant-negative character is presumably what allows these alleles to exert a strong phenotype in the presence of redundant factors.

Dominant-negative alleles can reveal critical regions of biochemical function. The novel and severe inflorescence phenotypes of *blr-7* and the *gorgon* allele of *STM*, as well as the homeotic transformation phenotypes of *blr-4* and *blr-5*, highlight the effects of mutations within different helices of the homeodomain [18]. Dominant-negative alleles can also reveal partner proteins whose activity is compromised in the presence of the mutant protein isoform. For example, in the case of *clv1* dominant-negative alleles resulting from missense mutations in the kinase domain, the alleles block the function of the partner protein BAM [30]. In the case of the *blr-7* allele, my observations are consistent with the blr-7 protein interfering with STM function.

Identifying DNA binding targets of transcriptional regulators such as STM, WUS and BLR will be necessary to determine specific cellular processes which maintain meristematic cells. In addition, a detailed map of temporal and spatial expression patterns for interacting homedomains will provide insight into how the various combinations regulate different aspects of development.

A recent study has demonstrated that CLV1 is targeted to the lytic vacuole upon ligand binding indicating a mechanism for intracellular signal transduction through endocytic trafficking [31]. Our lab has shown the effective ligand-binding for transiently expressed CLV1, BAM and CLV2 receptors only occurs in a lipid-insoluble membrane fraction [32] . Furthermore, a portion of CLV1/BAM/CRN

receptors are found in these membrane microdomains in Arabidopsis. Other studies indicated that CRN and CLV2 are ER localized and must dimerize in order to move from the ER to the plasma membrane [32,33]. The role of the endomembrane system and ligand mediated receptor endocytosis in CLV signaling could partially explain the lack of signaling intermediates identified in the CLV-WUS pathway. In the future, the analysis of subcellular behavior of CLV proteins and mutants and disruption of membrane transport pathways may be useful in determining mechanisms of CLV signaling.

The protein-protein interaction approach utilized in the identification of CCI1 is not dependent on the genetic function of the interacting protein. The first such CLV1-interacting protein identified in this fashion, KAPP, has little effect on the meristem in the null allele [34,35]. This may reflect an activity that is redundantly encoded or reflect a biochemical function in signaling that is not essential. For example, mutations in the ER quality control machinery that monitor and facilitate receptor folding have little to no phenotype when mutated on their own. For the CLV1-interacting protein I have characterized, CCI1, no phenotypes were observed in mutant alleles. In this case, it is unclear if this is because the alleles are loss-of-function or if CCI1 mutants do not disrupt meristem development.

CCI1 is differentially expressed in CZ region of the meristem in the L1 and L2 layers compared to cells of the PZ and RM [36]. The up-regulation of CCI1 in these cells coincides with CLV3, expressed in the CZ, over that of WUS and FIL

which are expressed in the PZ and RM respectively [37-39]. Further, the identification of CCI1 as directly upregulated by WUS highlights a probable role in the CLV3-WUS regulatory network within the shoot meristem [40]. Additionally, the localization and the co-immunoprecipitation of CCI1 with DRM-associated CLV factors suggest a possible role of CCI1 in a lipid raft-based signaling complex.

Future analysis of signal transduction focusing on characterizing biochemical functions and behavior of known components as well as identifying transcriptional regulation targets and mapping transcriptional networks will lead us to a greater understanding of meristem maintenance. Because of the nature of the meristem and the balance of stem cell with differentiation, understanding the mechanisms which lead to differentiation on a cellular and meristematic level, combined with those that maintain stem cells will be necessary to paint a clear picture of the plant meristem.

References

1. Reinholz E (1966) Radiation induced mutants showing changed inflorescence characteristics. Arabidopsis Information Service 3: 19-20.

2. Koornneef M, van Eden J, Hanhart CJ, Stam P, Braaksma FJ, et al. (1983) Linkage map of *Arabidopsis thaliana*. J Hered 74: 265-272.

3. Leyser HMO, Furner IJ (1992) Characterization of three shoot apical meristem mutants of *Arabidopsis thaliana*. Development 116: 397-403.

4. Clark SE, Running MP, Meyerowitz EM (1993) *CLAVATA1*, a regulator of meristem and flower development in Arabidopsis. Development 119: 397-418.

5. Barton MK, Poethig RS (1993) Formation of the shoot apical meristem in *Arabidopsis thaliana*: An analysis of development in the wild type and *shoot meristemless* mutant. Development 119: 823-831.

6. Kayes JM, Clark SE (1998) *CLAVATA2*, a regulator of meristem and organ development in *Arabidopsis*. Development 125: 3843-3851.

7. Clark SE, Running MP, Meyerowitz EM (1995) *CLAVATA3* is a specific regulator of shoot and floral meristem development affecting the same processes as *CLAVATA1*. Development 121: 2057-2067.

8. Laux T, Mayer KF, Berger J, Jurgens G (1996) The WUSCHEL gene is required for shoot and floral meristem integrity in Arabidopsis. Development 122: 87-96.

9. Miwa H, Betsuyaku S, Iwamoto K, Kinoshita A, Fukuda H, et al. (2008) The receptor-like kinase SOL2 mediates CLE signaling in Arabidopsis. Plant Cell Physiol 49: 1752-1757.

10. Muller R, Bleckmann A, Simon R (2008) The receptor kinase CORYNE of Arabidopsis transmits the stem cell-limiting signal CLAVATA3 independently of CLAVATA1. Plant Cell 20: 934-946.

11. Yu LP, Simon EJ, Trotochaud AE, Clark SE (2000) *POLTERGEIST* functions to regulate meristem development downstream of the *CLAVATA* loci. Development 127: 1661-1670.

12. Song SK, Clark SE (2005) POL and related phosphatases are dosage-sensitive regulators of meristem and organ development in Arabidopsis. Dev Biol 285: 272-284.

13. DeYoung BJ, Bickle KL, Schrage KJ, Muskett P, Patel K, et al. (2006) The CLAVATA1-related BAM1, BAM2 and BAM3 receptor kinase-like proteins are required for meristem function in Arabidopsis. Plant J 45: 1-16.

14. Venglat SP, Dumonceaux T, Rozwadowski K, Parnell L, Babi V, et al. (2002) The homeobox gene *BREVIPEDICELLUS* is a key regulator of inflorescence architecture in *Arabidopsis*. Proc Natl Acad Sci USA 99: 4730-4735.

15. Lincoln C, Long J, Yamaguchi J, Serikawa K, Hake S (1994) A knotted1-like homeobox gene in Arabidopsis is expressed in the vegetative meristem and dramatically alters leaf morphology when overexpressed in transgenic plants. Plant Cell 6: 1859-1876.

16. Ragni L, Belles-Boix E, Gunl M, Pautot V (2008) Interaction of KNAT6 and KNAT2 with BREVIPEDICELLUS and PENNYWISE in Arabidopsis inflorescences. Plant Cell 20: 888-900.

17. Ray A, Robinson-Beers K, Ray S, Baker SC, Lang JD, et al. (1994) Arabidopsis floral homeotic gene BELL (BEL1) controls ovule development through negative regulation of AGAMOUS gene (AG). Proc Natl Acad Sci U S A 91: 5761-5765.

18. Bao X, Franks RG, Levin JZ, Liu Z (2004) Repression of AGAMOUS by BELLRINGER in floral and inflorescence meristems. Plant Cell 16: 1478-1489.

19. Byrne ME, Groover AT, Fontana JR, Martienssen RA (2003) Phyllotactic pattern and stem cell fate are determined by the Arabidopsis homeobox gene BELLRINGER. Development 130: 3941-3950.

20. Bhatt AM, Etchells JP, Canales C, Lagodienko A, Dickinson H (2004) VAAMANA--a BEL1-like homeodomain protein, interacts with KNOX proteins BP and STM and regulates inflorescence stem growth in Arabidopsis. Gene 328: 103-111.

21. Roeder AH, Ferrandiz C, Yanofsky MF (2003) The role of the REPLUMLESS homeodomain protein in patterning the Arabidopsis fruit. Curr Biol 13: 1630-1635.

22. Kumar R, Kushalappa K, Godt D, Pidkowich MS, Pastorelli S, et al. (2007) The Arabidopsis BEL1-LIKE HOMEODOMAIN proteins SAW1 and SAW2

act redundantly to regulate KNOX expression spatially in leaf margins. Plant Cell 19: 2719-2735.

23. Otsuga D, DeGuzman B, Prigge MJ, Drews GN, Clark SE (2001) *REVOLUTA* regulates meristem initiation at lateral positions. Plant J 25: 223-236.

24. McConnell JR, Emery J, Eshed Y, Bao N, Bowman J, et al. (2001) Role of *PHABULOSA* and *PHAVOLUTA* in determinging radial patterning in shoot. Nature 411: 709-713.

25. Prigge MJ, Otsuga D, Alonso JM, Ecker JR, Drews GN, et al. (2005) Class III Homeodomain-Leucine Zipper Gene Family Members Have Overlapping, Antagonistic, and Distinct Roles in Arabidopsis Development. Plant Cell 17: 61-76.

26. Green KA, Prigge MJ, Katzman RB, Clark SE (2005) *CORONA*, a Member of the Class III Homeodomain-Leucine Zipper Gene Family in Arabidopsis, Regulates Stem Cell Specification and Organogenesis. Plant Cell In Press.

27. Byrne ME (2006) Shoot meristem function and leaf polarity: the role of class III HD-ZIP genes. PLoS Genet 2: e89.

28. Diévart A, Dalal M, Tax FE, Lacey AD, Huttly A, et al. (2003) *CLAVATA1* dominant-negative alleles reveal functional overlap between multiple receptor kinases that regulate meristem and organ development. Plant Cell 15: 1198-1211.

29. Yu LP, Miller AK, Clark SE (2003) *POLTERGEIST* Encodes a Protein Phosphatase 2C that Regulates CLAVATA Pathways Controlling Stem Cell Identity at *Arabidopsis* Shoot and Flower Meristems. Curr Biol 13: 179-188.

30. DeYoung BJ, Clark SE (2008) BAM receptors regulate stem cell specification and organ development through complex interactions with CLAVATA signaling. Genetics 180: 895-904.

31. Nimchuk ZL, Tarr PT, Ohno C, Qu X, Meyerowitz EM (2011) Plant stem cell signaling involves ligand-dependent trafficking of the CLAVATA1 receptor kinase. Curr Biol 21: 345-352.

32. Guo Y, Clark SE (2010) Membrane distributions of two ligand-binding receptor complexes in the CLAVATA pathway. Plant Signal Behav 5: 1442-1445.

33. Bleckmann A, Weidtkamp-Peters S, Seidel CA, Simon R (2010) Stem cell signaling in Arabidopsis requires CRN to localize CLV2 to the plasma membrane. Plant Physiol 152: 166-176.

34. Williams RW, Wilson JM, Meyerowitz EM (1997) A possible role for kinase-associated protein phosphatase in the arabidopsis CLAVATA1 signaling pathway. Proc Natl Acad Sci USA 94: 10467-10472.

35. Stone JM, Trotochaud AE, Walker JC, Clark SE (1998) Control of meristem development by CLAVATA1 receptor kinase and kinase-associated protein phosphatase interactions. Plant Physiol 117: 1217-1225.

36. Yadav RK, Girke T, Pasala S, Xie M, Reddy GV (2009) Gene expression map of the Arabidopsis shoot apical meristem stem cell niche. Proc Natl Acad Sci U S A 106: 4941-4946.

37. Fletcher JC, Brand U, Running MP, Simon R, Meyerowitz EM (1999) Signaling of cell fate decisions by *CLAVATA3* in *Arabidopsis* shoot meristems. Science 283: 1911-1914.

38. Mayer KF, Schoof H, Haecker A, Lenhard M, Jurgens G, et al. (1998) Role of *WUSCHEL* in regulating stem cell fate in the *Arabidopsis* shoot meristem. Cell 95: 805-815.

39. Heisler MG, Ohno C, Das P, Sieber P, Reddy GV, et al. (2005) Patterns of auxin transport and gene expression during primordium development revealed by live imaging of the Arabidopsis inflorescence meristem. Curr Biol 15: 1899-1911.

40. Yadav RK, Perales M, Gruel J, Ohno C, Heisler M, et al. (2013) Plant stem cell maintenance involves direct transcriptional repression of differentiation program. Mol Syst Biol 9: 654.